Molecular genetic approaches for the improvement of abiotic stress resistance in *Arabidopsis thaliana*

genehmigte Dissertation von
M.Sc. Mohamed Hassan Mohamed Ahmed Aboelmy
geboren am 13.06.1979 in Menia, Ägypten

2014

Parts of this work have already been published:

Publications:

1- Aboelmy, M.H. and Peterhansel, C. (2014). Enzymatic characterization of *Chlamydomonas reinhardtii* glycolate dehydrogenase and its nearest proteobacterial homologue. Plant Physiol. Biochem. **79**: 25–30.

2- Kebeish, R.*, Aboelmy, M.H.*., El-Naggar, A., El-Ayouty,Y., Peterhansel, C (2014). Simultaneous overexpression of cyanidase and formate dehydrogenase in Arabidopsis thaliana chloroplasts enhanced cyanide metabolism and cyanide tolerance. Environ. Exp. Bot. **DOI:** 10.1016/j.envexpbot.2014.09.004.
*Joint first authors

Conference contributions:

Aboelmy, M.H. and Peterhansel, C. Enzymatic characterization of *Chlamydomonas reinhardtii* glycolate dehydrogenase and its nearest proteobacterial homologue. 16th Photosynthesis congress, St. Louis, USA, 2013.

ABSTRACT

Abstract

Abiotic stresses limit plant growth, metabolism and productivity. In this study two different approaches were carried out to enhance plant tolerance to abiotic stresses. The first approach aimed to characterize biochemically a glycolate dehydrogenase (*Cr*GlcDH), a key enzyme in *Chlamydomonas reinhardtii* photorespiration. Photorespiration is now believed to be a part of stress response in plants through preventing accumulation of reactive oxygen species (ROS) and protecting photosynthesis from photoinhibition. *Cr*GlcDH is different in structure from the GlcDH enzymes of heterotrophic prokaryotes and the glycolate oxidases of higher plants. In this study, *Cr*GlcDH was recombinantly overexpressed, purified and its enzymatic properties were studied. It was found to use $_D$-lactate, but not $_L$-lactate, as an alternative substrate with similar catalytic proficiency compared to glycolate. Other short-chain organic acids were only very slowly oxidized. Only the artificial electron acceptors DCIP and PMS, but neither flavine mono- or dinucleotides nor nicotineamide dinucleotides or cytochrome c, were used as electron acceptors by the recombinant enzyme. The enzyme was sensitive to $CuSO_4$ suggesting function of reactive sulfhydryl groups in catalysis. Accordingly, mutational analysis of a putative Fe-S cluster indicated an important function of this domain in catalysis. Evolutionary sequence analysis revealed that *Cr*GlcDH belongs to a so far uncharacterized group of enzymes that was only found in chlorophytes and some proteobacteria. Other prokaryotic GlcDH enzymes were only distantly related. Moreover, the most related proteobacterial homologue from *Desulfovibrio vulgaris* was also recombinantly overexpressed and purified. It was found to be active with $_D$-lactate, but not glycolate as a substrate.

The second approach in this study was to introduce a novel pathway in plants for cyanide detoxification. Cyanide is a strong inhibitor of diverse metabolic reactions and easily absorbed by organisms. However, cyanide is also a byproduct of plant and microbial metabolism. This is why these groups of organisms contain pathways for cyanide detoxification. Large amounts of cyanides are also produced by industries and are today mostly removed by physical and chemical methods. Phytoremediation can provide an alternative to these techniques, but existing cyanide concentrations at contaminated sites often exceed the capacities of plant metabolism. In this study, a bacterial cyanidase together with a plant formate dehydrogenase were introduced to *Arabidopsis thaliana* in order to establish a synthetic pathway for cyanide degradation. Simultaneous overexpression of both enzymes would ultimately result in the formation of CO_2

ABSTRACT

and NH$_3$ from cyanide. Both enzymes were targeted to chloroplasts and shown to be active *in planta*. Growth on cyanide was tested for seedlings germinating on agar, plants in hydroponics, and plants growing in sand. In all three assays, plants overexpressing the synthetic pathway for cyanide degradation showed enhanced growth and biomass accumulation compared to controls. In addition, gas exchange measurements confirmed enhanced stress resistance of transgenic plants and suggested that cyanide degradation to CO$_2$ increased the leaf internal CO$_2$ concentration.

Zusammenfassung

Abiotischer Stress limitiert Wachstum, Metabolismus und Produktivität von Pflanzen. Im Rahmen dieser Arbeit wurden zwei unterschiedliche Ansätze zur Erhöhung der Toleranz von Pflanzen gegen abiotischen Stress getestet. Im ersten Ansatz wurde eine photorespiratorische Glycolatdehydrogenase (*Cr*GlcDH) aus *Chlamydomonas reinhardtii* biochemisch charakterisiert. Photorespiration wird heute als ein Bestandteil der Stressantwort von Pflanzen gesehen, da dieser Stoffwechselweg die Akkumulation reaktiver Sauerstoffspecies vermindert und die Photosysteme vor Photoinhibition schützt. *Cr*GlcDH unterscheidet sich in der Struktur von den Glycolatdehydrogenasen heterotropher Eukaryoten und der Glycolatoxidasen höherer Pflanzen. In dieser Arbeit wurde *Cr*GlcDH rekombinant überexprimiert, aufgereinigt und enzymatisch charakterisiert. $_D$-Lactat, aber nicht $_L$-Lactat, wurde als alternatives Substrat mit zu Glycolat vergleichbarer katalytischer Effizienz akzeptiert. Andere kurzkettige organische Säuren wurden nur sehr langsam oxidiert. Die artifiziellen Elektronenakzeptoren DCIP und PMS, aber weder Flavin mono- und dinucleotide noch Nikotinamid-dinucleotide oder Cytochrom c wurden als Elektronendonatoren akzeptiert. Das Enzym wurde durch $CuSO_4$ inhibiert, was für eine Funktion von Sulfhydryl-Gruppen bei der Katalyse spricht. Entsprechend konnte durch Mutationsanalysen eine wichtige Rolle eines Fe-S-Clusters bei der Katalyse belegt werden. Durch evolutionäre Sequenzanalysen wurde CrGlcDH einer bisher unbeschriebenen Gruppe von Enzymen zugeordnet, die nur in Chlorophyten und einigen Protobakterien vorkommen. Andere prokaryotische GlcDH Enzyme zeigten nur geringe Homologien zu *Cr*GlcDH. Das am nächsten verwandte proteobakterielle Homolog aus *Desulfovibrio vulgaris* zeigte ebenfalls Aktivität mit $_D$-Lactat als Substrat, aber nicht mit Glycolat.

In einem zweiten Ansatz wurde ein neuer Stoffwechselweg zum Zyanid-Abbau in Pflanzen etabliert. Zyanid ist ein starker Inhibitor zahlreicher metabolischer Reaktionen und wird von Organismen leicht aufgenommen. Auf der anderen Seite ist Zyanid auch ein natürliches Nebenprodukt des Metabolismus von Pflanzen und Mikroorganismen. Daher enthalten diese Organismengruppen Stoffwechselwege zum Zyanid-Abbau. Große Mengen an Zyanid werden auch in industriellen Prozessen erzeugt und heute zumeist über physikalische oder chemische Methoden entsorgt. Phytoremediation könnte als Alternative zu diesen Techniken genutzt werden, aber die Konzentrationen an kontaminierten Standorten übersteigen häufig die metabolische Leistungsfähigkeit von Pflanzen. Im Rahmen dieser Arbeit wurden eine bakterielle

Cyanidase und eine pflanzliche Formatdehydrogenase in *Arabidopsis thaliana* überexprimiert, um einen synthetischen Stoffwechselweg zum Zyanidabbau zu etablieren. Die gleichzeitige Überexpression beider Proteine würde letztlich zu einem Abbau des Zyanids zu CO_2 und NH_3 führen. Beide Enzyme wurden in Chloroplasten lokalisiert und die *in planta* Aktivität wurde nachgewiesen. Das Wachstum von Keimlingen unter Zyanidstress wurde auf Agar, in hydroponischer Kultur, und in Sand als Substrat getestet. In allen drei Ansätzen zeigten Pflanzen, die den synthetischen Stoffwechselweg zum Zyanidabbau überexprimierten, eine erhöhte Biomasseakkumulation im Vergleich zu Kontrollen. Gaswechselmessungen bestätigten die verbesserte Stressresistenz und ergaben Hinweise auf eine erhöhte CO_2 Konzentration in Blättern als Resultat der Zyaniddegradation.

Schlagworte:

Photorespiration

Bioremediation

Glycolat dehydrogenase

Key words:

photorespiration

bioremediation

glycolate dehydrogenase

Table of contents

1. Introduction

1.1. Photosynthesis

Photosynthesis is an important process for all living forms on earth. It is the process by which photoautotrophic organisms capture light energy and use it to convert atmospheric carbon dioxide and water into carbohydrates. The food that we eat, the oxygen that is required for all aerobic organisms, the fuel that is required for energy production, and the fibers that we wear are resulting from photosynthesis (Blankenship, 2010). Photosynthesis is generally divided up into two parts: the light reactions and the carbon reactions.

The light dependent reactions (Figure 1) are the processes in which the light is captured and conserved in the form of chemical bonds (Sugar). These processes take place in the thylakoid membrane of the chloroplasts. This is performed by photo-system I (PSI) and photo-system II (PSII) (Järvi et al., 2013). In the reaction center of PSII an electron from one of the chlorophylls is excited and subsequently transferred through a series of acceptors in the electron transport chain. The linear electron transport chain builds up a proton gradient over the thylakoid membrane, which is used to produce energy via converting ADP to ATP. In addition, the reducing agent NADPH is produced during the electron transport through PSI. The light reactions serve to produce the energy carriers which are further used in the carbon reactions to fix atmospheric CO_2 (Järvi et al., 2013).

The carbon reactions do not directly need light in order to occur, but they need the products of the light reaction (ATP and NADPH). The light independent reactions occur in the stroma of the chloroplast. During these reactions, the reducing power and energy equivalents (ATP and NADPH) provided by the light reactions are required for CO_2 assimilation. Most higher plants assimilate carbon dioxide through the C_3-photosynthetic pathway and thus are known as C_3 plants (Ku et al., 1999). The CO_2 assimilation pathway in C_3 plants is known as the Calvin cycle (Figure 3). The Calvin cycle proceeds in three stages, carboxylation, reduction and regeneration. During the carboxylation reaction, a molecule of CO_2 is covalently linked to a five-carbon skeleton called ribulose bisphosphate (RuBP) producing an unstable six-carbon intermediate that immediately breaks down into two molecules of the three-carbon compound phosphoglycerate (PGA). The carbon that was a part of inorganic CO_2 is now part of the carbon skeleton of an organic molecule.
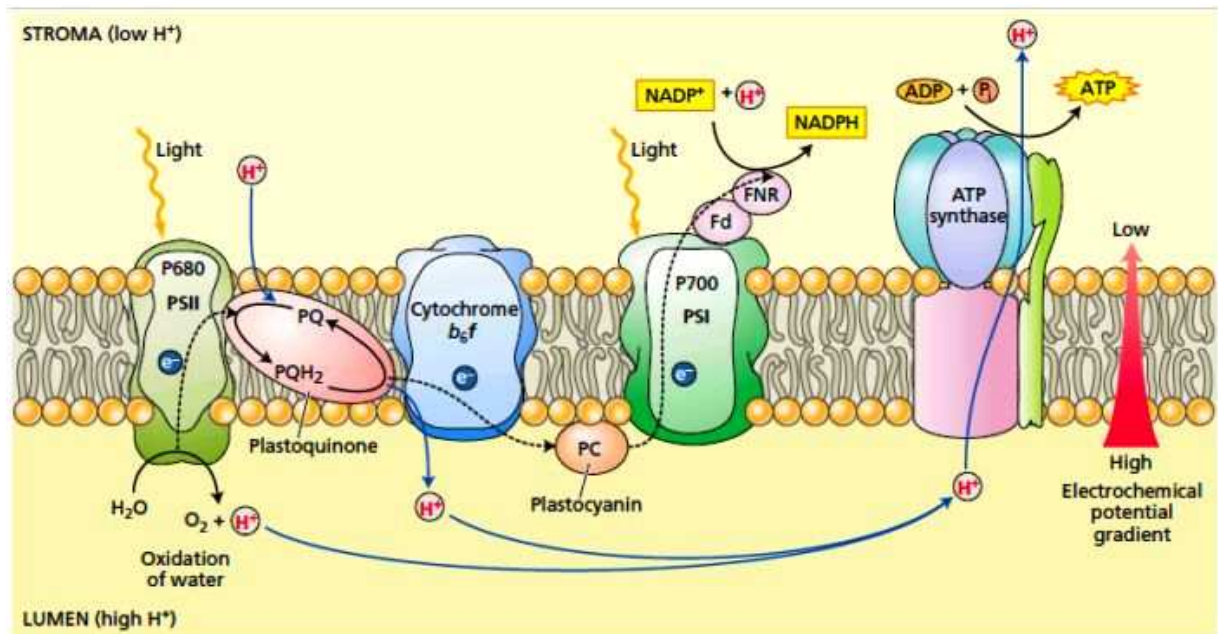
Figure 1. Schematic diagram for the transfer of electrons and protons in the thylakoid membrane. The figure was taken from Plant Physiology fifth edition (Taiz and Zeiger, 2010)

CO_2 fixation is catalyzed by a complex enzyme consisting of eight large subunits and eight small subunits (Miziorko and Lorimer, 1983; Parry, 2003; Whitney et al., 2011) known as ribulose-1,5-bisphosphate carboxylase/oxygenase (Rubisco, EC 4.1.1.39). In addition to CO_2 fixation, Rubisco accepts O_2 as a competitor substrate (Figure 2). Depending of certain conditions such as temperature and CO_2/O_2 ratio, the oxygenation reactions (photorespiration, see 1.2) of Rubisco are estimated to be quarter or even higher of its activity (Sharkey, 1988). Rubisco is produced in huge amount in higher plants to compensate for its slow activity (Tcherkez et al., 2006), as it can make up as much as 30-50% of total leaf protein in C_3 plants (Parry, 2003). During the reduction phase, the carboxylated compound is reduced on the expense of the photochemically derived ATP and NADPH. The PGA is converted to glyceraldehyde-3-phosphate (G3P), another three carbon compound. For every six molecules of CO_2 that enter the Calvin cycle, two molecules of G3P are produced. Some of the molecules of G3P, however, are used to synthesize glucose and other organic molecules.
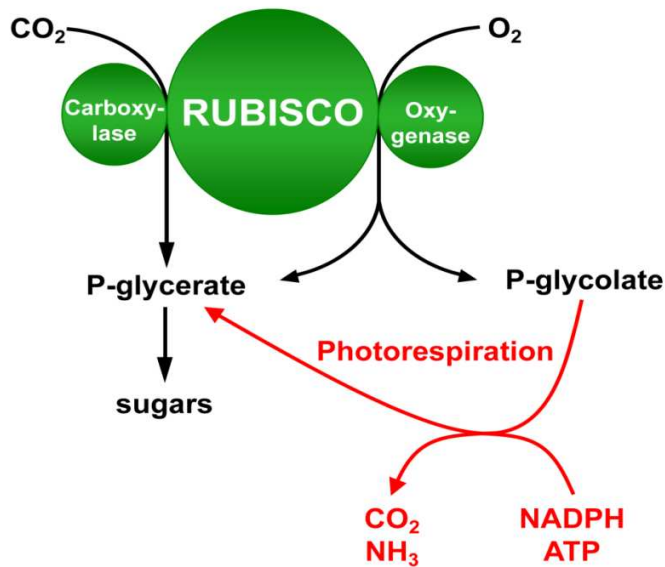
Figure 2. Schematic overview of the bi-functions (CO_2/O_2 fixation) of Rubisco in photosynthetic organisms.
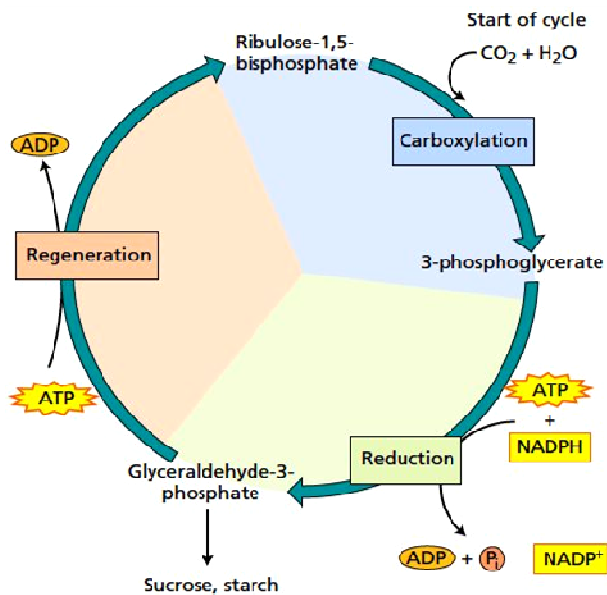
Figure 3. The carbon reactions pathway in C_3 plants (Calvin cycle). ATP, adenosine triphosphate. ADP, adenosine diphosphate. CO_2, carbon dioxide. NADPH, nicotinamide adenine dinucleotide phosphate (Reduced form). $NADP^+$, nicotinamide adenine dinucleotide phosphate (Oxidized form). The figure was taken from plants physiology fifth edition (Taiz and Zeiger, 2010).

3

During the regeneration phase, the CO_2 acceptor RuBP re-forms. Most of the G3P produced during the Calvin cycle are used to regenerate RuBP.

Ten molecules of the three-carbon compound G3P eventually form six molecules of the five-carbon compound ribulose phosphate (RP) which is then phosphorylated to produce RuBP, the starting compound for the Calvin cycle.

1.2. Photorespiration

Photorespiration occurs in all oxygen (O_2)-producing photosynthetic organisms (Bauwe et al., 2010). Biochemically, photorespiration begins with O_2 substituting for CO_2 in the first reaction of the photosynthetic CO_2 fixation that is catalyzed by Rubisco (Leegood et al., 1995; Wingler et al., 2000). The reductive reaction (Carboxylation reaction, or CO_2 fixation) of Rubisco enzyme is known as C_3 or Calvin cycle (See 1.1), and the oxidative reaction (O_2 fixation) is known as C_2 or photorespiration (Leegood et al., 1995; Wingler et al., 2000). The carboxylation of RubP produces two molecules of 3-phosphoglycerate (PGA) while its oxygenation yields one molecule of PGA and one molecule of phosphoglycolate (PG) (Andersson, 2008). PG is a toxic compound, it inhibits the Calvin-cycle enzyme triose- phosphate isomerase, thus it should be metabolized rapidly (Norman and Colman, 1991; Tolbert, 1997).

1.3. The photorespiratory pathway in higher plants (C_2 cycle)

In higher plants, metabolism of PG compound is achieved via several enzymes distributed in three different compartments: chloroplast, peroxisome, and mitochondria (Foyer et al., 2009; Bauwe et al., 2010). In the chloroplast, PG is dephosphorylated to glycolate through a highly specific enzyme known as phosphoglycolate phosphatase (PGLP) (Somerville and Ogren, 1979). In addition to the plastidial PGLP enzyme (At5g36700), *Arabidopsis thaliana* also has a second enzyme in the cytosol, but only knockout mutants of the plastidial enzyme result in a photorespiratory phenotype and require CO_2-enriched environment to survive (Schwarte and Bauwe, 2007). PGLP was reported as a light-induced gene (Foyer et al., 2009). Biochemical studies were performed on purified PGLP proteins from various organisms revealed the requirement of Mg^{2+} and Cl^{-1} for PGLP activity (Husic and Tolbert, 1984; Norman and Colman, 1991). The produced glycolate is transported from the chloroplast through a glycolate-glycerate antiporter and enters the peroxisome via porin-like channels (Reumann and Weber, 2006; Pick et al., 2013).

In the peroxisomes, glycolate is oxidized in an irreversible reaction into equimolar amounts of glyoxylate and H_2O_2. Glycolate oxidation is catalyzed by glycolate oxidase (GOX, EC 1.1.3.15) (Volokita et al., 1987). In Arabidopsis plants five genes were reported to encode GOX protein, three of them are localized in the peroxisome (Reumann et al., 2004; Reumann and Weber, 2006). GOX-mutants in rice plants (Xu et al., 2009) and in maize (Zelitch et al., 2009) require elevated CO_2 for survival, while no GOX-mutants were identified in Arabidopsis plants (Somerville and Ogren, 1982). Moreover, studies using down-regulated GOX mutants in tobacco plants revealed the potential regulatory effect of GOX proteins on photosynthesis (Xu et al., 2009). Furthermore, GOX protein was found to be induced during the pathogen infection (Taler et al., 2004). The H_2O_2 generated as a by-product during glycolate oxidation is detoxified by catalase (CAT, EC 1.11.1.6) in the peroxisome (Tolbert, 1997; Queval et al., 2007; Foyer et al., 2009). Three different CAT genes were identified in Arabidopsis, but only one gene (CAT2, At4g35090) was found to involve in photorespiration cycle (Queval et al., 2007). CAT2 was reported as light-induced gene and clock-regulated (Induced in the morning) (Zhong et al., 1997; Queval et al., 2007). Arabidopsis plants with CAT2-knock-out mutant showed reduction in rosette biomass and activation of oxidative signaling pathway (Queval et al., 2007). Glyoxylate is then transaminated to glycine. In Arabidopsis glyoxylate is transaminated to glycine through one of two parallel reactions catalyzed by glutamate:glyoxylate aminotransferase (GGAT, EC 2.6.1.4) or serine:glyoxylate aminotransferase (SGAT, EC 2.6.1.45). Two GGAT genes (At1g23310 encoding GGAT1 and At1g70580 encoding GGAT2) were identified in Arabidopsis (Igarashi et al., 2003, 2006). It was reported that each of GGAT1 and GGAT2 contributes in the total GGAT activity in photorespiration (Igarashi et al., 2006). In Arabidopsis SGAT is encoded by a single gene (At2g13360). SGAT knock-out mutants in Arabidopsis (Somerville and Ogren, 1980; Liepman and Olsen, 2001) or barley (Murray et al., 1987) were lethal under ambient air conditions.

In the mitochondria, two molecules of glycine are required to generate one molecule of serine by the combined action of two enzymatic complexes: glycine decarboxylase (GDC) and serine hydroxymethyltransferase (SHMT, EC. 2.1.2.1) (Peterhansel et al., 2010). Decarboxylation of one glycine molecule produces one molecule each of CO_2, NH_3, NADH, and 5,10 methylene tetrahydrofolate (CH_2-THF) (Oliver, 1994; Douce et al., 2001). GDC is a complex enzyme consisting of four different subunits (P (EC 1.4.4.2), H, T (EC 2.1.2.10), and L (EC 1.8.1.4)). In

Arabidopsis plants, eight different genes were identified for GDC complex protein, two genes for each subunit (P-protein (At4g33010 and At2g26080) and L-protein (At3g17240 and At1g48030), three genes for H-protein (At2g35370, At2g35120 and At1g32470) and one gene for T-protein (At1g11860)) (Bauwe and Kolukisaoglu, 2003). Enriched CO_2 air was not able to rescue Arabidopsis plants with double knock-out mutants in the two genes encoding the P-subunit (Engel et al., 2007) suggesting that GDC has a potential function in nucleic acids and amino acids metabolism (Cossins and Chen, 1997). The SHMT combines methylene-THF with a second molecule of glycine to produce one molecule of serine and regenerate THF (Leegood et al., 1995). In Arabidopsis, the SHMT is encoded by a single gene (At4g37930). Knock-out mutants of SHMT require elevated CO_2 to survive (Voll et al., 2006).

Back to the peroxisome, serine generated in the mitochondria goes back to the peroxisome and is converted to glycerate through the action of SGAT (See above: in the peroxisome) that produces hydroxypyruvate (HP). HP is reduced by NADH-dependent hydroxypyruvate reductase (HPR1, EC 1.1.1.29) to glycerate. In Arabidopsis, HPR1 is encoded by a single gene (At1g68010) (Givan and Kleczkowski, 1992). HPR1 knock-out mutants in Arabidopsis (Timm et al., 2008) and barley (Murray et al., 1989) do not show the photorespiratory phenotype suggesting that an alternative pathway for the conversion of hydroxypyruvate to glycerate may be exist (Peterhansel et al., 2010). Finally, glycerate is transported back to the chloroplast then phosphorylated to form PGA by catalysis of D-glycerate 3-kinase (GLYK, EC 2.7.1.31) at expense of ATP. In Arabidopsis, GLYK is encoded by a single gene (At1g80380) and knock-out mutants show the photorespiratory phenotype (Boldt et al., 2005).
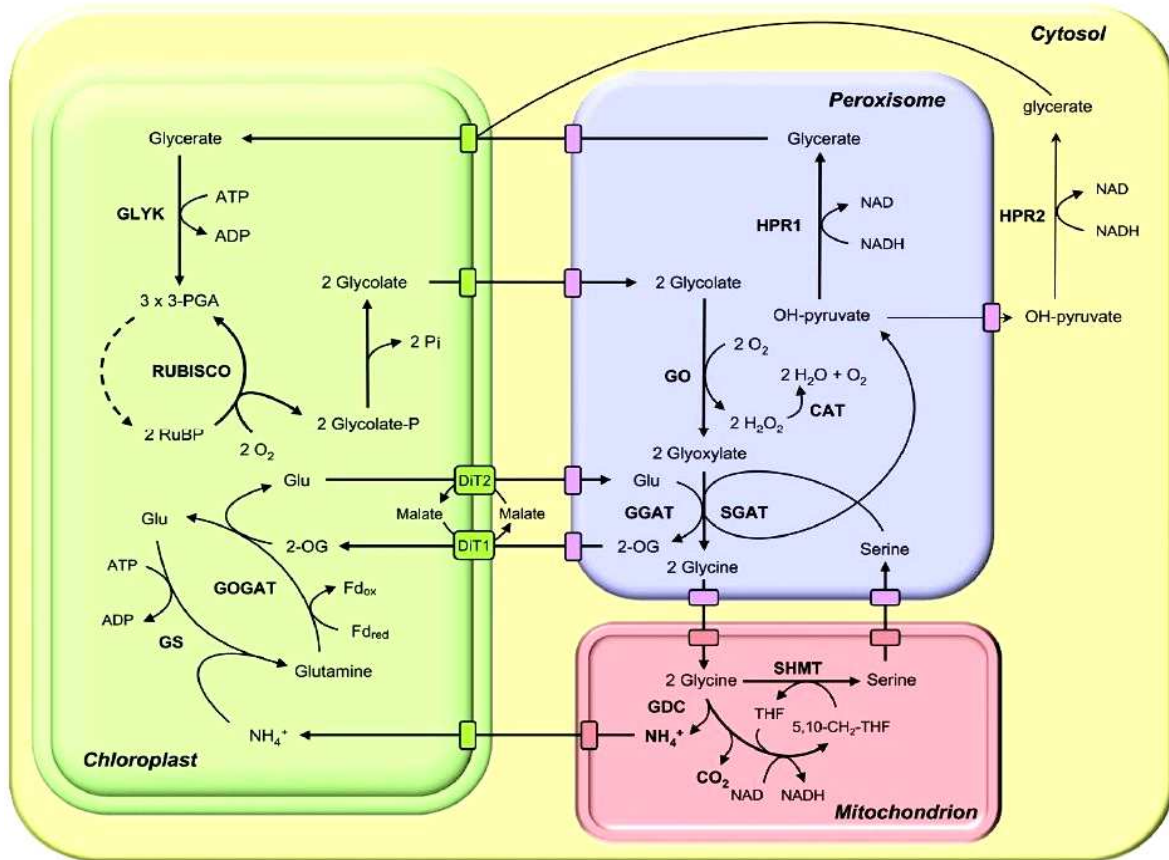
Figure 4. The major photorespiratory pathway. DiT1 and DiT2: dicarboxylate transporter 1 and 2; CAT: catalase; GDC: glycine decarboxylase; GGAT: glutamate:glyoxylate aminotransferase; GLYK: glycerate kinase; GO: glycolate oxidase; GOGAT: glutamate:oxoglutarate aminotransferase; GS: glutamine synthetase; HPR1: peroxisomal hydroxypyruvate reductase; HPR2: cytosolic hydroxypyruvate reductase; PGP: phosphoglycolate phosphatase; Rubisco: ribulose-1,5-bisphosphate carboxylase/oxygenase; RubP: ribulose-1,5- bisphosphate; SGAT: serine-glutamate aminotransferase; SHMT: serine hydroxymethyl transferase; THF: tetrahydrofolate; 5,10-CH2- THF: 5,10- methylene-THF; and 3-PGA: 3-phosphoglycerate. The dashed line represents the reductive and regenerative phases of the Calvin Cycle. The figure was taken from (Maurino and Peterhansel, 2010).

1.4. Glycolate and glyoxylate metabolism in other organisms

Several heterotrophic bacteria have been reported to use glycolate as a carbon source for growth (Edenborn and Litchfield, 1985). Heterotrophic bacteria oxidize glycolate to glyoxylate by catalysis of glycolate oxidase (GlcDH, see 1.6). Glyoxylate is then metabolized through various mechanisms: the glycerate pathway via tartronic semialdehyde (Hansen and Hayashi, 1962), the ß-hydroxyaspartate pathway (Kornberg and Morris, 1965), and dicarboxylic acid pathway (Kornberg and Sadler, 1960). In the glycerate pathway, glyoxylate carboxylase catalyzes the formation of tartronic semialdehyde from two glyoxylate molecules and CO_2 molecule is

released. Afterwards, tartronic semialdehyde is reduced to glycerate by tartronic semialdehyde reductase. Finally, glycerate is phosphorylated to form phosphoglycerate by glycerate kinase (Kornberg and Sadler, 1961). In the ß-hydroxyaspartate pathway, oxaloacetate is produced as an end product of glyoxylate utilization. The erythro ß-hydroxyaspartate compound was reported as a key intermediate compound in glyoxylate metabolism through this pathway (Kornberg and Morris, 1965). Dicarboxylic acid pathway was also reported in bacteria for glyoxylate metabolism and producing formate as an end product by catalysis of malate synthase G (Kornberg and Sadler, 1960).

In cyanobacteria, glycolate is produced from the dephosphorylation of phosphoglycolate that is generated from the oxygenative activity of Rubisco as in higher plants (See 1.1). Studies on *Synechocystis sp* revealed the existence of three different routes for glyoxylate metabolism (Figure 5). Beside the bacterial glycerate pathway, all the enzymes in the C_2 cycle (See 1.3) in higher plant were determined. In addition, decarboxylation of glyoxylate via oxalate was also reported (Eisenhut et al., 2008).

In green algae, several studies revealed the existence of most C_2 cycle genes (Tural and Moroney, 2005). However, two different genes were identified for glycolate oxidation among green algae. The charophycean algae were found to possess microbodies similar to the leaf peroxisomal type containing an active GOX enzyme (Stabenau et al., 2003; Stabenau and Winkler, 2005). While in *Chlamydomonas* and several other chlorophyta glycolate is oxidized to glyoxylate by a mitochondrial glycolate dehydrogenase GlcDH (See 1.6) (Nakamura et al., 2005; Stabenau and Winkler, 2005).

8
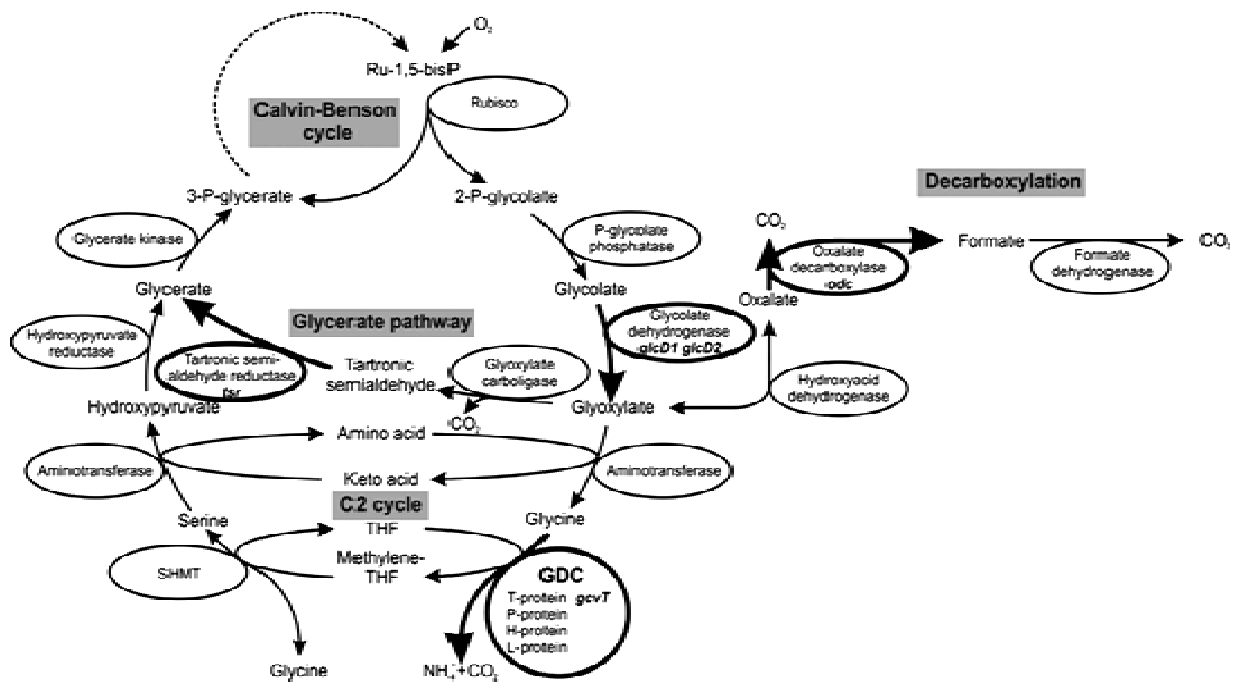
Figure 5. A scheme describing the different routes for PG metabolism in *Synechocystis sp*. The figure was taken from Eisenhut et al (2008).

1.5. Pros and Cons of photorespiration

Since its discovery in early 1960s by Krotkov (Hew and Krotkov, 1968), photorespiration in all oxygen (O_2) producing photosynthetic organisms remains controversial. Photorespiration undoubtedly represents a potential limitation on carbon gain in C_3 plants, and ultimately, crop yields. The oxygenation reactions catalyzed by Rubisco represent a wasteful process in plants because of its association with carbon and nitrogen loss (Ogren, 1984). During the oxygenation reaction, the RuBP the main precursor for CO_2 fixation is consumed and a toxic PG compound is produced. Recycling of the PG compound consumes ATP and reducing equivalents in the form of NAD/(P)H (Sage, 2004). The CO_2 release in the mitochondria during photorespiration results in 25% loss of the carbon from PG compound. Moreover, NH_3 is lost in this cycle that has to be refixed (Leegood et al., 1995).

Despite of the negative aspects mentioned above, the predominating view on photorespiration has completely changed since the pathway is recognized as an integral element of primary carbon metabolism that interacts with many other pathways (Maurino and Peterhansel, 2010). Moreover, photorespiration has been suggested to play an important role in maintaining the electron flow in the chloroplast. Photorespiration protects the stroma from its over reduction and

thus photoinhibition that might occur under stress conditions such as high-light, drought, salt-stress (Osmond et al., 1997; Wingler et al., 2000; Weise et al., 2006; Miller et al., 2010a)

1.6. Glycolate oxidizing enzymes

Glycolate oxidation to glyoxylate is an essential step in photorespiration in all photosynthetic organisms (Maurino and Peterhansel, 2010). In addition, glycolate can be used as a carbon source by various heterotrophic bacteria (Lau et al., 2007). Although the reaction is highly conserved, the different classes of organisms use different enzymes for glycolate oxidation.

As described previously (See 1.3), land plants and charophytes, their nearest sister group within green algae, use GOX for glycolate oxidation (Volokita et al., 1987; Stabenau et al., 2003; Hagemann et al., 2013). The GOX enzyme is a flavin mononucleotide (FMN) dependent enzyme that is using molecular oxygen as the terminal electron acceptor. This enzyme is using $_L$-lactate as an alternative substrate and cyanide inhibitors have no effect on its activity.

In *E. coli* and other prokaryotes, a completely unrelated enzyme named glycolate dehydrogenase (*Ec*GlcDH, EC 1.1.99.14) is used for glycolate oxidation. The enzyme is made up from three protein subunits encoded by the glcD, glcE, and glcF open reading frames of the glc operon (Sallal and Nimer, 1989; Pellicer, 1999). *Ec*GlcDH accepts $_D$-lactate, but not $_L$-lactate, as an alternative substrate and is highly sensitive to cyanide (Lord, 1972). In the photosynthetic cyanobacterium *Synechocystis*, two genes encoding homologues to glcD were identified, but homologues to glcE and glcF were not described so far (Eisenhut et al., 2008). Double knockout of the two glcD genes resulted in a disruption of photorespiration and a lethal phenotype that could only be rescued at high CO_2 concentrations (Eisenhut et al., 2008).

Furthermore, the chlorophyte green alga *Chlamydomonas reinhardtii* was reported to encode a protein (*Cr*GlcDH, gi|159474536) with homology to *Ec*GlcDH. A *Chlamydomonas* mutant in this gene was reported to require enriched CO_2 environment for growth (Nakamura et al., 2005) suggesting that photorespiration was disrupted in this mutant similar to what has been observed in cyanobacteria. Molecular characterization of *Cr*GlcDH was reported by Nakamura et al (2005). Interestingly, the amino acids sequence of *Cr*GlcDH has high homology to glcD in the N-terminal and to glcF in the C-terminal part of the protein sequence. This suggested that two of the three subunits of *Ec*GlcDH were merged in this enzyme (Nakamura et al., 2005).

1.7. Synthetic pathways to reduce photorespiratory losses

Considerable effort has been invested over the past decades to reduce photorespiratory losses either through attempts to modify Rubisco specificity (CO_2/O_2) or through modifying photorespiratory metabolism (Spreitzer and Salvucci, 2002; Kebeish et al., 2007; Andersson, 2008; Carvalho et al., 2011; Maier et al., 2012). In theory, disruption of the photorespiratory pathway should enhance CO_2 fixation and consequently growth. However, knockout mutants of several photorespiratory genes resulted in strongly retarded growth revealing its importance (See 1.3). Three different approaches were suggested by genetic engineering for modifying the photorespiratory pathway (Kebeish et al., 2007; Carvalho et al., 2011; Maier et al., 2012).

Kebeish et al (2007) proposed the installation of a bypass (Bypass1, Figure 6) of 5 different bacterial proteins targeted to the chloroplast of Arabidopsis plants in order to reduce photorespiratory losses. Bypass1 starts with glycolate and ends with glycerate. Glycolate is oxidized by the three subunits glycolate dehydrogenase enzyme from *E.coli* (*Ec*GlcDH) (See 1.6). Afterwards, two glyoxylate molecules (C_2 compound) are merged to form tartronic semialdehyde (C_3 compound) by catalysis of the bacterial glyoxylate carboligase enzyme (GCL) and CO_2 is released. Finally, tartronic semialdehyde is reduced to glycerate by tartronic semialdehyde reductase (TSR). Bypass1 pathway differs from the original photorespiratory pathway in shifting CO_2 release into the vicinity of Rubisco in the chloroplast. This might result in increasing the CO_2/O_2 ratio, and as a consequence should decrease oxygenation of RuBP. Furthermore, ammonia release is avoided that maintains the energy required for refixation.

Figure 6. Scheme of the original photorespiration pathway (black) and the three bypasses for the reduction of photorespiratory losses (red, numbers in boxes). The arrows indicate enzymatic reactions or transport steps. Enzymatic reactions (numbers in circles) are explained in table 1. The stoichiometry of the reactions is not included. 3-PGA, 3- phosphoglycerate. The scheme is deduced from Peterhansel et al (2013).

Table 1. Comparison of the enzymatic reactions of photorespiration and the three bypasses.

	Reaction	**Photorespiration**	**Bypass 1**	**Bypass 2**	**Bypass 3**
1	Phosphoglycolate-dephosphorylation	PGLP	PGLP	PGLP	PGLP
2a	Glycolate-oxidation	GOX	GlcDH	GOX	GOX
2b	H_2O_2 -detoxification	CAT	-	CAT	CAT
3	Transamination	GGAT	-	-	-
4a	Decarboxylation	GDC, SHMT	GCL	GCL	ME, PDH
4b	NH3-release	GDC, SHMT	-	-	-
5	Transamination	SGAT	-	-	-
6	Reduction	HPR	TSR	HPR	-
7	Glycerate-phosphorylation	GK	GK	GK	-
8	Other				MS

PGLP, phosphoglycolate phosphatase; GOX, glycolate oxidase; GlcDH, glycolate dehydrogenase; CAT, catalase; GGAT, glutamate:glyoxylate aminotransferase; GDC, glycine decarboxylase; SHMT, serine hydroxymethyltransferase; SGAT, serine:glyoxylate aminotransferase; HPR, hydroxypyruvate reductase; GK, glycerate kinase; GlycolateDH, glycolate dehydrogenase; GCL, glyoxylate carboxylyase; TSR, tartronic semialdehyde reductase; ME, malic enzyme; PDH, pyruvate dehydrogenase; HPI, hydoxypyruvate isomerase; MS, malate synthase.

Similar to bypass 1, bypass 2 starts with a photorespiratory intermediate and ends with another photorespiratory intermediate (Carvalho et al., 2011; Peterhansel et al., 2013). As well as bypass1, bypass 2 integrates bacterial proteins into plant metabolism to shorten the original photorespiratory pathway. However, these genes are targeted to the peroxisome. Bypass3 is unlike bypass1 and bypass2; its products are not reconnected to the major photorespiratory pathway (Fahnenstich et al., 2008; Maier et al., 2012). Glycolate oxidation is catalyzed by glycolate oxidase that was relocated from the peroxisome to the chloroplast. The H_2O_2 by-product generated during glycolate oxidation is detoxified by the relocated catalase enzyme in the chloroplast. Afterwards, glyoxylate is converted to malate by catalysis of malate synthase in the presence of acetyl-S-CoA. CO_2 release in the chloroplast is started by decarboxylation of malate to pyruvate by malic enzyme (ME). Finally, pyruvate is oxidized to CO_2 by pyruvate dehydrogenase (PDH), and acetyl-S-CoA is produced as a by-product.

1.8. Improvement of cyanide resistance by installing a novel detoxification pathway in *Arabidopsis thaliana*

The previous chapter described the photorespiration process that increased under various abiotic stresses and highlighted different strategies that attempt to manipulate this wasteful process. Another small compound that is generated in higher plants during abiotic stress is cyanide (Liang, 2003) that may cause severe toxicity to plants. Although cyanide is involved in several biochemical pathways, it could be highly toxic at higher concentrations (Yu et al., 2005). Generally, the endogenous cyanide produced under normal conditions is not harmful to plants as it usually found in concentrations under the metabolic capacity (Goudey et al., 1989; Manning, 1988). However, if the endogenous concentrations of cyanide exceed the metabolic capacity of plants, potential toxic effects could be induced that can lead to plant death. For example, treating of barnyard grass (*Echinochloa crus-galli*) with the herbicide quinolinecarboxylic acid (quinclorac) resulted in cyanide concentrations in the shoots by three times higher than the control plants. These levels caused severe symptoms to barnyard plants such as chlorosis, necrosis, loss in the fresh weight and reduction of the shoot growth (Siegień and Bogatek, 2006). The endogenous cyanide concentrations and thus the resulting symptoms were highly correlated with quinclorac concentrations (Siegień and Bogatek, 2006). Beside endogenous cyanide, plants are exposed to cyanide from various exogenous sources. Depending on cyanide concentration, it can function as a nitrogen source or a highly metabolic inhibitor to plants. For example, weeping willow trees (*Salix babylonica L*) grown in hydroponic solution containing low cyanide concentrations (KCN < or = 20µM) had no signs of toxicity, while at higher concentrations (KCN > or = 50µM) severe signs of toxicity were observed (Yu et al., 2005). Moreover, weeping willows grown in sandy soil irrigated with low doses of cyanide (KCN < or = 50µM) survived without any toxic effect the entire experiment time (nine days). However, higher doses of cyanide (KCN > or = 300µM) were lethal for weeping willows after nine days (Yu et al., 2005). In addition, cyanide application has been found to cause noticeable decrease of chlorophyll content in Arabidopsis plants when exposed to 50µM HCN (McMahon Smith and Arteca, 2000) and necrotic spots on tobacco leaves (Siefert et al., 1995). The toxic effect of cyanide is mostly associated with its ability to form metal complexes with several principle metalloenzymes such as cytochrome c oxidase , superoxide dismutase, peroxidase, catalase and Rubisco (Siegień and Bogatek, 2006).

1.9. Different sources of cyanide

Plants are exposed to cyanide from both natural and manufactured sources. Cyanide is produced naturally in plants as a by-product in the last step of ethylene biosynthesis during several plant growth stages such as germination, root-hair initiation, senescence and abscission, fruit ripening, and the response to various stresses (Goudey et al., 1989). Moreover, several plants have the ability to produce and store cyanide as cyanogenic glycosides including the plant families Rosaceae, Fabaceae, Limaceae, and Compositae (Poulton, 1988). Decomposition of cyanogenic plants might affect other plants in the neighborhood. Furthermore, plants might be influenced by cyanogenic bacteria that colonize the rhizosphere (Gallagher and Manoil, 2001). It has been reported that cyanide concentrations were higher as 100mg kg dw^{-1} in the rhizosphere of some plants colonized by cyanogenic bacteria (Owen and Zdor, 2001).

The major cyanide waste in the environment is coming from human activities. Cyanide is extensively used by industries such as plastics industries, organic chemicals production, photographic development, pharmaceuticals, electroplating, and metal finishing (Patil and Paknikar, 2000). A great amount of cyanide is used in gold and silver mining as a lixiviation to leach these precious metals from the ores. More than 90% of gold extraction is done by cyanidation (Trapp et al., 2003). Cyanide concentrations in soils near the industries that release cyanide can exceed 1000mg kg dw^{-1}, while in wastewater it may be an order of magnitude higher (Henny et al., 1994).

1.10. Bioremediation of cyanide

The widespread usage of cyanide for gold and silver extraction and many other industries imposes a serious ecological risk for ecosystems and mankind. Several disasters associated with cyanide waste have occurred worldwide such as release of methyl isocyanate in the Union Carbide Manufactory in Bhopal December 1984 (Sriramachari and Chandra, 1997), spilling of cyanide at Baia Mare, Romania 2000 (Korte et al., 2000), spilling of cyanide from the Ashanti gold fields in Ghana, and several accidents in China were reported (Yu et al., 2004). Although such accident is rare, it highlights the importance of detoxifying and cleaning cyanide waste. Several studies reported the capability of various micro-organisms including bacteria, fungi and algae to detoxify cyanide pollutant in wastewater of gold and silver mining industry (Naveen et al., 2011). Moreover, all the investigated higher plants including both cyanogenic and non

cyanogenic plants were found to possess one or more enzymes that assimilate cyanide (Miller and Conn, 1980). The uptake, and metabolism of cyanide by higher plants has been investigated (Ebbs et al., 2003; Larsen et al., 2005). However, tolerance and assimilation of higher plants to cyanide is highly depending on its metabolic capacity as described previously (See 1.9). Although, several chemical and physical methods have been established for cyanide detoxification, these methods tend to be complex and expensive processes (Akcil, 2003). Biological degradation of cyanide can be an alternative solution (Akcil and Mudder, 2003). Introducing novel genes into plant genome by genetic engineering techniques may enhance its degradation capacity to cyanide. Consequently, the transgenic approaches can provide an efficient, cheap and environment-friendly method for cyanide degradation.

There are several enzymes have already been reported to detoxify cyanide from various organisms including all phyla. For instance, ß-cyanoalanine synthase enzyme that is localized in the mitochondria of higher plants and is believed to have a principle role in detoxifying the endogenous cyanide (Yu et al., 2012). The enzyme catalyzes the substitution of a thiol in cysteine with cyanide producing ß-cyanoalanine that is then converted to asparagines by nitrile hydratase. Radioactive studies revealed the principle role of ß-cyanoalanine synthase in incorporating the exogenous cyanide into the amino acids pools in higher plants (Peiser et al., 1984). The reaction is shown in equation 1.

$$HCN + cysteine \longrightarrow \beta\text{- cyanoalanine} + acetate \qquad (1)$$
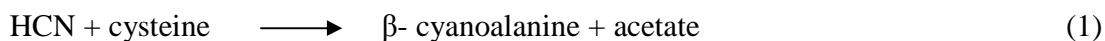
In bacteria, another type of enzymes was reported for cyanide detoxification known as cyanidases (Ingvorsen et al., 1991; Jandhyala et al., 2003). Cyanidases catalyze conversion of cyanide directly to formate and ammonia. The reaction is shown in equation 2.

$$HCN + 2H_2O \longrightarrow HCO_2H + NH_3 \qquad (2)$$
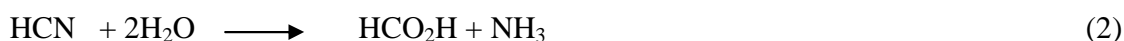
1.11. The aim of the present study

In the framework of this study, there were two main goals: the first main goal was the biochemical characterization of a putative glycolate dehydrogenase enzyme from *Chlamydomonas reinhardtii* (*Cr*GlcDH). Moreover, in order to better understand the importance of the Fe-S conserved domain for the activity of *Cr*GlcDH enzyme, different mutations were performed. Furthermore, the evolution of *Cr*GlcDH enzyme was explored *in silico* through analysis of the phylogenetic relationships, and studying the enzymatic properties of one of the nearest homologous sequences. These analyses should provide a basis for the optimization of the photorespiratory bypass reported by Kebeish et al (2007). Such approaches should reduce abiotic stress in higher plants.

The second main goal was to establish a novel method for bioremediation of cyanide toxicity using transgenic *Arabidopsis thaliana* as a model plant. Two functional transgenes (a cyanidase gene originated from bacteria and a formate dehydrogenase gene from *Arabidopsis thaliana*) were characterized and cloned into plant expression vectors. Afterwards, the two transgenes were transferred to the nuclear genome of wild type *Arabidopsis thaliana* plants through *Agrobacterium* mediated genetic transformation. Under cyanide stress, the combination of both transgenes should result in enhanced levels of CO_2 and ammonia that will be fixed by the chloroplastic enzymes and integrated in the basal plant metabolism as a source for carbon and nitrogen, respectively. This approach should also result in a reduction of photorespiration. Molecular, physiological, and biochemical studies were performed in order to ensure the success of implementing the method proposed in this study.

2. Materials and methods

2.1. Materials

2.1.1. Plant materials

Arabidopsis thaliana ecotype Columbia plants were used to generate stable expression lines of cyanidase and formate dehydrogenase.

2.1.2. Bacterial strains

Table 2. Bacterial strains used throughout this study.

Bacterial Strain	Features	Antibiotic resistance	Purpose
DH5α	It has recA1 and endA1 mutations that increase insert stability and improve the quality of plasmid DNA prepared from minipreps.		Plasmid - miniprep
XL1-Blue	This strain has recA1 and endA1 mutations which greatly improves the quality of miniprep DNA. The hsdR mutation prevents the cleavage of cloned DNA by the EcoK endonuclease system. The lacIqZΔM15 gene on the F′ episome allows blue-white screening for recombinant plasmids.	Tetracycline (12.5µg/ml)	Plasmid – miniprep
BL21(DE3)	DE3 lysogen contains T7 polymerase suitable for IPTG induction. This strain is deficient of lon and omp-t proteases and is therefore suitable for expression of non-toxic genes.		Protein expression
BL21 codon Plus	BL21 codon plus strain is recommended for expressing heterologous protein with codon bias. This strain possesses extra copies of the argU, ileY, and leuW tRNA genes. The tRNAs encoded by these genes recognize the AGA/AGG (arginine), AUA (isoleucine), and CUA (leucine) codons, Respectively.	Tetracycline (12.5ug/ml) Chloramphenicol (34ug/ml)	Protein expression
C41(DE3)	This strain is effective in expressing toxic and membrane proteins. It was derived from BL21 (DE3), and has at least one uncharacterized mutation that prevents cell death associated		Protein expression

	with expression of many toxic recombinant proteins.		
C43(DE3)	Similar to C41 (DE3), this strain is recommended for expressing toxic and membrane proteins.		Protein expression
Rosetta gami-pLysS	Rosetta-gami strains are suitable for expression of eukaryotic proteins that contain codons rarely used in *E. coli*. These strains supply tRNAs for AGG, AGA, AUA, CUA, CCC, GGA on a compatible chloramphenicol resistant plasmid. In addition, this strain enhances the disulfide bond formation resulting from trxB/gor mutations.	Kanamycin (25ug/ml) Tetracycline (12.5ug/ml) Chloramphenicol (34ug/ml)	Protein expression
ER2566	*E. coli* B cells engineered to form proteins containing disulfide bonds in the cytoplasm. Suitable for T7 promoter driven protein expression.		Protein expression
Agrobacterium strain GV3101 (pMP90RK)	This *Agrobacterium* strain contains a Ti plasmid pMP90RK that represents one component of the binary vector system. This plasmid contains the *vir*-region as well as the genes for gentamycin and kanamycin resistances. This bacterial strain is used for delivering heterologous genes to tobacco and *Arabidopsis* plants.	Gentamycin (50μg/ml) Kanamycin (50μg/ml) Rifampicin. (50μg/ml).	Plant transformat-ion

2.1.3. Chemicals and consumables

The chemicals were purchased from the following companies: Amersham Phamarcia Biotech (Freiburg), AppliChem (Darmstadt), BioRad Laboratories GmbH (München), Boehringer Roche (Mannheim), Calbiochem (Bad Soden), Carl Roth GmbH (Karlsruhe), Gibco BRL (Eggenstein), Hartmann Analytic (Braunschweig), Invitek (Berlin), Invitrogen (Leck, Netherlands), KMF Laborchemie Handels GmbH (St. Augustin), Kodak (Stuttgart), Life Technologies (Carlsbad, United states of America), Merck (Darmstadt), Metabion (Martinsried), Molbiol (Hamburg), New England Biolabs (Frankfurt), Peglab (Erlangen), Phamarcia (Freiburg), Promega (Madison, United States of America), Thermo Scientific Fermentas (St.- Leon-Rot), QIAGEN (Hilden), Roche Diagnostic GmbH (Mannheim), Serva (Heidelberg), Sigma-Aldrich (Taufkirchen), VWR (Darmstadt),Worthington (Lakewood, New Jersey, United States of America).

The consumables were obtained from: Applied Biosystems (Darmstadt), Beckman Coulter (Fullerton, United States of America), Biometra (Göttingen), BioRas Laboratories GmbH (München), Eppendorf (Hamburg), Fuji (Düsseldorf), Gibco BRL (Eggenstein), Greiner (Solingen), Hanna Instruments (Kehl), Heraeus (Osterode), Herolab (Wiesloch), Hettich Zentrifugen (Tuttlingen), Kodak (Stuttgart), Labomedic (Bonn), LI-COR® Biosciences (Lincoln, United States of America), Merck (Darmstadt), Millipore (Eschborn), MWG Biotech (München), Phamarcia (Freiburg), Raytest (Berlin), Serva (Heidelberg), Schott Glaswerke (Mainz), Sorvall (Bad Homburg), Wissenschaftliche Technische Werkstätten (Weilheim), Whatman (Maidstone, Kingdom of Great Britain), Zinsser Analytic (Frankfurt).

2.1.4. Instruments and equipment

Table 3. Instruments and equipment used in this study.

Instruments/Equipment	Company
Centrifuges and rotors	
5415R CI 023 (F45-24-11)	Eppendorf (Hamburg)
Optima L-100XP	Beckman - Coulter (Fullerton, USA)
Rotor SW 41 Ti	Beckman - Coulter (Fullerton, USA)
Sorvall RC 5 B Plus	Sorvall (Bad Homburg)
SpeedVac Savant	Thermo Scientific (Waltham, USA)
Electroporation	
Gene Pulser^{TM}	BioRad Laboratories GmbH (München)
Electrophoresis	
Acrylamide gel equipment	BioRad Laboratories GmbH (München)
Agarose gel equipment	Biozym Scientific GmbH (Hessisch Oldendorf)
ELISA-reader	
Incubators and climate cabinets	
MobyLux Gro Banks	CLF plantclimatic (Wertingen)
Minitron	Infors-HAT (Bottmingen)
Percival	
Photographic apparatus	
Intas GDS	Intas (Göttingen)
Photometer	
Genesys 10 UV scanning	Thermo Electron Corporation (Waltham, USA)
UV cuvette	Sarstedt (Nümbrecht)
One time cuvette	Sarstedt (Nümbrecht)
Real time PCR system	
ABI Prism 7300	Applied Biosystems (Darmstadt)
ABI Prism 7300 SDS software	Applied Biosystems (Darmstadt)

Thermocycler	
Vapo protect Mastercycler Pro	Eppendorf (Hamburg)

2.1.5. Specific chemicals

Table 4. Specific chemicals used throughout this study.

Specific chemicals	Company
Antibiotics	
Ampicillin	AppliChem (Darmstadt)
Carbenicillin	Duchefa (St. Louis, USA)
Chloramphenicol	Duchefa (St. Louis, USA)
Kanamycin	Duchefa (St. Louis, USA)
Rifampicin	Duchefa (St. Louis, USA)
Tetracycline	Duchefa (St. Louis, USA)
cDNA synthesis/PCR dNTPs	Thermo Scientific Fermentas
KCN	Sigma-Aldrich (Taufkrichen)

2.1.6. Markers

Table 5. DNA and protein markers used throughout this study.

Marker	Company
GeneRuler 1kb DNA Ladder	Thermo Scientific Fermentas
GeneRuler 50bb DNA Ladder	Thermo Scientific Fermentas
pageRuler plus protein Ladder	Thermo Scientific Fermentas
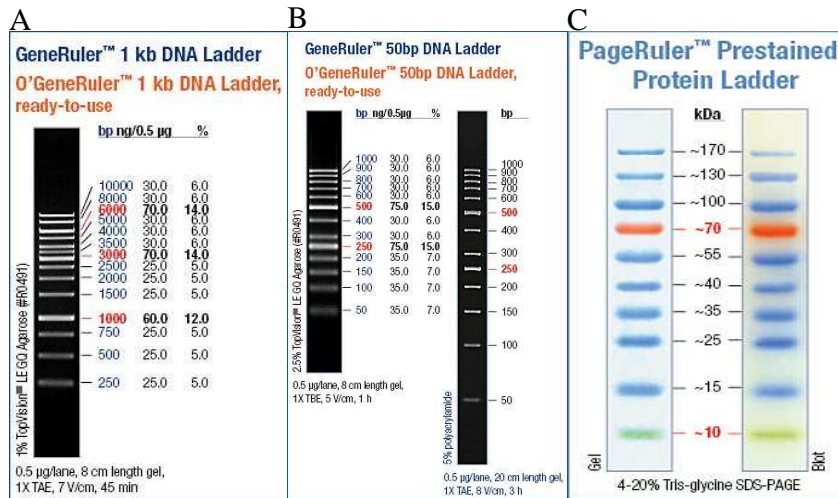
Figure 7. Markers used throughout this work for gel-electrophoresis. (a) GeneRuler™ 1kb DNA Ladder (b) GeneRuler™ 50bp DNA Ladder, (c) PageRuler plus protein Ladder.

2.1.7. Reaction kits

Table 6. Reaction kits used throughout this study.

Reaction kit	Company
Extraction of DNA from agarose gel slices Invisorb® spin DNA extraction kit	Invitek (Berlin)
Purification of PCR and restriction products MSB spin PCRapace	Invitek (Berlin)
Plasmid preparation kit GeneJet plasmid miniprep kit	Thermo Scientific Fermentas
qPCR Platinum® SYBR® Green qPCR SuperMix-UDG with Rox	Life Technologies (Carlsbad, USA)
Protein extraction from *E.coli* strains Bugbuster master mix	Novagen (Germany)

2.1.8. Enzymes

Table 7. List of enzymes used throughout this study.

Enzyme	Company
cDNA synthesis *Moloney Murine Leukemia virus reverse transcriptase (M-MLV-RT)*	*Thermo Scientific Fermentas*
DNA digestion *DNAse I*	*Thermo Scientific Fermentas*
Ligation *T4 DNA ligase*	*Thermo Scientific Fermentas*
PCR amplification *Dream TaqTM polymerase* *Phusion® hot Start II*	*Thermo Scientific Fermentas* *Thermo Scientific Fermentas*
Restriction enzymes *XhoI* *NcoI* *XbaI* *BamHI* *HindIII* *EcoRI* *NotI* *PstI* *SalI*	*Thermo Scientific Fermentas* *Thermo Scientific Fermentas* *Thermo Scientific Fermentas* *Thermo Scientific Fermentas* *Thermo Scientific Fermentas* *Thermo Scientific Fermentas* *Thermo Scientific Fermentas* *Thermo Scientific Fermentas* *Thermo Scientific Fermentas*

2.1.9. Oligonucleotides

Table 8. Different synthetic oligonucleotides used throughout this study.

Primer	Sequence (5´-> 3´)	Purpose
1. *Cr*GlcDH fw1	TAGGTACCATGGGCGCGAGAGGT	Cloning of *Cr*GlcDH into pET22
2. *Cr*GlcDH rev1	GTG CTA GCT CAA GCC GTC TTA GCT	Cloning of *Cr*GlcDH into pET22
3. *Cr*GlcDH fw2	TAGAATTCGGCGCGAGAGGT	Cloning of *Cr*GlcDH into pET41
4. *Cr*GlcDH rev2	ACGTCGACT CAA GCC GTC TTA	Cloning of *Cr*GlcDH into pET41
5. *Cr*GlcDH fw3	TAGTCGACGGCGCGAGAGGT	Cloning of *Cr*GlcDH into pMAL
6. *Cr*GlcDH rev3	ACG AAT TCT CAA GCC GTC TTA GCT	Cloning of *Cr*GlcDH into pMAL
7. *Cr*GlcDH fw4	TAGTCGACGTTGCGCAAGTTGC	Cloning of truncated *Cr*GlcDH
8. *Cr*GlcDH fw5	CAGAAGTATCGAGAGCGGATT-CAGCGAGTCTAACAGTCCATCA	Cloning of *Cr*GlcDH mut1 into pET22
9. *Cr*GlcDH rev5	TGATGGACTGTTAGACTCGCT-GAATCCGCTCTCGATACTTCTG	Cloning of *Cr*GlcDH mut1 into pET22
10. *Cr*GlcDH fw6	CTA GCG CAG CTG ATG GAA TGA -GCC AAG AGA AGA GTC CA	Cloning of *Cr*GlcDH mut2 into pET22
11. *Cr*GlcDHrev6	TGGACTCTTCTCTTGGCTC-ATTCCATCAGCTGCGCTAG	Cloning of *Cr*GlcDH mut2 into pET22
12. *Cr*GlcDH fw7	GCTTATGTGGGAGCTAAAGG	*Cr*GlcDH mut. sequencing
13. *Cr*GlcDHrev7	GCATAGCGTTGACGATGTTC	*Cr*GlcDH mut. sequencing
14. *Dv*GlcDH fw1	ATT AGG ATC CAT GCT CCC CGCCGC	Cloning of *Dv*GlcDH
15. *Dv*GlcDHrev1	ATATCTCGAGCGCGGGCTTCG GCGT	Cloning of *Dv*GlcDH
16. *Dv*GlcDH fw2	AAATACCTGCTGCCGACCGCTGCTG	Sequencing of *Dv*GlcDH

17. *Dv*GlcDH rev2	ATCATTTCCACGGCGGACAC	Sequencing of *Dv*GlcDH
18. *Dv*GlcDH fw3	GTCCGCCGTGGAAATGATGG	Sequencing of *Dv*GlcDH
19. *Dv*GlcDH rev3	GCGCAGTTCCTTGATGAACG	Sequencing of *Dv*GlcDH
20. *Dv*GlcDH fw4	TCAACACCGGCGCGTTCATC	Sequencing of *Dv*GlcDH
21. *Dv*GlcDH rev4	GTTAGCAGCCGGATCTCAGTGGTGG	Sequencing of *Dv*GlcDH
22. T7-universe	AAT TAA TAC GAC TCA CTA TAG GG	pET sequencing
23. T7-reverse	GCT AGT TAT TGC TCA GCG G	pET sequencing
24 Actin Fw	GGT AAC ATT GTG CTC AGT GGTGG	*A. thaliana* Actin gene
25. Actin Rev	GGT GCA ACG ACC TTA ATC TTCAT	*A. thaliana* Actin gene
26. pS5'	GAC CCT TCC TCT ATA TAA GG	pTRA-K sequencing
27. pS3'	CAT GAG CGA AAC CCT ATA AGA CC	pTRA-K sequencing
28. 3'g7-Rev	ATA TCA GCT GGT ACA TTG CCGTAG	pTRA-K sequencing
29. pS3'-2	CAC ACA TTA TTC TGG AGA AA	pTRA-K sequencing
30. FDH-fw1	GCT GTT GTT GAT GCT GTT GAA	qPCR of FDH gene
31. FDH-rev1	AAC AGT CAA TCC AGC AGC AG	qPCR of FDH gene
32. FDH-fw2	GGC TAT GAC TCC TCA TACT TCT GG	qPCR of FDH gene
33. FDH-rev2	TCC TTA GGA GCT GGT TGT GG	qPCR of FDH gene
34. FDH-rev3	TGT TGG GAA ATC TTC ACC CT	qPCR of FDH gene
35. CYND-fw1	CGC CGA AAT TGA TAT TGA GAA	qPCR of CYND enzyme
36. CYND-rev1	GGG ATA ACC CGG AAT GAA TG	qPCR of CYND enzyme
37. CYND -fw2	GCC TAA CCC AGT TGT CAG AAA	qPCR of CYND enzyme
38. CYND -rev2	CTG AGT CTC ACA GAG CAT ATC T	qPCR of CYND enzyme
39.CYND -Rev3	ACA ACT GGG TTA GGC GAT TG	qPCR of CYND enzyme
40. CYND-rev4	GCA AGG AAC GCA CTA CTG G	qPCR of CYND enzyme
41. Random nanomer	NNNNNNNNN	[d(N)9] 1st strand synthesis

2.1.10. Solutions, buffers and media

Table 9. List of buffers and media used during the present work.

Name	Component	Concentration
1. Acrylamide/bis-acrylamide	Acrylamide	30% (w/v)
	N',N'– Methylen bisacrylamide	0.8% (w/v)
2. Ammonium per sulphate (APS)		10% (w/v)
3. Anti-His HRP conjugate blocking buffer	From Qiagen, Germany	
4. Bradford–solution	Coomassie brilliant blue G 250	100mg/L
	Ethanol 96 % (v/v)	50ml/L
	Phosphoric acid 85 % (v/v)	100ml/L
5. Coomassie-fixation solution	Methanol	30% (v/v)
	Acetic acid	10% (v/v)
6. Coomassie-staining solution	Coomassie-brilliant-blue (Serva-blue R250, Fa. Serva)	0.5% (w/v)
	Methanol	80% (v/v)
	Acetic acid	20% (v/v)
7. dNTP–mix	dATP	2.0mM
	dCTP	2.0mM
	dGTP	2.0mM
	dTTP	2.0mM
8. Electrophoresis buffer 5x	Glycine	1.92M
	Tris base	500mM
	SDS	0.5 %(w/v)
	pH should be 8.8 without adjusting	
9. Grinding buffer (GB)	HEPES-KOH pH 8.0	50mM
	EDTA	10mM
	Sorbitol	0.33M
	BSA	0.5g/l
	Ascorbate	5mM
10. HEPES buffer I	HEPES –KOH pH 7.5	1mM
11. HEPES buffer II	HEPES–KOH pH 7.5	1mM
	Glycerol	10% (v/v)

12. Induction medium	YEB medium	
	MES pH 5.6	10mM
	Acetosyringone	20µM
13. Laemmli-loading buffer 5x	Tris–HCl, pH 6.8	225mM
	SDS	5%(w/v)
	Glycerol	50%(w/v)
	Bromophenol blue	0.05 %(w/v)
	DTT	225mM
14. LB–ampicillin	LB–medium	
	Ampicillin	100µg/ml
15. LB–amp–plate	Bactotrypton	10g/L
	Yeast extract	5g/L
	NaCl	10g/L
	Agar	15g/L
	Ampicillin	100µg/ml
16. LB–medium	Bactotrypton	10g/L
	Yeast extract	5g/L
	NaCl	10g/L
17. Ligase–buffer	Tris–HCl, pH 7.8	40mM
	$MgCl_2$	10mM
	DTT	10mM
	ATP	0.5mM
	PEG 8000	5%(w/v)
18. MS medium	Murashige and Skoog basal medium	
19. MS + Kanamycin plates (for Arabidopsis)	MS salt	2.2g/L
	Agar	0.7% (w/v)
	Kanamycin	20mg /ml
20. Orange G loading dye (6x)	Glycerin (99.8%)	60%
	EDTA pH 8.0 (0,5 M)	60mM
	Tris/HCl pH 7.6 (1M)	10mM
	Orange G	0.03% (w/v)
	H_2O	Ad to 500ml
21. PCR–buffer (10x)	Tris–HCl pH 8.5	100mM
	KCl	500mM
	Tween 20	0.5% (v/v)

22. Ponceau S–Red–solution	Ponceau S–Red	0.25% (w/v)
	Acetic acid	1% (v/v)
23. Protein elution buffer	Na-phosphate pH 8.0	50mM
	NaCl	300mM
	Imidazol	250mM
24. Protein extraction buffer from plant materials	Protein resuspension buffer	
	Ascorbate	0.5 % (w/v)
	DTT	5mM
	Polyclar	2% (w/v)
25. Protein resuspension buffer	HEPES–KOH pH 7.5	50mM
	$MgCl_2$	5mM
	EDTA	1mM
26. Protein wash buffer I	Na-phosphate buffer pH 8.0	100mM
	NaCl	300mM
	Imidazol	10mM
	Triton x 100	0.1%
27. TAE (1x)	Tris–acetate, pH 8.0	40mM
	EDTA, pH 8,0	1mM
28. TBS buffer	Tris-HCL (pH 7.5)	10mM
	NaCl	150mM
29. TBS-Tween –Triton buffer	Tris-HCl (pH 7.5)	20mM
	NaCl	500mM
	Tween 20	0.05% (v/v)
	Triton X-100	0.2% (v/v)
30. TE (1x)	Tris–HCl, pH 8.0	10mM
	EDTA, pH 8.0	1mM
31. TFB I (pH 5.8)	K–acetate	30mM
	$MnCl_2$	50mM
	RbCl	100mM
	$CaCl_2$	10mM
	Glycerin	15% (v/v)
32. TFB II (pH 6.8)	RbCl	10mM
	$CaCl_2$	75mM
	MOPS	10mM
	Glycerin	15% (v/v)

33. Tank-blotting transfer buffer (1x)	Tris base	25mM
	Glycine	150mM
	Methanol	20% (v/v)
	pH should be 8.3 without adjusting	
34. YEB medium	Nutrient broth or beef extract	5g/L
	Yeast extract	1g/L
	Peptone	5g/L
	Sucrose	5g/L
	$MgSO_4$	2mM
	pH	7.4

2.1.11. Matrix and membranes

- Hybond^{TM}-ECL^{TM}-nitrocellulose membrane (0.45 μm) from Amersham Pharmacia biotech (Braunschweig).

- Whatman no.1 paper from Whatman.

2.1.12. Plasmids

Table 10. List of plasmids generated in course of this study.

No.	Construct name	Usage
1	pTRA-K-TL- ctp-CYND-His	Chloroplastic expression of cyanidase (CYND) enzyme.
2	pTRA-K-TL-FDH	Cytosolic expression of formate dehydrogenase (FDH) enzyme.
3	pTRA-K-ctp-FDH-CYND-His	Chloroplastic expression of both FDH and CYND genes enzyme.
4	pET22-*Cr*GlcDH-His	Bacterial expression of *Cr*GlcDH enzyme.
5	pET22-mut1-*Cr*GlcDH-His	Bacterial expression of mutant1 of *Cr*GlcDH enzyme.
6	pET22-mut2-*Cr*GlcDH-His	Bacterial expression of mutant2 of *Cr*GlcDH enzyme.
7	pET22-delta-*Cr*GlcDH-His	Bacterial expression of delta *Cr*GlcDH
8	pET22-*Dv*DLDH-His	Bacterial expression of *Dv*DLDH enzyme.
9	pET41- GST- *Cr*GlcDH-His	Bacterial expression of *Cr*GlcDH with GST fusion tag.
10	pMAL-*Cr*GlcDH	Bacterial expression of *Cr*GlcDH with maltose binding fusion tag.
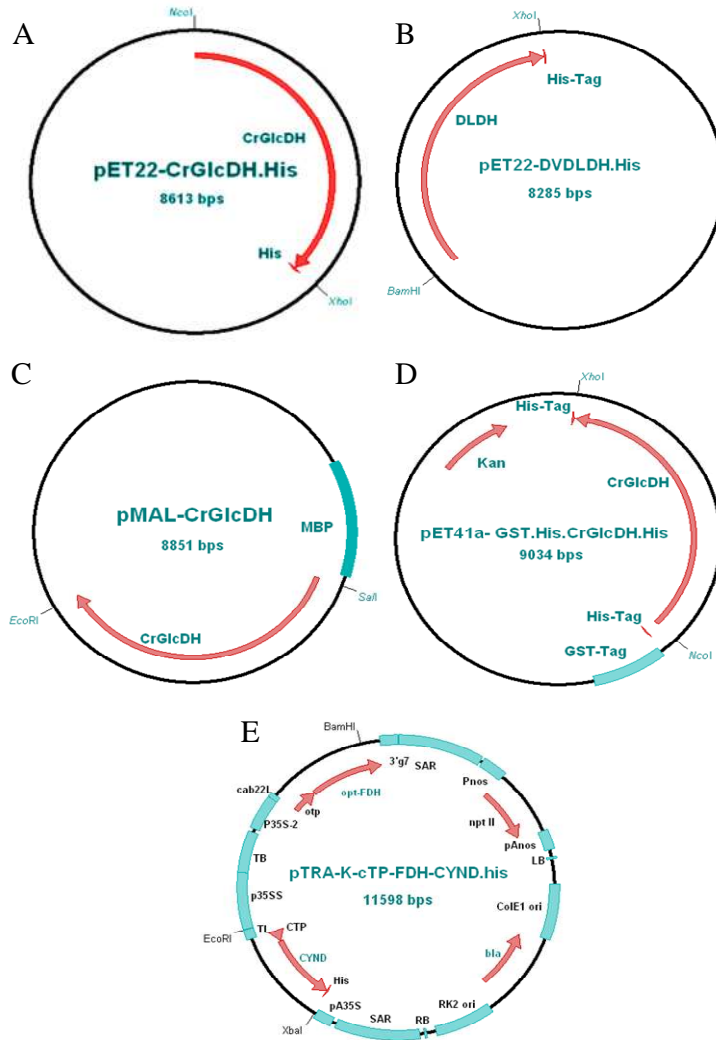
Figure 8. Structure of different plasmids constructed during this study. A, pET22-His plasmid that was used for expression of *Cr*GlcDH protein and its mutants with His-tag fusion at C-terminal. B, pET22-*Dv*DLDH-His plasmid was used for expressing of $_D$-Lactate dehydrogenase from *Desulfovibrio vulgaris* with His-tag fusion at C-terminal. C, pMAL-*Cr*GlcDH plasmid was used for expression of *Cr*GlcDH protein with maltose binding fusion tag. D, pET41-GST-His plasmid was used for expressing of *Cr*GlcDH with a glutathione-S-transferase fusion tag at N-terminal and His-tag at C-terminal. And E, pTRA-K-CTP-FDH-CYND-his plant expression vector, was used for expressing of cyanidase protein in the chloroplast of *Arabidopsis thaliana*.

2.1.13. Software and internet programs

Table 11: Software and internet-programs used throughout this study.

Software/internet-program	Characteristics
ABI Prism® 7300 SDS software 1.4	Software for enforcement and evaluation of ABI Prism® 7300 sequence detection system.
Clone manager professional 9	Nucleic acid sequence analysis.
Mega 5	MEGA software is an integrated tool for conducting sequence alignment, inferring phylogenetic trees, estimating divergence times (Tamura et al., 2011). http://www.megasoftware.net/.
Multiple sequence alignment by CLASTALW	Internet program for sequence alignment, http://www.genome.jp/tools/clustalw/.
National centre for biotechnology information (NCBI)	Internet database for sequencing, http://ncbi.nlm.nih.gov/.
Oligonucleotides properties calculator (OligoCalc)	Internet program for oligonucleotides analyses, http://www.basic.northwestern.edu/biotools/ oligocalc.html.
SeqLab	Internet program for sequencing, http://seqlab.de/

2.2. Methods

2.2.1. Molecular methods

2.2.1.1. DNA and RNA extraction (Combined method) from plant material

A frozen and well ground plant material was used for extraction of DNA and RNA in a combined method. 100mg ground plant material was mixed with 500µl DNA/RNA extraction buffer (Table 9). Afterwards, 1 volume of water saturated phenol was added and was mixed gently for 10 to 15min on a shaker followed by centrifugation at 16000xg for 10min. The upper phase was transferred to a new tube and 0.1 volumes of 3M NaAc (pH 5.2) and 2 volumes of ethanol (96%) were added and mixed well. The DNA and RNA were precipitated by centrifugation at 16000xg for 10min at 4°C. The aqueous phase was removed and the resulting pellet was washed by adding 300µl 70% ethanol. The mixture was centrifuged for 10min (16000xg, 4°C). Finally, the ethanol was completely removed, and the pellet was dissolved in 100µl sterile H_2O and stored at -20°C until used.

2.2.1.2. Polymerase chain reaction

The Polymerase chain reaction (PCR) is a powerful amplification technique that can generate a huge amount of a specific segment of DNA (Saiki *et al.*, 1988). Two synthetic oligonucleotides with known sequences designated as primers (a forward and a reverse primer) are required to initialize the amplification process. The target is flanked by the primers, which are complementary two the (+) and (-) strands of the DNA. The new strands are synthesized between the two primers by catalysis of *Taq* DNA polymerase enzyme. Amplification of the DNA fragment is performed by repeating the reaction several cycles. Each cycle contains three main stages: the denaturation, the annealing, and the extension (Lorenz, 2012). Repeating the cycles of denaturation, primer annealing and extension results in an exponential accumulation of the target DNA fragment. See below the reaction composition and conditions used in this study (Table 12&13).

2.2.1.3. Multiplex PCR

With help of this technique, it is possible to amplify more than one DNA fragment using more than one primer pair in the same PCR reaction mixture (Table 12). In this study this method was used to amplify the actin2 (Plant control) together with the different transgenic constructs. The standard multiplex PCR conditions were used for fragment amplification (Table 13).

Table 12. PCR reaction mixture.

Reagent	Final concentration
Dream-*Taq* Buffer (10X)	1x
dNTP mix	200µM
Forward primer	0.2µM
Reverse primer	0.2µM
Taq polymerase	0.02µM
Template	1 – 2ng/µl
H$_2$O	Ad 25µl

Table 13. Standard PCR conditions.

Reaction step	Temperature	Duration	Cycle
Initial denaturation	94°C	5min	1x
Denaturation	94°C	30sec	
Annealing	50-60°C ??	30sec	35x
Elongation	72°C	2min ??	
Deactivation	72°C	5min	
Rest	16°C		

2.2.1.4. Purification of PCR products and digested DNA fragments

The MSB Spin PCRapace kit (Invitek, Berlin) was used to purify PCR products and the digested plasmids. The kit was used according to the manufacturer's instruction.

2.2.1.5. Isolation of plasmid DNA

Plasmid DNA mini kits (GeneJet Plasmid Miniprep Kit, Thermo Scientific Fermentas) was used to isolate plasmid DNA. The kit was used according to the manufacturer's instruction.

2.2.1.6. Agarose gel electrophoresis

Agarose gel electrophoresis method enables researchers to separate and visualize DNA fragments. DNA fragments are forced to migrate through an agarose matrix in response to an electric field. Agarose is a polysaccharide that produces cross-linked matrix during its polymerization with a particular size depending on agarose concentration. Therefore, small fragments run more quickly than the bigger fragments through the agarose matrix. All agarose gel electrophoreses for DNA separation was performed as previously published (Sambrook and Russell, 2001). Briefly, 0.8-2% (w/v) agarose was dissolved in 1x TAE buffer (Table 9) by heating in a microwave. Ethidium bromide was added to the melted agarose solution at a relationship of 1:20,000. In order to create pockets inside the gel, the solution was poured in a plastic template with a comb placed inside. After gel solidification, the comb was removed and the DNA samples, mixed with loading buffer, were loaded in the pockets. To enable subsequent size determination of the DNA fragments 5µl of the DNA ladder (Invitrogen) was also loaded. The DNA samples were run at 1.5 mA/cm^2 in 1x TAE buffer. Finally, the separated DNA fragments were visualized on a UV table.

2.2.1.7. Purification of DNA fragments from agarose gels

To purify DNA fragments (70bp - 10kb) from agarose gels, the Invisorb$^®$ Spin DNA Extraction Kit (Invitek, Berlin) was used according to the manufacturer's instruction.

2.2.1.8. Restriction enzyme digestion

Restriction reactions were performed as described in the manufacturer's instruction.

2.2.1.9. Ligation

Ligation of DNA is performed using DNA ligase enzyme (Thermo Scientific Fermentas, Germany). DNA ligases catalyze the formation of a phosphodiester bond between the 3' hydroxyl and 5' phosphate of adjacent DNA residues. The reaction was performed as described in the manufacturer's instruction, except the incubation step, which was performed over night at 16°C.

2.2.1.10. DNA Sequencing

DNA sequencing was performed by the Seqlab Company. For this purpose, approximately 600-700ng of the required plasmid was mixed with 20pmol of the used primers followed by adding water to a volume of 7µl.

2.2.1.11. cDNA synthesis from RNA

Complementary DNA (cDNA) is catalyzed by the reverse transcriptase enzyme. During this process, DNA is synthesized from the messenger RNA (mRNA). Briefly, the isolated DNA/RNAs samples (See 2.2.1.1) were digested by *DNAse* enzyme. The samples were incubated with *DNAse* enzyme for 30min at 37°C followed by additional 15min at 70°C. Afterwards, 1µl of the random primer (Table 8, primer no. 41) was added to the samples and incubated for 5min at 75°C followed with cooling on ice. Then, 7µl of the RT-reaction mix (Table 14) was added to each sample. The mixture was incubated for 1h at 37°C. Finally, the enzyme was inactivated by incubation at 70°C for 10min. As control, reaction mixtures without *DNAse* enzyme were used. The samples were diluted 1:4 and 1:16 with H_2O before cDNA synthesis. Finally, the resulting cDNA samples were diluted 1:2 and used as templates for gene expression analysis (qPCR).

Table 14. RT reaction mix.

Compound	End concentration
dNTP mix	20nmol
MMLV buffer	1 x
MMLV RT	200u
H2O	7µl

2.2.1.12. Quantitative RT-PCR

RNA was prepared from *Arabidopsis thaliana* leaves following the BCP (1-bromo-3-chloropropane) protocol (Chomczynski and Mackey 1995). Preparation of first strand cDNA was performed as described by Niessen et al. (2007). Quantitative PCRs were performed on an ABI PRISM 7300 Sequence Detection System (Applied Biosystems, Darmstadt, Germany) in the presence of SYBR Green following the manufacturer's instructions. Reaction mix was obtained from Invitrogen, Karlsruhe, Germany, and oligonucleotides were purchased from Metabion, Planegg, Germany. For the detection of FDH transcripts, primers 5'-GCT GTT GTT GAT GCT GTT GAA-3' and 5'-TCC TTA GGA GCT GGT TGT GG-3' were used. For the detection of CYND transcripts, primers 5'-GCC TAA CCC AGT TGT CAG AAA-3' and 5'-GCA AGG AAC GCA CTA CTG G-3' were used. For the detection of Actin*2* transcripts, primers 5'- GGT AAC ATT GTG CTC AGT GGT GG-3' and 5'-GGT GCA ACG ACC TTA ATC TTC AT-3' were used. The final primer concentration was 200nM in the reaction mixture. Amplification conditions were 10 min of initial denaturation at 95°C, followed by 40 cycles each of 15s denaturation at 95°C and 1min combined annealing and extension at 60°C.

2.2.1.13. Phylogenetic tree assembly

Amino acid sequences from bacteria, fungi, algae and plants were obtained from the NCBI databases using a combination of queries based on key terms and BlastP searches (Altschul *et al.*, 1997). Protein sequence alignments were performed with MEGA5.1 software (Tamura *et al.*, 2011). Phylogenetic analyses were inferred in MEGA5.1 using neighbor joining (NJ) method. The NJ tree was constructed from pairwise amino acid distances estimated using a Poisson correction and different rates among sites (gamma distributed). Bootstrap values (%) are for 500 replicates. Arabidopsis GOX was used as an outgroup.

2.2.2. Biochemical methods

2.2.2.1. Protein extraction from plant leaves

Frozen leaves were finely ground in liquid nitrogen. Approximately 150mg ground leaf material was placed in 1.5ml eppendorf tube and mixed with 700µl of protein extraction buffer (Table 9) followed by centrifugation (30000xg/15min/4°C). The supernatant was transferred into a new

1.5ml eppendorf tube and centrifuged once more to remove any remaining debris. Finally, the supernatant was transferred into clean eppendorf tube and placed in ice. Protein concentration was measured using Bradford solution.

2.2.2.2. Determination of protein concentrations

Proteins concentrations were determined according to the method described by (Bradford, 1976). From protein samples 2µl was mixed with 1ml of Bradford reagent (Table 9) and incubated for 5 min at room temperature (RT). The extinction at 595nm was measured against a reagent blank prepared from 2µl of the corresponding extraction buffer and 1ml of Bradford reagent. Different concentrations of bovine serum albumin protein (pH 7.0, Serva) were used to prepare a standard curve in a range between 1 and 20µg.

2.2.2.3. Expression and Purification of recombinant proteins

A single colony of *E. coli* strain harboring the gene of interest was inoculated in 5ml of LB medium containing the appropriate antibiotics and cultivated ON at 37°C. On the second day, the ON culture was transferred into 1000ml LB + antibiotics and left to grow until OD_{600nm} of 0.9. Protein expression was induced by addition of IPTG to a final concentration of 1mM for 2hr. The culture was centrifuged (4000xg/4°C/10min) and bacterial pellets were immediately frozen with liquid nitrogen and were kept in -80 freezer. The bugbuster master mix (Novagen) was used for protein extraction. The His-tagged recombinant protein was purified by Ni^{2+}-NTA resin (Qiagen). The purification was performed according to the manufacture's instruction with some modifications. The binding step was performed in batch using 15ml falcon tube for 1h at 4°C. Afterwards, the resin was carefully transferred into 1.5ml eppendorf

 tube. The non-specifically bound proteins were removed by washing with 5 resin volume of protein-wash-buffer. Finally, the recombinant protein was eluted using 3x 100µl of protein elution buffer. All the purification steps were performed at 4°C. The centrifugation steps were performed at 1000xg.

2.2.2.4. SDS-polyacrylamide gel electrophoresis

The size-dependent separation of denatured protein was performed according to (Laemmli, 1970). The polyacrylamide gels required for this purpose were cast in a mini gel system (The

Bio-Rad min protein II apparatus). After gel preparation, each protein sample was mixed with 5x SDS-PAGE-samples buffer (Table 9), boiled at 95°C for 5min, and spun down for 30sec. The boiled sample was then loaded into polyacrylamide gel (Ausubel et al., 2001). To be able to estimate the protein size, pre-stained molecular weight markers were used (Thermo Scientific Fermentas). 1x SDS-PAGE electrophoresis buffer (Table 9) was used for the electrophoresis that was performed for 120min at 120V/cm. Separated proteins were visualized by gel staining with Coomassie brilliant blue R250 (Table 9) or transferred onto a nitrocellulose membrane for western blotting analysis (Table 9).

2.2.2.5. Coomassie brilliant blue staining

Although, the presence of around 40 dyes called Coomassie[TM] xy, only Coomassie[TM] G250 and Coomassie[TM] R250 play a crucial role in biochemical analyses. Coomassie Brilliant Blue R-250 was first used to stain proteins in a polyacrylamide gel by (Meyer and Lamberts, 1965). Coomassie[TM] Brilliant Blue forms strong but non-covalent complexes with proteins, most probably based on a combination of van der Waals forces and electrostatic interactions. Formation of the protein/dye complex stabilizes the negatively charged anionic form of the dye producing the blue color in the gel.

The polyacrylamide gel containing the separated protein was placed carefully in coomassie dye solution (Table 9) and stained for 30min at RT while shaking gently. Non-specific background staining was removed using coomassie-destaining solution (Table 9) overnight at RT.

2.2.2.6. Western blot

Transfer of the electrophoretically separated proteins from polyacrylamide gels onto a Hybond[TM]-ECL[TM]-nitrocellulose membrane (0.45μm) was achieved using a tank-blotting transfer chamber (Biorad). The tank-blotting western blot was performed according to qiaexpress detection and assay handbook (Qiagen, Hilden, Germany). Briefly, a nitrocellulose membrane was cut according to the gel size and soaked in the tank-blotting transfer buffer for some minutes (Table 9). The gel was placed in between a sandwich-like structure of two filter papers and two fiber pads as shown in figure 9. The air bubbles between the gel and the membrane were carefully removed. The sandwich-like structure was hold with a plastic supporter. The tank was filled with transfer buffer and protein transfer was performed at 250mA for 1h. Afterwards, the

membrane was washed two times 10min each with TBS buffer (Table 9) at RT then incubated 1h in blocking buffer (Table 9) at 4°C. The blocked membrane was washed 2 times 10min each at RT with TBS-Tween/Triton buffer (Table 9) followed by two times with TBS buffer for 10min each then incubated in Anti-His HRP conjugate solution (Qiagen, Hilden, Germany) containing 1/2000-1/1000 dilution of antibody in blocking buffer (Qiagen, Hilden, Germany) at RT for 1h. Finally, the membrane was washed 2 times with TBS-Tween/Triton buffer (Table 9) followed by 2 times 10min each with TBS buffer (Table 9). The signals were visualized by adding lumi-light western blotting substrate (Lumi-light stable peroxide solution : lumi-light luminol/enhancer solution = 1:1 from Roche Diagnostics GmbH, Mannheim, Germany) to the membrane and incubated in dark for 5min then luminescence was recorded on a LAS3000 CCD camera (Raytest) according to the manufacturer's recommendations.
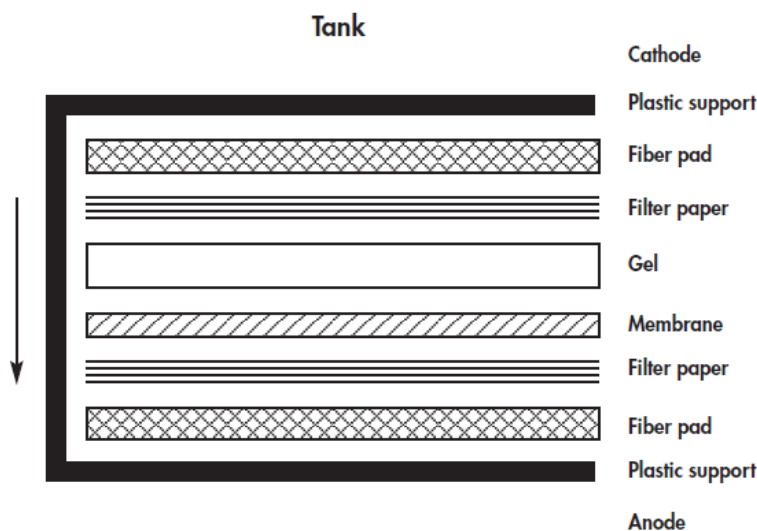

Figure 9. Schematic drawing of indicated tank- blotting methods. Arrow shows direction of the transfer (Qiagen Handbook).

2.2.2.7. Truncated protein version and site-directed mutagenesis

Oligonucleotides 5´-TAT GCC ATG GGC GCG AGA GGT CCT GCA TCT-3´ as forward primer and 5´- GAT GCT CGA GGA ACT TGA TGT GAG CGT CCT GAT CT-3´ as reverse primer were used to amplify a truncated version (660aa from the N-terminus) of *Cr*GlcDH. Site-directed mutagenesis was performed with the lightning quick-change site-directed mutagenesis kit (Agilent Technologies, Boeblingen, Germany) following the manufacturer's instructions to change cysteine 673, 676, 679 and 683 to serine. Synthetic oligonucleotide primers were 5′-

CAGATGTATCGAGAGCGGATTCAGCGAG-TCTAACAGTCCATCA-3′ for mut1 and 5′-CAGAAGTATCGAGAGCGGATTCAGCGAG-TCTAACAGTCCATCA-3′ for mut2. The reverse primer was 5′-TGATGGACTGTTAGA-CTCGCTGAATCCGCTCTCGATACTTCTG-3′. Constructs were amplified in *E. coli* XL10-Gold ultracompetent cells provided with the kit and screened using primers 5´-TAGCGCAGCTGATGGAATGAGCCAAGAGAAGAG TCCA-3´as forward primer and 5´-GACTCTTCTCTTGGCTCATTCCATCAGCTGCGCTAG-3´ as reverse primer. Positive constructs were sequenced by Seqlab (Goettingen, Germany). Expression and purification conditions were as described above (See 2.2.2.3).

2.2.2.8. Enzymatic activity assays

Enzymatic activity was assayed according to (Lord, 1972) with few modifications. Bacterial cell extract containing 100µg of total protein or 0.5µg of the purified protein was added to 100µM Na-phosphate buffer (pH 8.0), 50µM 2,6-dichlorophenolindophenol (DCIP), 3mM phenazine methosulfate (PMS), and 10mM glycolate or D/L-lactate in a final volume of 0.2mL. At fixed time intervals, individual assays were terminated by the addition of 8µL 32% HCl. After standing for 10min, 42µl of 0.1M phenylhydrazine-HCl was added. The mixture was allowed to stand for a further 10min, and then the extinction due to the formation of glyoxylate-phenylhydrazone or pyruvate-phenylhydrazone, respectively, was measured at 324nm.

For testing substrate specificity, enzymatic activity was tested spectrophotometrically with a different assay. Reaction mixture contained 50mM Na-phosphate buffer (pH 8.0), 3mM PMS, 200µM DCIP, and 10mM of the tested substrate in a final volume of 0.2ml. Activities were measured at RT ~ 21°C by recording the reduction of DCIP at 600nm (ε, 22 cm^{-1} mM^{-1}).

Cytochrome c reduction was tested in the same buffer containing 50mM Na-phosphate buffer pH 8.0, 10mM glycolate/$_D$-Lactate and 200µM equine cytochrome c (Sigma, Taufkirchen, Germany) instead of DCIP. OD change was measured at 550nm (ε, 18.6 cm^{-1} mM^{-1}). The resulting activity was divided by two since two moles of cytochrome c are reduced for each mole of substrate oxidized.

2.2.3. Biological methods

2.2.3.1. Culture of bacteria

I) *Escherichia coli*

Different *E. coli* strains (Table 2) were cultured in Luria-Bertani (LB) rich medium (Bertani, 2004). The bacteria were grown at 37°C.

II) *Agrobacterium tumefaciens*

Agrobacterium tumefaciens bacteria were cultured in YEB medium Broth (Table 9) that is based on the formula described by (Song et al., 2004). The bacteria were grown at 28°C.

2.2.3.2. Preparation of competent E. coli cells for heat shock transformation

From a fresh *E. coli* culture a single colony was inoculated into 5ml LB medium and incubated ON at 37°C with continuous shaking (200xg). On the second day, the ON culture was used to inoculate fresh 200ml LB medium and the culture was left to grow at the same conditions until the OD_{600nm} reached 0.5 - 0.6. Afterwards, bacterial culture was spun down for 10min (4000xg/ 4°C) and the pellet was then resuspended with 15ml ice-cold TFBI buffer (Table 9) and left in ice for 10min. The bacterial cells were centrifuged and the pellet was resuspended in 4ml TFBII buffer (Table 9). Finally, aliquots of 200μl of the suspension were dispensed into pre-chilled Eppendorf tubes, and were immediately frozen in liquid nitrogen and stored at -80°C.

2.2.3.3. Transformation of competent bacteria by heat-shock

The competent *E. coli* cells prepared as shown previously (See 2.2.3.2) were defrosted in ice before using. Plasmid DNA (10-100ng) or the ligation products (1-3μl) were added to the competent cells and gently mixed and incubated in ice for 30min. Afterwards, the cells were heat-shocked (45sec at 42°C), and were immediately rested in ice. The transformed cells were recovered by adding 1ml of LB medium without antibiotics and were incubated at 37°C for 60min with continuous shaking (180xg). Different volumes: 50, 100 and 150µl of the transformed cells were placed on LB-agar plates supplemented with appropriate antibiotics (Table 4) and incubated at 37°C ON.

2.2.3.4. Preparation of competent Agrobacterium cells for electroporation

From a fresh culture of *Agrobacterium tumefaciens* grown on YEB-agar plates containing 100µg/ml rifampicin (Rif) and 25µg/ml kanamycin (Kan) (YEB+Rif+Kan), a single colony was used to inoculate 5ml of YEB+Rif+Kan medium and incubated at 28°C for two days with shaking (200xg). Afterwards, 1ml of the culture was transferred into 200ml fresh YEB+Rif+Kan medium and the culture was left to grow until the OD_{660nm} reached 1-1.5. Then, cells were centrifuged (4000xg/4°C/10min) and the bacterial pellet was washed three times with 100ml, 50ml and 25ml cold HEPES buffer I (Table 9), respectively, and one time with 10ml HEPES buffer II (Table 9). Finally, the cells were resuspended in 500µl of sterile HEPES buffer II (Table 9) and aliquots of 45µl were dispensed into pre-chilled Eppendorf tubes, frozen immediately in liquid nitrogen and stored at -80°C.

2.2.3.5. Transformation of *Agrobacterium tumefaciens* by electroporation

The competent *A. tumefaciens* cells (See 2.2.3.4) were defrosted before using. The plasmid DNA (0.2-1.0µg) was added to the *Agrobacteria* and left in ice for 5min. The mixture was transferred into an electroporation cuvette and exposed to the electric pulse (25 F/2.5 kV/200). The cells then were diluted with 1ml of YEB medium without antibiotics and incubated at 28°C with shaking (200xg) for 60min. Finally, 50µl and 100µl of the transformed cells were placed on YEB plates containing Rif+Kan and the antibiotic suitable to the plasmid. The plates were incubated at 28°C for 3-4 days.

2.2.3.6. Plant culture, generation and characterization of transgenic plants

Transformation of *Arabidopsis* plants was performed through *Agrobacterium*-mediated floral dip transformation.

I) Preparation of Agrobacterium

A pre-culture of *Agrobacterium tumefaciens* carrying the gene of interest was prepared by inoculating a single colony into 5ml YEB medium (100µg/ml Rif+25µg/ml Kan+ 100µg/ml carbenicillin) and incubated at 28°C for 2 days with shaking at 150xg. Afterwards, the pre-culture was transferred into fresh 200ml YEB medium (100µg/ml Rif+25µg/ml Kan+ 100µg/ml carbenicillin) and incubated for additional 2 days at 28°C with shaking at 200xg. The bacterial

cells were spun down (4000xg /4°C/20min), and the bacterial pellet was resuspended in 5% sucrose until OD_{600nm} ~ 0.8. Finally, 0.04 % silwet l-77 (400μl/1000ml) was added to the resuspended and was used directly for floral dip transformation of Arabidopsis plants.

II) Transformation of Arabidopsis plants (floral dip transformation)

The floral dip transformation of Arabidopsis plants was performed as described by (Clough and Bent, 1998). Briefly, the Arabidopsis plants were grown under short day conditions (8h/16h, 22/20°C, day/night) to produce biomass. Afterwards, the plants were transferred to a long day conditions (16h light and 8h dark at 23-25°C) to enhance flowering. Bacterial cultures of Agrobacteria harboring plasmid with CYND or CYND and FDH together were prepared. The flowers were dipped in the Agrobacterium solution for 3 to 10min (Figure 10). The dipped plants were covered ON (16h) in order to maintain humidity. The plants were then transferred to normal growth conditions (16h light and 8h dark at 23-25°C) until plant maturation and seeds harvesting.

III) Selection of the transgenic plants

Selection of transgenic lines was performed on MS+Kan plates as described by (Clough and Bent, 1998). The harvested seeds were sterilized using 98% (v/v) ethanol for 15min then washed three times with 75% (v/v) ethanol, and then the seeds were left to dry. The seeds were placed on MS+Kn plates and left to grow in short day conditions (16h light and 8h dark at 23-25°C) for 10-15 days. The survived plants were transferred to soil. The transgenic plants were confirmed by PCR (See 2.2.1.2) using specific primer. The positive plants were continued growing for seeds production.
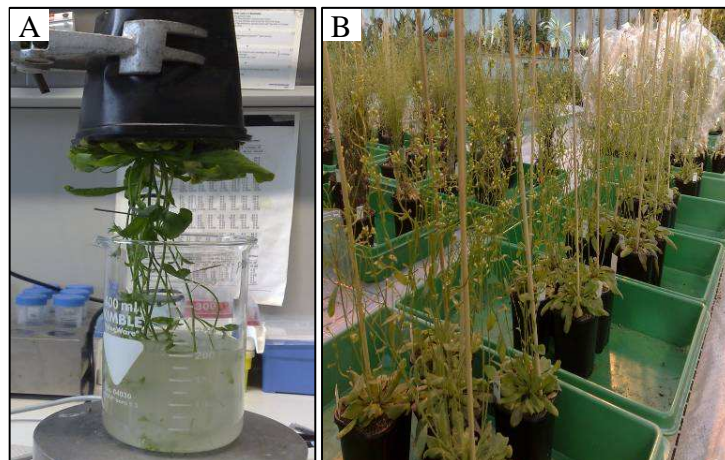

Figure 10. Floral dip *Agrobacterium* mediated transformation of wild type *Arabidopsis* plants.

2.2.3.7. Growth assay conditions

Three different systems were used for growth assays under cyanide stress. For determination of root growth in seedlings, plants were grown on vertical MS medium agar plates with or without 250µM KCN (plate assay). For determination of rosette size, and fresh weight plants were grown in a hydroponic system in MS medium under short day conditions (8h/16h, 22/20°C, day/night). After two weeks, plants were treated with MS supplemented with 50µM KCN for another two weeks (hydroponic assay). Alternatively, plants were grown in sand and watered with MS medium. After four weeks, plants were treated with MS supplemented with 300µM KCN for another two weeks in 3-day intervals (Sand assay).

2.2.3.8. Gas exchange measurements

Plants grown in sand and watered with MS+300µM KCN for two weeks (Sand assay, see 2.2.3.7.) were used for gas exchange measurements using the LI-6400 system (Li-Cor, Lincoln, NE). Parameters were calculated with the software supplied by the manufacturer. Measuring conditions were photon flux density = 1000µmol m^{-2} s^{-1}, chamber temperature = 26°C, flow rate =100 µmol s^{-1}, relative humidity = 60–70%, and CO_2 = 400ppm. Plant leaves were allowed to adapt for 20–30min to the measuring chamber before each measurement.

3. Results

3.1. Enzymatic characterization of *Chlamydomonas reinhardtii* glycolate dehydrogenase and its nearest proteobacterial homologue

A mitochondrial glycolate dehydrogenase (*Cr*GlcDH) in *Chlamydomonas reinhardtii* was initially described by (Nakamura et al. (2005). Although *Cr*GlcDH was reported to encode a GlcDH based on its homology to GlcD and GlcF from *E. coli* (Nakamura *et al.*, 2005), the enzymatic properties of this enzyme were not identified. In order to investigate whether the *Cr*GlcDH gene product is a true glycolate dehydrogenase and to determine whether it can be used for the chloroplastic bypass (Figure 6), biochemical characterization of the enzyme was undertaken in this study.

3.1.1. Phylogenetic analysis

A phylogenetic analysis was conducted for *Cr*GlcDH gene to get better understanding of the distribution of its orthologous sequences. The *Cr*GlcDH amino acid sequence was used for a basic alignment search (BLAST) in the NCBI databank. Representative sequences from bacteria, archaea, chlorophyta and other eukaryotes were selected and used to construct a phylogenetic tree through the neighbor joining method (Figure 11). Arabidopsis GOX (gi|25083945) gene was used as an outgroup for rooting of the phylogenetic tree. The nearest homologues to *Cr*GlcDH were found in sequenced genomes of other chlorophytes. All available genome sequences of this clade contained sequences homologous to *Cr*GlcDH (data not shown). Surprisingly, the sister-group to the chlorophyta enzymes was made up from proteobacterial enzymes. The selected species represent the subclades alpha (*Azospirillum*), beta (*Dechloromonas*), gamma (*Pseudomonas*), delta (*Desulfovibrio*) and epsilon (*Arcobacter*). However, we did not identify a *Cr*GlcDH homologue in the *E. coli* genome (gammaproteobacteria). All the identified *Cr*GlcDH homologues in proteobacteria contained homology domains to both GlcD and GlcF over the full length of the protein sequence (Figure 12). Proteins with homology to *E. coli* GlcD, but not GlcF were clustered in a separate clade. This clade contained sequences from different groups of prokaryotes including archaea and cyanobacteria. Many of the proteobacteria that contained a *Cr*GlcDH homologue (see above), in addition, were found to contain a GlcD homologue. Putative $_D$-lactate dehydrogenases from different evolutionary groups including ascomycetes (*Saccharomyces*), ameobozoa (*Dictyostelium*), and plants (*Arabidopsis*, *Physcomitrella*) formed

a sister group to the GlcD-homologues. Thus, *Cr*GlcDH represents a group of proteins found in chlorophyta and some proteobacteria that is evolutionary separated from other GlcD homologues.
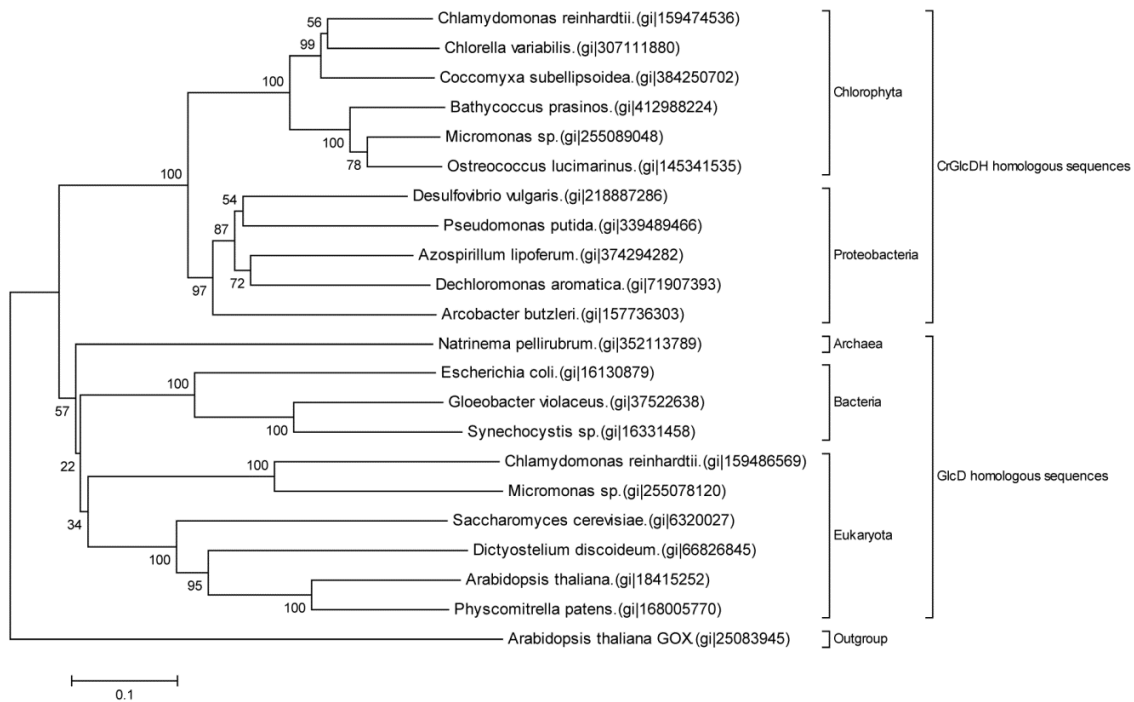

Figure 11. Evolutionary relationship of *Cr*GlcDH using neighbor-joining method. Bootstrap values (%) are for 500 replicates. Evolutionary distances were computed using the p-distance method. Sequence alignment and evolutionary analyses were conducted in MEGA5.1 software (See 2.2.1.13). Arabidopsis GOX was used as an outgroup. Numbers in parentheses are Genbank accession numbers.

3.1.2. Alignment of *Cr*GlcDH to its closest proteobacterial sequence

The *Cr*GlcDH amino acid sequence was aligned to the nearest proteobacterial *Desulfovibrio vulgaris* (*Dv*DLDH, gi|218887286) protein. It was found that the similarity extended over the full length covering the GlcD and GlcF domains. Thus, both proteins might share similar enzymatic characteristics (Figure 12).

```
CrGlcDH : MPRGQGKRLAQLLGAQLKQYAAEVRGISTAGGASRGGARGPASPSSLEQQTRQVAQVAVQQSTQQAVKVVVPAIKVDLVGAVS :    83
DV-DLDH : -----------------------------------------------------------------------MLPA--------- :     4


CrGlcDH : SVSESDKVEPGVFKNVDGHRFEDGRYAAFVEEITKFIPKERQYSDPVRTFAYGTDASFYRLNPKLVVKVHNEDEVRRIMPIAE :   166
DV-DLDH : -----------------------AYQAFIKELLEFIPRRNVFTDPLRTLAYGTDASFYRLIPKIVVDTHNEDEVVGVIKLAN :    63


CrGlcDH : RLQVPITFRAAGTSLSGQAITDSVLIKLSHTGKNFRNFTVHGDGSVIIVEPGLIGGEVNRILAAHQKKNKLPIQYKIGPDPSS :   249
DV-DLDH : KHRLPMTFRAAGTSLSGQAVTDSILVRL---GDGWRKYAIFDNATKIRLQPGIIGSHANRLLAEFGK-------KIGPDPAS :   135


CrGlcDH : IDSGMIGGIVSNNSSGMCCGVSQNTYHTLKDMRVVFVDGTVLDTADPNSCTAFMKSHRSLVDGVVSLARRVQADKELTALIRR :   332
DV-DLDH : IDTGKIGGIVANNASGMCCGVAENSYKTLSHMRVVFHDGTVLDTSDTKSRAAFQRTHPEIVNGVAAMRAQIMNKPELADLITR :   218


CrGlcDH : KFAIKCTTGYSLNALVDFPVDNPIEIIKHLIIGSEGTLGFVSRATYNTVPEWPNKASAFIVFPDVRAACTGASVLRNETSVDA :   415
DV-DLDH : KFKIKNTTGYSLNALVDFA--DPFDIIQHLMVGSEGTLGFISEVTYHTVTEHAHKASALVIFPTIRDACEATIILRQQP-VSA :   298


CrGlcDH : VELFDRASLRECENNEDMMRLVPD-IKGCDPMAAALLIECRGQDEAALQSRTEEVVRVLTAAGLPFGAKAAQPMAIDAYEFHH :   497
DV-DLDH : VEMMDRASLRSVEDKPGM----PDGLQGLPDDAAALLVETRAGDKATLEDQISRITASIEA--IP----KIRPVAFTDVPAEF :   371


CrGlcDH : DQKNAKVFWDVRRGLIPIVGAAREPGTSMLIEDVACPVDKLADMMIDLIDMFQRHGYHDASCFGHALEGNLHLVFSQGFRNKE :   580
DV-DLDH : G-----TLWNVRKGLFPAVGAVRKVGTTVIIEDVAFPIASLADATPELQTLFAKHGYSEAIIFGHALEGNLHFVFTQDFNTQS :   449


CrGlcDH : EVQRFSDMYEEMCHLVATKHSGSLKGEHGTGRNVAPFVEMEWGNKAYELMWELKALFDPSHTLNPGVILNRDQDAHIKFLKPS :   663
DV-DLDH : EVDRYRAFMDDVAAMVVGTYSGSLKAEHGTGRNMAPFVELEWGRDAFLLMRELKTLFDPYGLLNPGVIINPDAEAHIRNLKPL :   532


CrGlcDH : PAASPIVNRCIECGFCESNCPSRDITLTPRQRISVYREMYRLKQLGPGASEEEKKQLAAMSSSYAYDGEQTCAADGMCQEKCP :   746
DV-DLDH : PAAHSIIDKCIECGFCEPICPSKDVTFTPRQRIVGWREISRMK-----AGDEKSGLLKQLFSGYDYLGCDNTCATDGLCATRCP :   610


CrGlcDH : VKINTGDLIKSMRAEHMKEEKTASGMADWLAANFGVINSNVPRFLNIVNAMHSVVGSAPLSAISRALNAATNHFVPVWNPYMP :   829
DV-DLDH : VGINTGAFIKELRAD--KVGPRAQKAADWVARHYGGVCRTISTALTGVDLLHRVLGTEVMDKGAQFLRVVSLKKAPLWTRAMP :   691


CrGlcDH : KGA-APLKVPAPPAPAAAEASGIPRKVVYMPSCVTRMMGPAASDTETAAVHEKVMSLFGKAGYEVIIPEGVASQCCGMMFNSR :   911
DV-DLDH : TGASAPAHAPRGPVS-------DRKVVYFPSCIARSMGPARDDEQRDPLPAKTIGLLLKAGYHVLFPEKLGDLCCGQPFESK :   766


CrGlcDH : GFKDAAASKGAELEAALLKASDNGKIPIVIDTSPCLAQVKSQISEPSLRFALYEPVEFIRHFLVDKLEWKKVRDQVAIHVPCS :   994
DV-DLDH : GFKAQADMKAKELSEALLKVSDNGAIPVLCDTSPCLYRMKETLDK---RLKLYEPIEFALEHLTQALDFRKAERTIAIHSTCT :   846


CrGlcDH : SKKMGIEESFAKLAGLCANEV-VPSGIPCCGMAGDRGMRFPELTGASLQHLNLP-KTCKDGYSTSRTCEMSLSNHAGINFRGL :  1075
DV-DLDH : AVKLGLPGKFKQLAFLCAEQVIVPEDVFCCGFAGDRGFSFPELNTGALKELRRQVEICEEGYSTSRTCEIGLSLHGKIPYRNI :   929


CrGlcDH : VYLVDEATAPKKQAAAAKTA : 1095
DV-DLDH : LYLVDEVTTPKSA------- :  942
```

Figure 12. Alignment of *Cr*GlcDH against a putative ᴅ-lactate dehydrogenase from *Desulfovibrio vulgaris* (*Dv*DLDH). I, GlcD homologous domain; II, GlcF homologous domain. The black boxes show the similarities among the amino acids.

3.1.3. Cloning, heterologous expression and purification of *Cr*GlcDH

To optimize expression of the recombinant *Cr*GlcDH protein, significant efforts were invested during this study. The *Cr*GlcDH gene was cloned into several expression plasmids: pET22 with C-terminal 6-histidine fusion tag, pET41 with N-terminal glutathione S-transferase (GST) fusion tag and C-terminal 6-histidine fusion tag, and pMAL with N-terminal maltose binding protein fusion tag. The bacterial strain *E. coli* BL21 codon plus was used to analyze the expression level of the different constructs. In all constructs, the majority of *Cr*GlcDH protein was found to accumulate as inclusion bodies, and only a small amount was detected in the soluble fraction by western blotting (data not shown). The construct pET22-*Cr*GlcDH with the short histidine fusion tag was used for further investigations. Moreover, several *E. coli* strains: ER2566, BL21 codon plus, Rosette gami, C41 and C43, were used to analyze expression of the recombinant *Cr*GlcDH protein. Among the tested bacterial strains, *E. coli* BL21 codon plus was selected for further investigations as it showed the best expression level of *Cr*GlcDH in soluble form (data not shown). Further optimization for expression of recombinant *Cr*GlcDH in BL21 codon plus was undertaken: expression at different temperatures (4, 17, 25, 30 and 37°C), induction of the expression at different bacterial densities OD_{600nm} (0.6, 0.9, 1.5 and 2), induction of the expression with different IPTG concentrations (0.05, 0.1, 0.5, 1 and 2mM) (data not shown) and induction for different time points (1, 2, 3, 4 ,5, 6 hours and ON). Eventually, the expression conditions: grown in LB medium, protein induction at 37°C for 2h by 1mM IPTG were routinely used for *Cr*GlcDH expression in *BL21* codon plus. The soluble *Cr*GlcDH protein was purified by Ni^{2+}-NTA chromatography (Qiagen). The purification was performed according to the manufacturer's instructions with some modifications (See 2.2.2.3). The purified *Cr*GlcDH protein was analyzed by SDS-PAGE (See 2.2.2.4) and western-blotting (See 2.2.2.6). A protein of the expected size and two additional protein bands were observed in the eluate (Figure 13). Blotting the purified proteins against anti-His antibodies resulted in two signals: one matched the full-length *Cr*GlcDH protein size and the other matched the smallest band of the two contaminating bands (Figure 13). I speculated that the contaminations were derived from *Cr*GlcDH protein that was degraded during purification. All the three eluted bands were analyzed by mass spectrometry (Mass spectrometry was done at the Institute of Plant Genetics, Leibniz University Hannover). As expected, all three bands contained peptides derived from *Cr*GlcDH (See 6.1, S2).
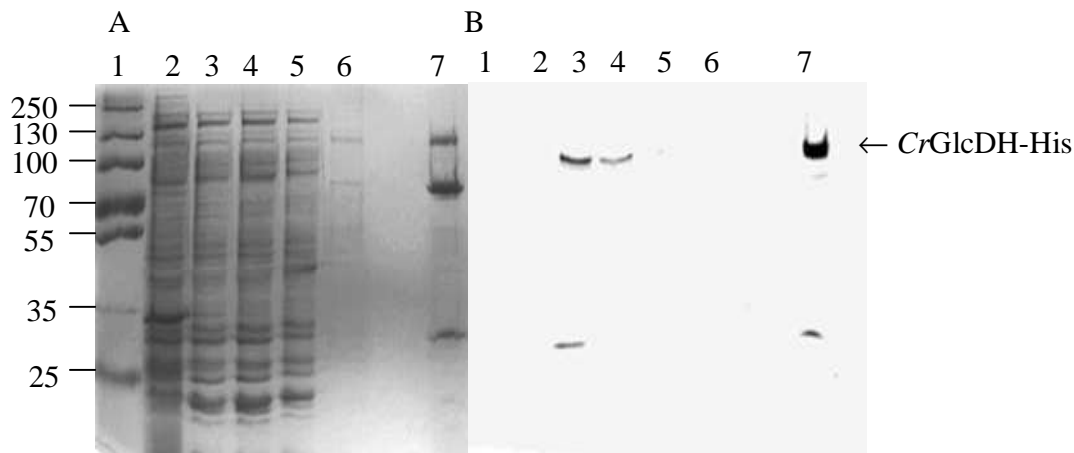
Figure 13. Purification of *Cr*GlcDH-His using Ni^{2+}-NTA affinity chromatography. A, Coomassie stained SDS-PAGE of the progress of recombinant *Cr*GlcDH purification. B, Western blot of the SDS gel using anti-His antibodies. Lane 1, protein marker. Lane 2, 20µg of soluble protein extract after IPTG induction from bacteria transformed with an empty vector. Lane 3, 20µg of soluble protein extract after IPTG induction from bacteria transformed with the *Cr*GlcDH-His construct. Lane 4, 20µg flow-through fraction. Lane 5-6, washing fractions. Lane 7, 5µg of purified *Cr*GlcDH-His protein.

3.1.4. Cloning, heterologous expression, purification of D-LDH from *Desulfovibrio vulgaris*

In order to compare the catalytic properties of *Cr*GlcDH protein with *Dv*DLDH protein, the gene was isolated and cloned into pET22 vector (See 6.1, S1 and figure 8). After confirming the sequence, the construct was transformed into *E. coli* BL21 codon plus and was overexpressed using the same conditions that were previously determined for *Cr*GlcDH (See 2.2.2.3). Although, the expression was as low as for *Cr*GlcDH protein, the soluble protein was purified as described with *Cr*GlcDH protein. The eluate fraction was analyzed with SDS followed by western blot (Figure 14). As expected, a signal was detected at molecular weight of 100kDa.
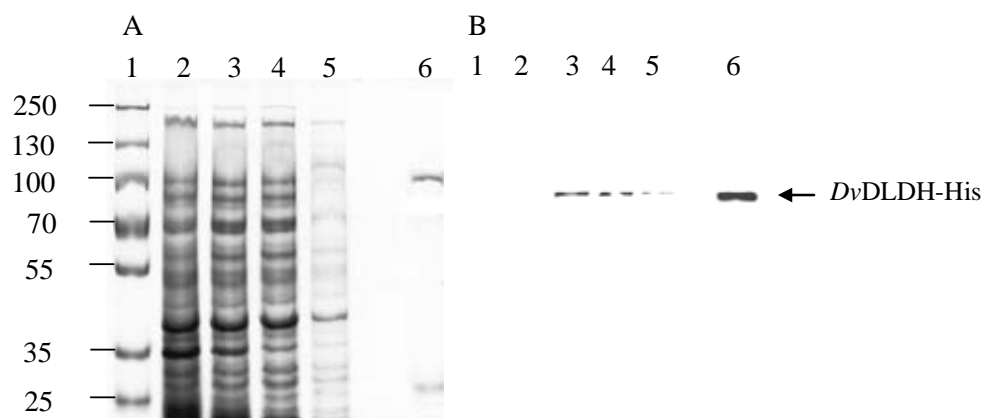
Figure 14. Purification of *Dv*DLDH-His using Ni^{2+}-NTA affinity chromatography. A, Coomassie stained SDS-PAGE of the progress of recombinant *Dv*DLDH purification. B, Western blot of the SDS gel using anti-His antibodies. Lane 1, protein marker. Lane 2, 20μg of soluble protein extract after IPTG induction from bacteria transformed with an empty vector. Lane 3, 20μg of soluble protein extract after IPTG induction from bacteria transformed with the *Dv*DLDH-His construct. Lane 4, 20μg flow-through fraction. Lane 5, washing fraction. Lane 6, 5μg of purified *Dv*DLDH-His protein.

3.1.5. Screening of the substrate specificity of recombinant *Cr*GlcDH

Other GlcDH homologues have been shown to accept wide range of substrates such as glycolate and $_D$-lactate. However the activity of the purified *Cr*GlcDH enzyme was tested spectrophotometrically against various substrates by recording the reduction of DCIP at 600 nm (ε, 22 cm^{-1} mM^{-1}) as was described in (See 2.2.2.8). The highest activity was detected with $_D$-lactate. Therefore, the activity with $_D$-lactate was set to 100% (Table 15). Slightly lower activity was observed with glycolate. Moreover, activities with $_L$-lactate and succinate were around 10% compared to $_D$-lactate, and only very low activities were observed with glyoxylate and glycerate as substrates. The other tested short-chain organic acids were not accepted as substrates.

Table 15. Substrate specificity of recombinant *Cr*GlcDH. Activity was measured under standard assay conditions described in experimental procedures. Activity with $_D$-lactate as a substrate (1.0 ± 0.06 μmol min^{-1} mg^{-1}) was set to 100%. Parameters represent mean ± SE of three independent enzyme preparations.

Substrate	Relative specific activity (% of $_D$-lactate)
No substrate	0.0 ± 0.03
Glycolate	72 ± 1.3
$_L$-lactate	12.5 ± 0.016

$_D$-lactate	100.0 ± 0.0
Formate	0.0 ± 0
Malate	0.0 ± 0
Succinate	8.5 ± 0.001
Acetate	0.06 ± 0.03
Glycerate phosphate	2.8 ± 0.013
Glyoxylate	1.8 ± 0.01
Pyruvate	0.0 ± 0.001

4.1.6. Substrate specificity of *Dv*DLDH

The substrate specificity of *Dv*DLDH was determined using purified protein. The activity was measured with glycolate and $_D$-lactate as substrates as described by Lord (1971) (See methods 2.2.2.8). *Dv*DLDH protein showed activity with $_D$-lactate similar to *Cr*GlcDH protein (Figure 15). However, no activity was observed for *Dv*DLDH when glycolate was used as a substrate.
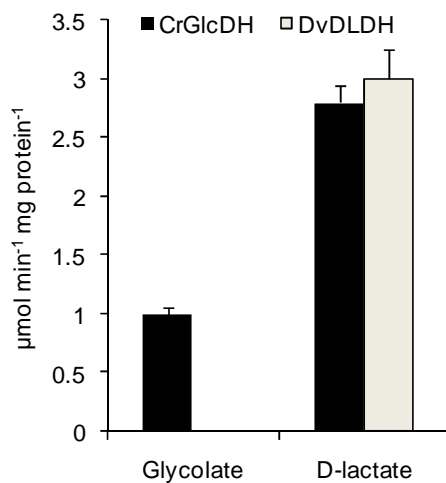

Figure 15. Comparison of substrate specificity of *Cr*GlcDH and its nearest proteobacterial homologue (*Dv*DLDH). Recombinant proteins were purified by affinity chromatography and tested with glycolate and $_D$-lactate as substrates. Data points represent mean $\pm$ SE of three independent replicates.

3.1.7. The effect of temperature and pH on the activity of purified *Cr*GlcDH

The effect of the temperature on enzyme activity was measured in the temperature range of 4–50 °C at pH 8 using 100mM sodium phosphate buffer. The effect of pH on the activity was measured at 30°C within pH range of 6-9 using 100mM of sodium phosphate buffer. The optimum temperature for the reaction with glycolate as a substrate was determined to 30°C and the optimum pH to 8.0 (Figure 16). These parameters were used for the further analysis.
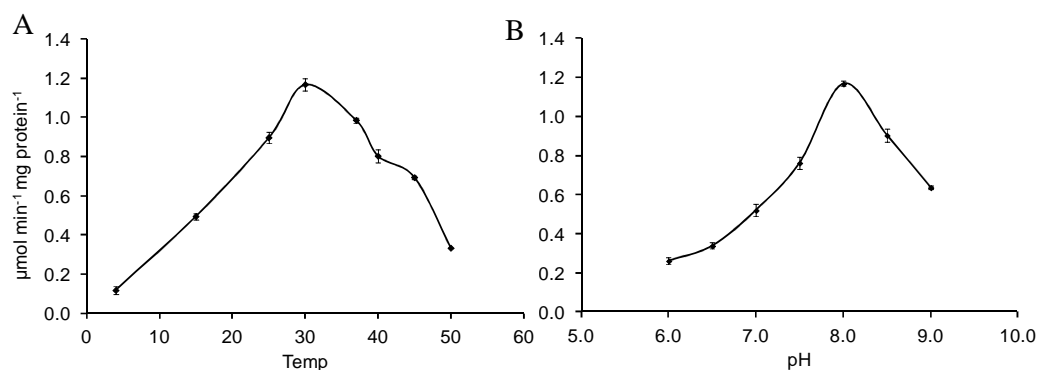

Figure 16. Effect of temperature and pH on the catalytic activity of recombinant *Cr*GlcDH protein. *Cr*GlcDH-His was purified from overexpressing bacteria and glycolate dehydrogenase activity was assayed at different temperatures (A) or different pH (B). Data points represent mean ± SE of three independent replicates.

3.1.8. Co-factor analysis of recombinant *Cr*GlcDH

The co-factor preference of the partially purified *Cr*GlcDH was analyzed by measuring the extinction due to formation of glyoxylate-phenylhydrazone at 324nm as described by Lord (1971) (See 2.2.2.8). Activity of *Cr*GlcDH with glycolate as a substrate was only detected with DCIP and/or PMS as co-factors. Neither flavine nucleotides (FMN, FAD), nor nicotineamide dinucleotides (NAD$^+$, NADP$^+$) were accepted. Furthermore, there was no activity with molecular oxygen or oxidized cytochrome c as electron acceptors (Table 16).

Table 16. Electron acceptor specificity of the recombinant CrGlcDH relative to DCIP reduction. Data points represent mean ± SE of three independent replicates. *different assay (See 2.2.2.8).

Electron acceptor	Relative specific activity (% of DCIP)
O_2	0
DCIP	100 ± 0.02
PMS	93 ± 3.41
DCIP+PMS	127 ± 3.87
FAD	0
FMN	0
NAD^+	0
$NADP^+$	0
Cytochrome C*	0

3.1.9. Determination of kinetic properties of the recombinant CrGlcDH

Kinetic parameters (Table 17) were determined for glycolate and the two lactate enantiomers as was described in 2.2.2.8. The partially purified CrGlcDH enzyme showed high affinity to glycolate with a Km value of 200µM and a catalytic rate of 116 min^{-1}. The resulting catalytic efficiency ($Kcat/Km$) was 655min^{-1} mM^{-1}. Similarly, the kinetic properties for CrGlcDH using $_D$-lactate were very close to that with glycolate. The Km value for $_D$-lactate was 450µM, and the catalytic rate was 324min^{-1}. Furthermore, the catalytic efficiency ($Kcat/Km$) for $_D$-lactate was very close to that for glycolate, it was determined to be 781min^{-1}mM^{-1}. In contrast, with $_L$-lactate, the Km value was almost 100-fold higher than for glycolate, and the catalytic rate was reduced by 2-fold. This resulted in a very low catalytic efficiency with $_L$-lactate as a substrate.

Table 17. Kinetic parameters of recombinant *Cr*GlcDH. Kinetic data were best fit by non-linear regression analysis. Parameters represent mean ± SE of three independent enzyme preparations.

	K_m (mM)	K_{cat} (min^{-1})	K_{cat}/K_m (min^{-1} mM^{-1})
Glycolate	0.21 ± 0.06	116 ± 7	655
$_D$-lactate	0.45 ± 0.1	325 ± 17	781
$_L$-lactate	19 ± 1.3	92 ± 27	5

3.1.10. Effect of different inhibitors on *Cr*GlcDH activity

The enzymatic activity of purified *Cr*GlcDH was tested in presence of different potential inhibitors using glycolate as a substrate and DCIP as an electron acceptor as was described in (2.2.2.8). EDTA showed almost no inhibitory effect on *Cr*GlcDH activity even at high concentrations. However, $CuSO_4$ inhibited activity already at moderate concentrations (0.1mM) providing evidence that disulfide bonds are required for protein activity. KCN sensitivity is another joint property of GlcDH enzymes (Bari et al., 2004). *Cr*GlcDH activity was inhibited by KCN in a concentration dependent manner (Table 18).

Table 18. Effect of inhibitors on the activity of recombinant *Cr*GlcDH. Data represent mean ± SE of three independent replicates.

Inhibitors	Concentration (mM)	Inhibition (%)
EDTA	1	6 ± 3.75
	10	8 ± 6.05
$CuSO_4$	0.1	28 ± 4.91
	0.5	95 ± 4.74
	2	100 ± 0.06
KCN	0.1	31 ± 1.89
	0.5	98 ± 0.77
	2	100 ± 0.01

3.1.11. Mutational analysis of the glcF homology domain

In order to understand the importance of the GlcF-homology region in the C-terminus of the *Cr*GlcDH protein for catalytic activity, a deletion mutant and two point mutations were generated. The truncated *Cr*GlcDH gene (*Cr*GlcDHΔC660) and the two substitution mutations were cloned into pET22 vector and overexpressed in *E.coli* BL21 codon plus (Figure 8). The enzymatic activities of *Cr*GlcDH and the three different mutants were determined with crude protein extracts, but an extract from *E. coli* transformed with the empty vector was always used as a negative control (Figure 17 & 18). Deletion of the GlcF homology region resulted in a complete loss of *Cr*GlcDH activity in this assay. Furthermore, substituting of 3 or 4 cysteine residues (673, 676, 679, and 683) with serine residues in a putative 4Fe-4S (aa 673-683) cluster in GlcF-homology region resulted in loss of activity. These results indicate the importance of this region for *Cr*GlcDH activity.
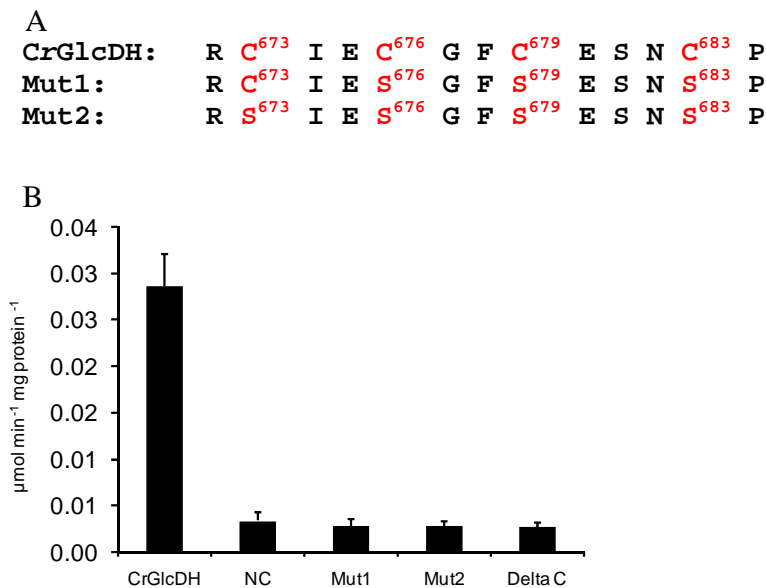
A

CrGlcDH:	R	C^{673}	I	E	C^{676}	G	F	C^{679}	E	S	N	C^{683}	P
Mut1:	R	C^{673}	I	E	S^{676}	G	F	S^{679}	E	S	N	S^{683}	P
Mut2:	R	S^{673}	I	E	S^{676}	G	F	S^{679}	E	S	N	S^{683}	P

B

Figure 17. Enzymatic properties of different *Cr*GlcDH mutants. Protein extracts were used to compare the enzymatic activity of *Cr*GlcDH and the three different mutants. Columns represent mean ± SE of three independent replicates. NC, empty vector control. Mut1/Mut2, *Cr*GlcDH-His constructs with cysteine to serine mutations as indicated in the figure 17A. Delta C, *Cr*GlcDH-His construct truncated at amino acid position 660.
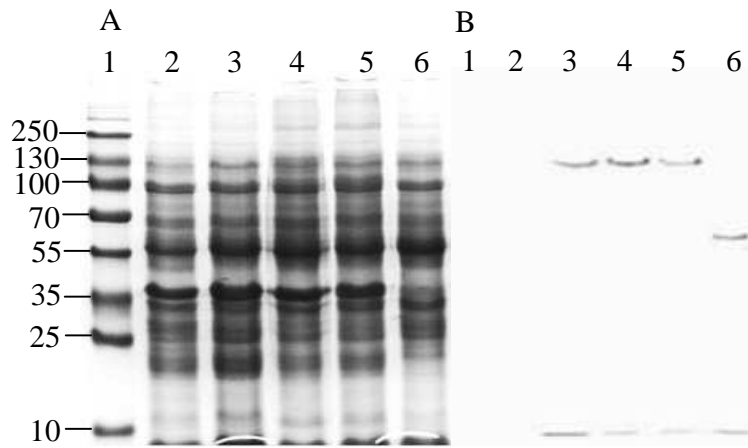
Figure 18. Overexpression of *Cr*GlcDH and its mutants. A, Coomassie stained SDS-PAGE. B, Western blot of the SDS gel using anti-His antibodies. Lane 1, protein marker. Lane 2, *Cr*GlcDH-His. Lane 3, mutant 1. Lane 4, mutant2. Lane 5, delta C. Equal amount from the soluble protein extract of each contract was loaded.

3.2. Simultaneous overexpression of cyanidase and formate dehydrogenase in *Arabidopsis thaliana* chloroplasts enhanced cyanide metabolism and cyanide tolerance

I wanted to test whether overexpression of cyanidase (CYND, from *Pseudomonas stutzeri*) could confer enhanced cyanide resistance to plants and whether formate resulting from the reaction could be further converted to CO_2 by formate dehydrogenase (FDH, from *Arabidopsis thaliana*). Before transfer to plants, the activity of both enzymes was tested in crude extracts from bacteria overexpressing the respective cDNA (This part was done by Dr. Rashad Kebeish, Zagazig University /Egypt). Clear increases in activity relative to the empty vector controls could be observed for both enzymes in specific assays.

3.2.1. Generation of CYND and FDH transgenic Arabidopsis plants

The genes were transferred separately (CYND, FDH) or in combination (CYND+FDH) to Arabidopsis plants. The enzymes were constitutively expressed, but targeted to chloroplasts to make best potential use of CO_2 resulting from the combined reactions of CYND and FDH. Transgenic lines were selected based on kanamycin resistance. Transgenes expression was initially tested by quantitative PCR in the CNYD+FDH lines. As shown in Figure 19A, three independent lines were selected. Lines CYND+FDH-4 and CYND+FDH-6 showed higher expression of both transgenes compared to line CYND+FDH-2. Expression of CYND in transgenic plants was also determined on the protein level by using an antibody specific for the His-tag. A strong signal at the expected molecular weight for CYND protein of around 44kDa was detected (Figure 19B&C). In addition, the activity of CYND and FDH was tested in extracts from chloroplasts isolated from CYND+FDH plants (This part was done by Dr. Rashad Kebeish, Zagazig University /Egypt).
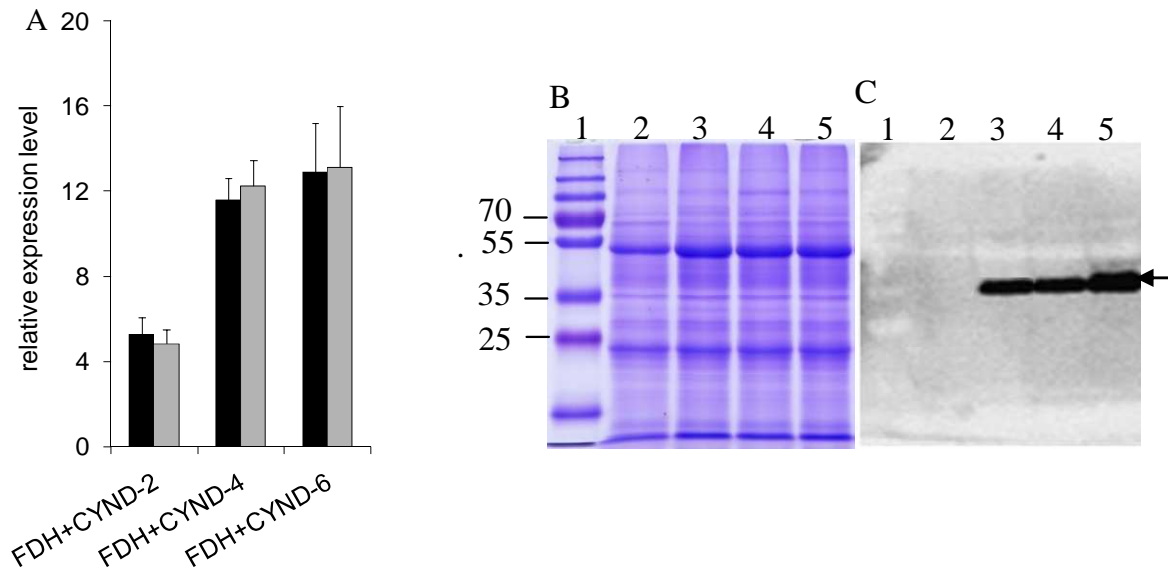
Figure 19. Characterization of FDH and CYND enzymes used in this study. A, Amount of FDH (black bars) and CYND (gray bars) transcripts relative to actin2 transcripts in three independent Arabidopsis lines overexpressing the FDH+CYND construct. Samples were collected from the youngest fully expanded leaf 6h after onset of light. B, Coomassie stained SDS-PAGE of the total protein extract from Arabidopsis plants. C, Western blot of the SDS gel using anti-His antibodies. Lane 1, protein marker. Lane 2, azygous plants. Lane 3, FDH+CYND-2 line. Lane 4, FDH+CYND-4 line. Lane 5, FDH+CYND-6 line. Equal amount of proteins were loaded.

3.2.2. Analysis of the performance of transgenic plants under different cyanide stress conditions

I) Performance of transgenic plants on MS/KCN plates

 Plants were germinated on vertical MS/agar plates containing 250µM KCN (See 2.2.3.7). The root length was measured after two weeks. A pool of azygous plants derived from the same mother plant was used as the control. In each plate, both the transgenic and azygous plants were represented. Average root length was significantly increased from 1.6 to 2.5cm (+56%) in CYND+FDH plants compared to controls. However, root length was almost identical for both genotypes in the absence of KCN.
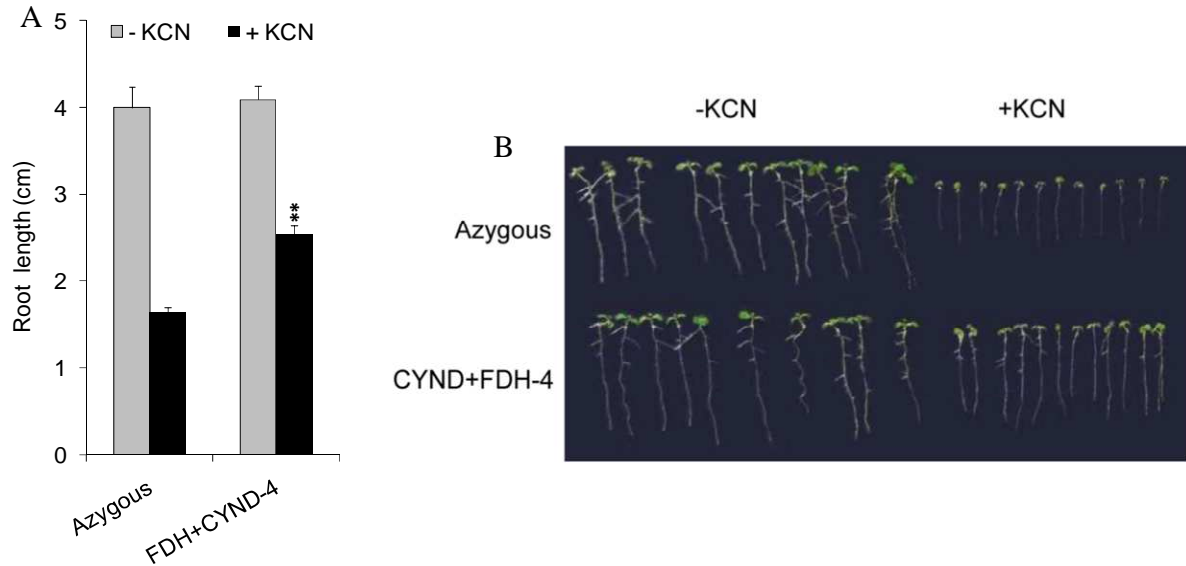
Figure 20. Growth of transgenic Arabidopsis plants and controls on vertical agar plates (A&B) containing 250µM KCN (+KCN) or not (-KCN). Azygous: Segregants from FDH+CYND plants that lost the transgene; FDH+CYND-4: Plant line transgenic for formate dehydrogenase and cyanidase. Data are means of three independent experiments each with at least ten plants per genotype ± SE. Asterisks represent statistically significant differences compared to azygous control plants (* = p<0.05, ** = p<0.01, *** = p<0.001).

II) Performance of the transgenic plants in hydroponic systems

Arabidopsis plants were grown in hydroponics for two weeks without KCN and then KCN was added for two weeks or not (See 2.2.3.7). Rosette diameter and fw were used as indicators for KCN resistance. CYND+FDH plants and controls showed very similar growth when KCN was omitted from the medium. However, KCN addition resulted in a reduction of both rosette diameter and fw (Figure 21 A, B and C) by approximately 30% relative to untreated plants in the azygous control line. In contrast, the CYND+FDH line was hardly affected under these conditions (+ 3% for fw and -10% for diameter).
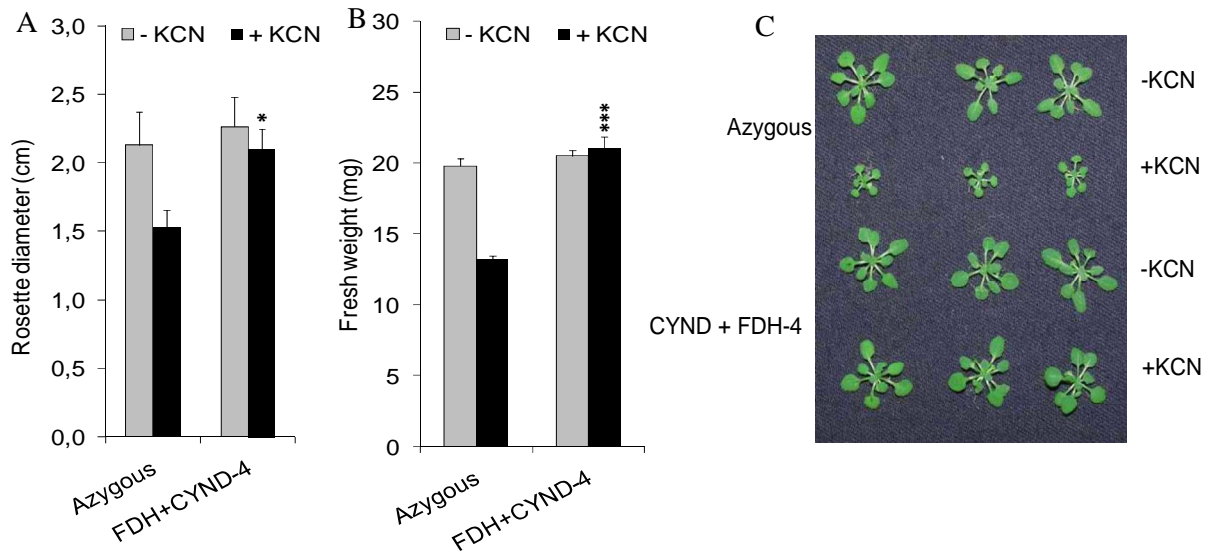
Figure 21. Growth of transgenic Arabidopsis plants and controls in hydroponic systems (A, B and C). Azygous: Segregants from FDH+CYND plants that lost the transgene; FDH+CYND-4: Plant line transgenic for formate dehydrogenase and cyanidase. Data are means of three independent experiments each with at least six plants per genotype ± SE. Asterisks represent statistically significant differences compared to azygous control plants (* = $p<0.05$, ** = $p<0.01$, *** = $p<0.001$).

III) Performance of transgenic plants grown in sand

As further analysis of the synthetic pathway, I grew the transgenic plants in sand supplemented with MS medium for four weeks and then MS/500µM KCN was applied for another two weeks (See 2.2.3.7). The rosette diameter and fresh weight were recorded (Figure 22). No differences were observed between the genotypes in the –KCN controls. Addition of KCN reduced rosette diameter by 30% and fw by 50% in the control. In the CYND+FDH line, diameter and fw were both only reduced by 17% when compared to untreated plants. These assays provided independent evidence that CYND+FDH double overexpressors performed superior when KCN was supplied via the root system.
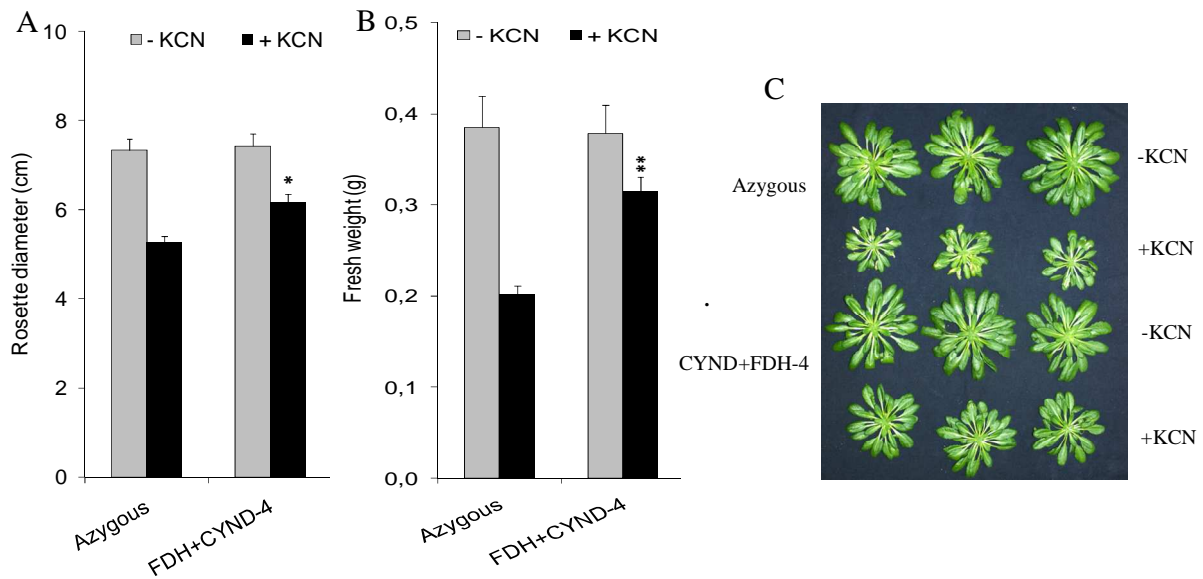
Figure 22. Growth of transgenic Arabidopsis plants and controls in sand (A, B and C). Azygous: Segregants from FDH+CYND plants that lost the transgene; FDH+CYND-4: Plant line transgenic for formate dehydrogenase and cyanidase. Data are means of three independent experiments each with at least six plants per genotype ± SE. Asterisks represent statistically significant differences compared to azygous control plants (* = p<0.05, ** = p<0.01, *** = p<0.001).

IV) Gas exchange measurements

In order to study the potential physiological effect of the established pathway, gas exchange characteristics of CYND+FDH and control lines were determined after two weeks of KCN treatment. In parallel, plants were grown without KCN treatment and tested (Table 19). As observed before in growth assays, CYND+FDH plants and control plants performed very similar under non-stressed conditions (-KCN). KCN treatment reduced CO_2 assimilation rate by 14% in the control whereas CYND+FDH plants remained unaffected. Similar trends were observed for transpiration (-14% for control vs. +7% for CYND+FDH) and stomatal conductance (-14% for control vs. +10% for CYND+FDH). Interestingly, leaf internal CO_2 concentration was largely unaffected in control plants by the treatment, but significantly increased in CYND+FDH plants by 10%. These data suggest that leaf internal CO_2 might be enhanced in CYND+FDH plants by CO_2 release from KCN.

Table 19. Gas exchange measurements of transgenic lines and azygous controls in the presence and absence of KCN (means derived from at least six independent plants ± SE).

	-KCN		+KCN	
	Azygous	**FDH+CYND-4**	**Azygous**	**FDH+CYND-4**
Assimilation rate (μmol CO_2 $m^{-2}s^{-1}$)	15.11 ($\pm$ 0.58)	15.39 ($\pm$ 0.35)	13.01 ($\pm$ 0.5)	15.76 ($\pm$0.55)[**]
Internal CO_2 concentration (C_i) (μmol $m^{-2}s^{-1}$)	211.31 ($\pm$ 9.2)	217.76 ($\pm$ 5.7)	201.41 ($\pm$ 7.9)	237.23 ($\pm$ 4.0)[***]
Stomatal Conductance (mol H_2O $m^{-2}s^{-1}$)	0.152 ($\pm$ 0.016)	0.164 ($\pm$ 0.011)	0.130 ($\pm$ 0.012)	0.149 ($\pm$ 0.013)
Transpiration (mol H_2O $m^{-2}s^{-1}$)	1.81 ($\pm$ 0.19)	1.93 ($\pm$ 0.12)	1.56 ($\pm$ 0.15)	1.78 ($\pm$ 0.16)

* = $p<0.05$, ** = $p<0.01$, *** = $p<0.001$ relative to azygous control.

4. Discussion

The goal of this study was to provide additional methods to enhance plant tolerance to abiotic stresses. Two different approaches were carried out during this study. The first objective was to improve the photorespiration cycle that is now known to be an important part in stress response in green tissues to prevent ROS accumulation and protect photosynthesis from photoinhibition (Voss et al., 2013). Photorespiration was reported to increase under abiotic stresses (Miller et al., 2010b). Several attempts were reported in the past few years to manipulate the photorespiration pathway to save CO_2, NH_3 and energy (Kebeish et al., 2007; Andersson, 2008; Carvalho et al., 2011; Maier et al., 2012). Kebeish et al. (2007) established a chloroplastic pathway in Arabidopsis plants aiming to improve photorespiration and provide CO_2 in the vicinity of Rubisco. In that pathway a bacterial GlcDH consisting of three functional genes was used to oxidize glycolate. In this study, I introduced a new GlcDH candidate from *Chlamydomonas* consisting of a single gene that could replace the three genes in the Kebeish et al (2007) bypass.

The second objective was to introduce a novel pathway into Arabidopsis plants to improve cyanide detoxification. The cyanide was reported to be biosynthesized as a co-product of ethylene and can increase under certain conditions such as abiotic stresses (Tittle et al., 1990) that could be a threat to the plants. Introduction of an efficient pathway to enhance cyanide detoxification and assimilation could have advantages for crop improvement.

4.1. Biochemistry and physiological relevance of GlcDH enzymes

When comparing enzymatic properties of the *Cr*GlcDH recombinant enzyme in this study to those reported previously for a *Chlamydomonas* protein fraction containing GlcDH activity (Nelson and Tolbert, 1970), multiple similarities were observed indicating that *Cr*GlcDH is indeed the enzyme that was enzymatically described in the previous study. The K_m for glycolate was almost identical, whereas the K_m for D-lactate was slightly lower for the recombinant enzyme compared to the enriched fraction (Table 17). The pH optimum was in the slightly alkaline range in both studies (Figure 13) and the degree of inhibition by various inhibitors (Table 18) was very much comparable. Specifically, both the recombinant enzyme and the enriched fraction only showed enzymatic activity with artificial electron acceptors, but not with any of the tested naturally occurring electron acceptors (Table 16). It has been shown for several chlorophytes green algae that mitochondrial GlcDH activity *in vivo* is linked to O_2 consumption

via the mitochondrial electron transport chain (METC) (Paul et al., 1975; Stabenau and Winkler, 2005). Moreover, both in chlorophytes (Beezley et al., 1976) and *E. coli* (Sallal and Nimer, 1989), GlcDH activity has been shown to be associated with membranes by cytochemical assays or subcellular fractionation, respectively. Membrane association is also in agreement with the low solubility of the recombinant protein in our assays (data not shown). Therefore I suggest that *Cr*GlcDH is a membrane-bound mitochondrial enzyme that feeds electrons from oxidation of glycolate into the METC.

Consistent with this hypothesis, mutational analyses of a potential Fe-S-cluster in the C-terminal GlcF-homology region indicate an important function of this domain in electron transport (Figure 14). However, there are conflicting data in the literature concerning the strict requirement of GlcF or a GlcF-homology region for GlcDH activity. A glcF knockout in *E. coli* resulted in a complete loss of GlcDH activity in protein extracts (Pellicer et al., 1996). On the other hand, the recombinantly expressed GlcD protein from Synechocystis showed GlcDH activity (Eisenhut et al., 2006). Previous studies provided physiological evidence that a GlcD homologue in higher plant mitochondria (encoded by At5g06580, Bari et al., 2004; Niessen et al., 2007, 2012)) oxidizes glycolate to glyoxylate. This enzyme also does not contain a GlcF homology domain and was suggested to oxidize glycolate in parallel to the peroxisomal GOX that is typical for plants. However, a recent enzymatic characterization revealed that the recombinant enzyme showed much higher activity with D-lactate compared to glycolate as a substrate questioning its role in glycolate metabolism and suggesting a function in the methylglyoxal pathway (Engqvist et al., 2009). Side-by-side activity assays with proteins from different sources would be required to conclusively judge about the role of the GlcF domain in function of GlcDH enzymes from different sources.

Why do different clades use different enzymes for glycolate oxidation? Table 20 provides a comparison with data from selected previous studies on GOX and GlcDH enzymes. The most evident difference between the enzymes is the lower specific activity of GlcDH compared to GOX enzymes. The recruitment of GOX into photorespiration might therefore be a consequence of the much higher flux rates through photorespiration in most land plants compared to aquatic photosynthetic organisms that express carbon concentrating mechanisms (Raven et al., 2008; Wang et al., 2011; Price et al., 2013).

4.2. Evolution of glycolate dehydrogenases

*Cr*GlcDH was originally identified in a mutant screen in *Chlamydomonas* and suggested to encode a GlcDH based on its homology to GlcD and GlcF from *E. coli* (Nakamura et al., 2005). However, when searching nearest homologues to *Cr*GlcDH in the available sequence information, another so far biochemically uncharacterized group of enzymes from proteobacteria was identified as the nearest homology group (Figure 11). There was not obvious homology to GlcE, the third subunit of *Ec*GlcDH, in any of these proteins, although GlcE has been shown to be essential for activity of the 3-subunit GlcDH enzymes by mutant analyses in *E. coli* (Pellicer et al., 1996). The tested proteobacteria containing a *Cr*GlcDH homologue still in addition contained the glc operon with separated GlcD, GlcE and GlcF subunits. Consistent with this observation, the nearest homologue from *Desulfovibrio* did not accept glycolate as a substrate (Figure 18). Thus, enzymes of the *Cr*GlcDH homology group probably only evolved specificity for glycolate as a substrate in chlorophytes.

There is no simple explanation for the appearance of *Cr*GlcDH homologues in only two evolutionary widely separated lineages. Mitochondria and some alpha-proteobacteria share a common ancestor (Richards and Archibald, 2011). The gene might therefore have been transferred during mitochondrial endosymbiosis. This is consistent with the mitochondrial localization of *Cr*GlcDH (Beezley et al., 1976; Nakamura et al., 2005). However, this scenario would imply that the homologue was lost in most eukaryotic lineages after mitochondrial endosymbiosis. Thus, the more parsimonious explanation for the observed clustering is that *Cr*GlcDH homologues in chlorophytes and proteobacteria evolved independently and might serve different functions in lactate and glycolate metabolism, respectively.

Table 20. Comparison of specific activities of GlcDH and GOX from different organisms.

Enzyme	Organism	Specific activity (μmol min^{-1} mg^{-1})	K$_m$ values (for glycolate, mM)	Reference
GlcDH	*E.coli* extract	0.14-3.1	0.04	Lord et al (1971)
GlcDH	*Chlamydomonas* (E. coli derived)	1	0.21	This publication
GOX	Pea leaf extract	30	0.25	Kerr and Groves (1975)
GOX	Spinach (*E.coli* derived)	26	0.2	Macheroux et al (1992)

4.3. Establishment of a novel pathway in *Arabidopsis thaliana* for cyanide detoxification

In this study I tested an approach for the enhancement of cyanide tolerance in plants. The introduced pathway is synthetic, since it combines bacterial and plant elements (CYND and FDH; respectively). The used cyanidase (CYND) enzyme in this study was derived from *Pseudomonas stutzeri* AK61. The enzyme was previously characterized and its catalytic properties were reported (Watanabe et al., 1998). Furthermore, formate dehydrogenase (FDH) was derived from *Arabidopsis thaliana*. Combination of both enzymes would result in complete oxidation of cyanide to NH_3 (resulting from the CYND reaction) and CO_2 (resulting from the FDH reaction). This was not further enhanced by simultaneous expression of FDH as expected. CO_2 release from formate is difficult to measure because of the refixation of CO_2 in the chloroplast by photosynthesis. However, gas exchange measurements data indicated that leaf internal CO_2 was enhanced in CYND+FDH plants and that this effect was dependent on KCN application. This suggested that both enzymes cooperate *in planta* in the decomposition of cyanide to two gases that are both useful substrates for plant biosynthesis.

Photosynthetic measurements indicated that FDH is important for CO_2 production from cyanide in the leaf. An alternative interpretation of the importance of FDH in the synthetic detoxification pathway would be that FDH simply removed toxic formate resulting from the CYND reaction

that might otherwise accumulate. Formate is an natural endogenous compound in plants resulting from non-enzymatic decarboxylation of photorespiratory glyoxylate in peroxisomes (Wingler et al., 2000). It can be used as a C1-donor (Wingler et al., 2000) or can be oxidized by the endogenous formate dehydrogenase that is mainly targeted to mitochondria (Hourton-Cabassa et al., 1998) (although dual targeting to mitochondria and chloroplasts has been reported for Arabidopsis (Herman et al., 2002). There are different reports about the impact of externally applied formate on plants. Whereas low amounts of formate in the growth substrate might even promote growth (Shiraishi et al., 2000), higher concentrations delay germination or affect plant growth (Li et al., 2002; Himanen et al., 2012). Consequently, FDH overexpression protected plants from formate toxicity (Li et al., 2002). This detoxification of excess formate might be also the major function of FDH in our synthetic cyanide degradation pathway.

4.4. Influence of the synthetic pathway on plant resistance to cyanide

Soil contamination is the major source of cyanide toxicity to plants (Trapp et al., 2003). Noteworthy, a significant amount of exogenously applied cyanide is not metabolized in roots, but ends up in shoots (Yu et al., 2012). I used three different methods to test resistance of CYND+FDH plants to cyanide contamination of growth substrates (See 2.2.3.7). In all these assays, CYND+FDH plants performed significantly better than controls and this effect was always dependent on cyanide application indicating that the observed phenotype is not due to any secondary effect of transgene overexpression on growth. Thus, CNYD+FDH plants might be suitable for detoxification of soils containing increased amounts of cyanides that are not tolerated by other plants. For example, willow trees can detoxify up to 10 mg cyanide per kg fw, but rapidly die at concentrations of > 2 mM (Larsen and Trapp, 2006). Sorghum bicolor can even survive such concentrations in the growth substrate by degrading cyanide that was uptaken (Trapp et al., 2003). Seedlings of the model plant Arabidopsis are sensitive to cyanides and show growth defects even when exposed to concentrations around 50-100μM of cyanide (García et al., 2010; McMahon Smith and Arteca, 2000; O'Leary et al., 2014). In contrast, CYND+FDH plants survived concentrations up to 300μM without visible signs of stress. It remains to be shown in further studies whether this approach is also effective in other species that have higher capacities for endogenous cyanide metabolism.

It is useful to compare observed effects of CYND+FDH overexpression to another recently published transgenic approach towards enhanced cyanide resistance of Arabidopsis that was based on enhancing the endogenous pathway for cyanide detoxification (O'Leary et al., 2014) through boosting the downstream flux of cyanide to asparagine. O'Leary et al (2014) overexpressed the *Pseudomonas fluorescens* β-cyanoalanine nitrilase pinA in Arabidopsis plants. PinA enzyme is a downstream enzyme in the cyanide assimilation pathway that metabolizes the toxic ß-cyanoalanine compound that results from the incorporation of cyanide and cysteine by catalysis of the mitochondrial ß-cyanoalanine synthase (CAS) enzyme. Plant growth analyses in this study were focused on seedlings grown on agar plates containing 50µM KCN and are, thus, best compared to the root length data shown in Figure 20 (250µM cyanide in agar plates). In both studies, root growth was reduced by approximately 50% after cyanide treatment in the WT, but fully restored by the transgenic intervention. Whereas carbon and nitrogen from cyanide was assimilated via formation of the amino acid asparagine in the endogenous pathway, the synthetic pathway released gaseous NH_3 and CO_2 that were probably re-assimilated by plant primary carbon and nitrogen assimilation pathways. Additional energy and reducing power would be required for re-fixation via gaseous intermediates (Peterhansel et al., 2010) compared to direct formation of amino acids. Together, these results indicate that both boosting the endogenous pathway and addition of a synthetic pathway were instrumental in enhancing cyanide resistance. It would be interesting to see whether both approaches can additively enhance cyanide metabolism in plants and facilitate the use of plants in bioremediation of toxic cyanide contaminations.

5. Conclusion

Overall most of the goals were fulfilled by this study: *Cr*GlcDH protein from *Chlamydomonas reinhardtii* was recombinantly overexpressed successfully purified and its enzymatic properties were studied. This protein was confirmed to be a glycolate dehydrogenase enzyme using both glycolate and $_D$-lactate as substrates, a typical feature of GlcDH enzymes. Additional mutational experiments would be interesting to identify the active site of this enzyme and figure out the evolutionary role of different amino acids controlling substrate specificity.

In addition, the second goal was also achieved: a new pathway for cyanide detoxification was established in *Arabidopsis thaliana*. The results showed that the pathway was effective in cyanide detoxification under tested conditions in this study. The results are still preliminary and additional studies might be required to test this pathway in other plants and under different conditions. Comparing this synthetic pathway with other plants that have reported to normally detoxify cyanide would be interesting experiments to see how efficient is the synthetic pathway described in this study.

6. Appendix

6.1. Supplementary material

S1: Codon-optimized nucleotide sequence of *Cr*GlcDH.

```
ATGGGCGCGAGAGGTCCTGCATCTCCTTCAAGTCTTGAGCAACAAACCAGACAAGTTGCGCAAGT
TGCTGTTCAACAGTCTACGCAACAGGCTGTTAAGGTTGTTGTGCCTGCTATCAAGGTTGATCTAG
TTGGAGCTGTCTCATCTGTGTCTGAGTCTGACAAGGTTGAACCTGGTGTCTTCAAGAACGTTGAT
GGACATCGTTTCGAAGACGGAAGATACGCTGCATTCGTTGAGGAGATCACGAAGTTCATCCCTAA
GGAGAGGCAATACTCCGATCCAGTTAGAACCTTCGCTTACGGTACAGATGCTTCTTTCTACAGGC
TCAACCCTAAGCTAGTCGTTAAGGTCCATAACGAGGACGAAGTTAGAAGAATCATGCCAATCGCT
GAGAGACTGCAAGTTCCAATCACTTTCAGAGCAGCTGGAACATCTCTTTCTGGACAAGCTATCAC
GGATTCTGTCCTTATCAAGCTTTCCCATACTGGTAAGAACTTCAGGAACTTCACGGTTCACGGTG
ATGGTTCTGTGATCACTGTTGAACCTGGACTTATCGGAGGAGAGGTTAACAGAATCCTGGCAGCT
CATCAGAAGAAGAACAAGCTGCCGATACAGTACAAGATTGGACCTGATCCCAGTTCTATCGACTC
TTGCATGATCGGAGGTATCGTCTCCAACAACTCTTCAGGAATGTGTTGTGGCGTTTCCCAAAACA
CCTACCATACTCTGAAGGACATGCGAGTCGTTTTCGTTGACGGAACAGTCTTGGATACAGCTGAT
CCTAACAGCTGCACTGCTTTCATGAAGAGTCATAGGTCTCTCGTTGATGGTGTTGTTTCCCTTGC
TAGGAGAGTTCAAGCTGATAAGGAGTTGACTGCCCTAATCCGCAGAAAGTTCGCTATCAAATGCA
CTACAGGATACTCCCTTAACGCTCTTGTTGACTTCCCTGTCGATAACCCTATCGAGATCATCAAG
CACCTCATCATAGGATCAGAAGGCACTCTTGGATTCGTGTCGAGAGCTACATACAACACCGTTCC
TGAATGGCCTAACAAGGCTTCTGCTTTCATCGTCTTCCCTGATGTTAGAGCAGCTTGCACAGGAG
CTTCAGTTCTGAGAAACGAGACGTCTGTTGATGCGGTTGAGTTGTTCGATAGAGCATCCTTGAGA
GAGTGCGAGAACAACGAGGATATGATGAGGCTGGTTCCAGACATCAAGGGATGCGATCCTATGGC
AGCTGCTCTTCTAATCGAGTGTAGAGGACAAGATGAAGCAGCTCTTCAGTCTAGAATCGAGGAGG
TTGTTCGTGTTCTTACTGCAGCTGGACTTCCTTTTGGAGCTAAAGCAGCTCAACCAATGGCTATC
GATGCTTACCCTTTCCATCACGATCAGAAGAACGCTAAGGTCTTCTGGGACGTTAGAAGAGGTCT
CATACCGATAGTTGGAGCTGCAAGAGAACCTGGAACTTCTATGCTCATCGAAGACGTTGCTTGTC
CTGTTGATAAGCTTGCGGACATGATGATCGACCTCATCGATATGTTCCAACGACACGGCTACCAT
GATGCTTCATGTTTCGGACATGCTCTAGAGGGAAACCTCCATCTTGTGTTCAGTCAAGGATTCCG
CAACAAGGAAGAGGTTCAACGGTTCAGTGACATGATGGAGGAGATGTGCCATCTTGTTGCTACAA
AGCACTCTGGTTCGCTTAAGGGAGAACATGGGACTGGAAGAAACGTTGCACCCTTTGTTGAGATG
GAATGGGGAAACAAGGCTTATGAGCTTATGTGGGAGCTAAAGGCACTTTTCGATCCAAGCCATAC
CCTAAACCCTGGGGGTTATCCTAAACCGAGATCAGGACGCTCACATCAAGTTCCTTAAGCCATCTC
CAGCTGCATCTCCAATCGTCAACAGATGTATCGAGTGCGGATTCTGCGAGTCTAACTGTCCATCA
CGAGACATCACTCTGACACCTAGGCAAAGGATCTCTGTGTACAGAGAGATGTACAGACTCAAGCA
ACTTGGACCTGGAGCATCTGAAGAGGAAAAGAAGCAACTTGCAGCTATGTCGTCTTCATACGCTT
ACGATGGAGAGCAAACTTGCGCAGCTGATGGAATGTGCCAAGAGAAGTGTCCAGTCAAGATCAAC
ACTGGAGATCTGATCAAGTCTATGAGAGCCGAGCACATGAAGGAAGAGAAAACAGCTTCTGGAAT
GGCAGATTGGCTTGCTGCAAACTTCGGTGTTATCAACTCCAACGTTCCCAGATTCCTGAACATCG
TCAACGCTATGCATTCTGTCGTTGGAAGTGCTCCTCTTTCAGCTATCTCTAGAGCACTTAACGCT
```

GCTACCAACCATTTCGTTCCAGTTTGGAACCCTTACATGCCTAAAGGAGCTGCTCCACTTAAGGT
TCCTGCACCTCCTGCTCCTGCTGCTGCTGAGGCTTCTGGTATCCCTAGAAAGGTTGTGTACATGC
CCAGTTGTGTTACTCGGATGATGGGTCCTGCTGCATCTGATACTGAGACTGCTGCTGTTCACGAG
AAAGTGATGTCTCTCTTCGGTAAGGCAGGATACGAAGTGATCATACCAGAAGGTGTTGCAAGCCA
ATGTTGCGGAATGATGTTCAACTCTAGAGGCTTCAAGGATGCTGCTGCTTCAAAAGGAGCTGAAC
TTGAGGCAGCTCTTTTGAAGGCATCTGACAACGGAAAGATCCCTATCGTTATCGACACTTCTCCA
TGCCTTGCTCAAGTTAAGTCTCAGATCTCGGAGCCTTCTCTAAGATTTGCCCTTTACGAGCCTGT
TGAGTTCATCAGACACTTCCTTGTTGACAAGCTTGAGTGGAAGAAGGTTCGTGATCAAGTTGCCA
TCCATGTTCCTTGCTCCTCAAAGAAGATGGGAATCGAGGAGTCTTTCGCTAAACTTGCTGGACTT
TGTGCTAACGAGGTGGTTCCATCTGGAATACCATGTTGTGGAATGGCTGGAGATCGTGGAATGAG
ATTCCCTGAGCTAACAGGAGCTTCTCTACAACACCTGAACCTTCCTAAGACGTGTAAGGACGGTT
ACTCAACGTCTAGAACCTGTGAGATGAGCCTTTCAAACCATGCTGGAATCAACTTCCGTGGACTT
GTTTACCTAGTCGATGAGGCTACTGCACCTAAGAAACAAGCAGCTGCAGCTAAGACGGCTTAA

S2. Identification of partially purified *Cr*GlcDH by mass spectrometry. band 1-3 refers to protein bands that were cut from the gel after purification of His-tagged *Cr*GlcDH (see Figure 1 of the main text). Proteins are listed sorted according to Mascot Scores (cut-off =50).

Location	Accession	Name	DB Name	MW [kDa]	Mascot Score	Peptides	SC [%]
band 1	gi|159474536	glycolate dehydrogenase [Chlamydomonas reinhardtii]	NCBInr (NCBInr_20130109.fa	118.8	2813.8	95	53.9726
band 1	gi|14719762	Chain A, Methylobacterium Extorquens Methanol Dehydrogenase	NCBInr (NCBInr_20130109.fa	65.8	1044.9	24	41.90317
band 1	gi|11935049	keratin 1 [Homo sapiens]	NCBInr (NCBInr_20090925.fa	66.0	813.3	17	20.18634
band 1	gi|375314779	keratin 1 [Homo sapiens]	NCBInr (NCBInr_20120322.fa	66.0	741.0	16	20.18634
band 1	gi|28317	unnamed protein product [Homo sapiens]	NCBInr (NCBInr_20100610.fa	59.5	671.8	17	24.78921
band 1	gi|240142560	hypothetical protein MexAM1_META2p0918 [Methylobacterium extorquens AM1]	NCBInr (NCBInr_20130109.fa	32.1	470.5	13	36.51316
band 1	gi|435476	cytokeratin 9 [Homo sapiens]	NCBInr (NCBInr_20100513.fa	62.1	424.5	10	15.56982
band 1	gi|431921648	Keratin, type II cytoskeletal 1 [Pteropus alecto]	NCBInr (NCBInr_20130109.fa	138.1	392.8	8	5.15625
band 1	gi|240142554	protein disaggregation chaperone [Methylobacterium extorquens AM1]	NCBInr (NCBInr_20130109.fa	106.2	386.1	9	12.24066
band 1	gi|403296723	PREDICTED: uncharacterized protein LOC101046470 [Saimiri boliviensis boliviensis]	NCBInr (NCBInr_20130109.fa	65.9	349.2	6	6.965944
band 1	gi|163854178	chaperonin GroEL [Methylobacterium extorquens PA1]	NCBInr (NCBInr_20130109.fa	57.4	292.3	7	15.38462
band 1	gi|153011789	hypothetical protein Oant_4474 [Ochrobactrum anthropi ATCC 49188]	NCBInr (NCBInr_20130109.fa	31.8	265.4	6	18.64407
band 1	gi|291406077	PREDICTED: keratin 13-like [Oryctolagus cuniculus]	NCBInr (NCBInr_20110811.fa	44.4	230.7	6	13.26781
band 1	gi|136429	Trypsin precursor	NCBInr (NCBInr_20080408.fa	24.4	229.5	7	16.45022
band 1	gi|60594122	Chain A, Structure Of The Tetrahydromethanopterin Dependent Formaldehyde-Activating Enzyme (Fae)	NCBInr (NCBInr_20130109.fa	17.9	136.7	4	23.07692
band 1	gi|163851982	phasin [Methylobacterium extorquens PA1]	NCBInr (NCBInr_20130109.fa	17.2	133.7	3	20.88608
band 1	gi|23011810	COG0050: GTPases - translation elongation factors [Magnetospirillum magnetotacticum MS-1]	NCBInr (NCBInr_20130109.fa	46.9	124.3	3	9.411765
band 1	gi|163851229	citrate (pro-3S)-lyase [Methylobacterium extorquens PA1]	NCBInr (NCBInr_20130109.fa	35.4	119.1	4	10.80247
band 1	gi|163850897	F0F1 ATP synthase subunit alpha [Methylobacterium extorquens PA1]	NCBInr (NCBInr_20130109.fa	54.8	100.7	2	4.3222
band 1	gi|434010	unnamed protein product [Escherichia coli]	NCBInr (NCBInr_20080408.fa	99.6	93.0	2	2.595937
band 1	gi|163852837	aldehyde dehydrogenase [Methylobacterium extorquens PA1]	NCBInr (NCBInr_20130109.fa	55.6	90.9	2	3.747535
band 1	gi|15800191	acridine efflux pump [Escherichia coli O157:H7 EDL933]	NCBInr (NCBInr_20080408.fa	113.5	90.0	3	3.527169
band 1	gi|163851438	nucleoside diphosphate kinase [Methylobacterium extorquens PA1]	NCBInr (NCBInr_20130109.fa	15.4	89.1	2	11.42857
band 1	gi|163853870	ROSMUCR transcriptional regulator [Methylobacterium extorquens PA1]	NCBInr (NCBInr_20130109.fa	19.5	85.9	2	10.79545
band 1	gi|23004112	COG0222: Ribosomal protein L7/L12 [Magnetospirillum magnetotacticum MS-1]	NCBInr (NCBInr_20130109.fa	12.8	85.1	3	14.28571
band 1	gi|163852882	acetyl-CoA acetyltransferase [Methylobacterium extorquens PA1]	NCBInr (NCBInr_20130109.fa	40.8	83.0	3	13.45178
band 1	gi|21535798	serine-glyoxylate aminotransferase [Methylobacterium extorquens DM4]	NCBInr (NCBInr_20130109.fa	40.6	79.7	2	6.860158
band 1	gi|84499888	translation elongation factor Tu [Oceanicola batsensis HTCC2597]	NCBInr (NCBInr_20130109.fa	42.8	59.9	2	8.184143
band 1	gi|163851861	ROSMUCR transcriptional regulator [Methylobacterium extorquens PA1]	NCBInr (NCBInr_20130109.fa	15.1	59.6	1	11.88811
band 2	gi|16130190	fused UDP-L-Ara4N formyltransferase/UDP-GlcA C-4'-decarboxylase [Escherichia coli str. K-12 substr. ...	NCBInr (NCBInr_20080408.fa	74.2	1798.6	73	50.15152
band 2	gi|43268	unnamed protein product [Escherichia coli]	NCBInr (NCBInr_20080408.fa	66.8	1276.3	43	44.99179
band 2	gi|11935049	keratin 1 [Homo sapiens]	NCBInr (NCBInr_20090925.fa	66.0	839.6	16	21.73913
band 2	gi|375314779	keratin 1 [Homo sapiens]	NCBInr (NCBInr_20120322.fa	66.0	816.6	16	21.73913
band 2	gi|28317	unnamed protein product [Homo sapiens]	NCBInr (NCBInr_20100610.fa	59.5	722.0	16	22.42833
band 2	gi|181402	epidermal cytokeratin 2 [Homo sapiens]	NCDInr (NCDInr_20090925.fa	65.0	542.6	11	10.44961
band 2	gi|14719762	Chain A, Methylobacterium Extorquens Methanol Dehydrogenase	NCBInr (NCBInr_20130109.fa	65.8	448.7	8	15.35893
band 2	gi|435476	cytokeratin 9 [Homo sapiens]	NCBInr (NCBInr_20100513.fa	62.1	394.3	7	11.55698
band 2	gi|109659947	glycolate dehydrogenase [Chlamydomonas reinhardtii]	NCBInr (NCBInr_20130109.fa	118.8	305.7	8	6.30137
band 2	gi|136429	Trypsin precursor	NCBInr (NCBInr_20080408.fa	24.4	226.3	7	16.45022
band 2	gi|15799694	molecular chaperone DnaK [Escherichia coli O157:H7 EDL933]	NCBInr (NCBInr_20080408.fa	69.1	211.2	7	7.053292
band 2	gi|240142560	hypothetical protein MexAM1_META2p0918 [Methylobacterium extorquens AM1]	NCBInr (NCBInr_20130109.fa	32.1	177.3	4	15.46053
band 2	gi|417401704	Putative nuclear envelope protein lamin intermediate filament superfamily [Desmodus rotundus]	NCBInr (NCBInr_20130109.fa	52.2	176.8	6	7.5
band 2	gi|87119170	succinate dehydrogenase [Marinomonas sp. MED121]	NCBInr (NCBInr_20130109.fa	63.8	159.0	2	3.898305
band 2	gi|60594122	Chain A, Structure Of The Tetrahydromethanopterin Dependent Formaldehyde-Activating Enzyme (Fae)	NCBInr (NCBInr_20130109.fa	17.9	77.2	3	8.87574
band 2	gi|163851982	phasin [Methylobacterium extorquens PA1]	NCBInr (NCBInr_20130109.fa	17.2	73.7	2	12.65823
band 2	gi|254254087	extracellular solute-binding protein [Burkholderia dolosa AUO158]	NCBInr (NCBInr_20130109.fa	34.2	69.5	2	4.100946
band 2	gi|46206059	COG1795: Uncharacterized conserved protein [Magnetospirillum magnetotacticum MS-1]	NCBInr (NCBInr_20130109.fa	7.8	66.2	2	21.12676
band 2	gi|786230	atpA intron1 ORF [Marchantia polymorpha]	NCBInr (NCBInr_20080408.fa	156.9	62.5	1	0.78853
band 2	gi|195375913	GJ13049 [Drosophila virilis]	NCBInr (NCBInr_20130109.fa	309.0	58.8	2	0.454704
band 3	gi|375314779	keratin 1 [Homo sapiens]	NCBInr (NCBInr_20120322.fa	66.0	866.2	23	23.91304
band 3	gi|11935049	keratin 1 [Homo sapiens]	NCBInr (NCBInr_20090925.fa	66.0	859.3	23	23.91304
band 3	gi|28317	unnamed protein product [Homo sapiens]	NCBInr (NCBInr_20100610.fa	59.5	568.7	18	24.95784
band 3	gi|14719762	Chain A, Methylobacterium Extorquens Methanol Dehydrogenase	NCBInr (NCBInr_20130109.fa	65.8	438.3	12	20.03339
band 3	gi|435476	cytokeratin 9 [Homo sapiens]	NCBInr (NCBInr_20100513.fa	62.1	428.1	12	14.60674
band 3	gi|15803862	FKBP-type peptidyl-prolyl cis-trans isomerase (rotamase) [Escherichia coli O157:H7 EDL933]	NCBInr (NCBInr_20080408.fa	20.8	422.5	28	68.87755
band 3	gi|110643589	FKBP-type peptidyl-prolyl cis-trans isomerase (rotamase) [Escherichia coli 536]	NCBInr (NCBInr_20080408.fa	20.9	402.4	26	55.10204
band 3	gi|15803975	cell division protein FtsE [Escherichia coli O157:H7 EDL933]	NCBInr (NCBInr_20080408.fa	24.4	354.6	10	32.43243
band 3	gi|431921648	Keratin, type II cytoskeletal 1 [Pteropus alecto]	NCBInr (NCBInr_20130109.fa	138.1	347.6	8	4.21875
band 3	gi|15803841	30S ribosomal protein S3 [Escherichia coli O157:H7 EDL933]	NCBInr (NCBInr_20080408.fa	26.0	343.6	6	21.45923
band 3	gi|119617032	keratin 6B, isoform CRA_a [Homo sapiens]	NCBInr (NCBInr_20090925.fa	59.9	320.7	9	10.83481
band 3	gi|181402	epidermal cytokeratin 2 [Homo sapiens]	NCBInr (NCBInr_20090925.fa	65.8	314.8	7	7.751938
band 3	gi|344286072	PREDICTED: keratin, type I cytoskeletal 14-like [Loxodonta africana]	NCBInr (NCBInr_20120322.fa	51.9	260.9	7	10.06289
band 3	gi|136429	Trypsin precursor	NCBInr (NCBInr_20080408.fa	24.4	245.6	9	25.10823
band 3	gi|109659947	glycolate dehydrogenase [Chlamydomonas reinhardtii]	NCBInr (NCBInr_20130109.fa	118.8	199.4	7	4.383562
band 3	gi|417376295	FKBP-type peptidyl-prolyl cis-trans isomerase SlyD, partial [Salmonella enterica subsp. enterica serovar	NCBInr (NCBInr_20130109.fa	10.5	197.2	10	20.83333
band 3	gi|60594122	Chain A, Structure Of The Tetrahydromethanopterin Dependent Formaldehyde-Activating Enzyme (Fae)	NCBInr (NCBInr_20130109.fa	17.9	117.0	2	8.87574
band 3	gi|417336877	FKBP-type peptidyl-prolyl cis-trans isomerase SlyD, partial [Salmonella enterica subsp. enterica serovar	NCBInr (NCBInr_20130109.fa	8.8	114.5	9	22.5
band 3	gi|15800428	succinate dehydrogenase iron-sulfur subunit [Escherichia coli O157:H7 EDL933]	NCBInr (NCBInr_20080408.fa	26.8	104.1	2	9.243697
band 3	gi|12513109	orf; Unknown function [Escherichia coli O157:H7 EDL933]	NCBInr (NCBInr_20080408.fa	31.1	89.3	2	6.382979
band 3	gi|153011788	hypothetical protein Oant_4473 [Ochrobactrum anthropi ATCC 49188]	NCBInr (NCBInr_20130109.fa	32.2	81.0	2	9.210526

S3. Evolutionary relationships of *Cr*GlcDH using neighbor-joining method. Bootstrap values (%) are for 500 replicates. Evolutionary distances were computed using the p-distance method. Sequence alignment and evolutionary analyses were conducted in MEGA5.1 software. *Arabidopsis thaliana* GOX was used as an outgroup. Numbers in parentheses are Genbank accession numbers.
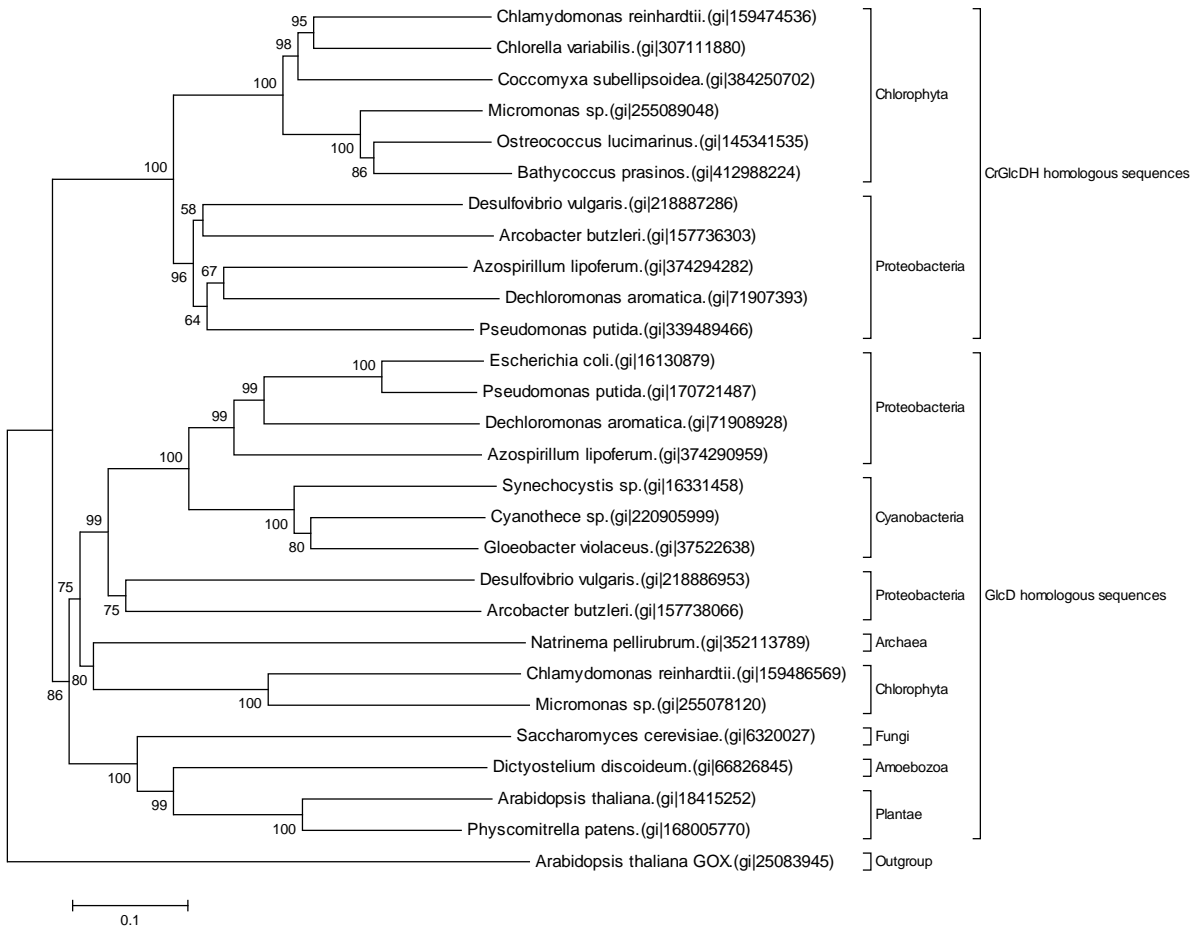
6.2. List of abbreviations

Abbreviation	Full form
Amp	Ampicillin
APS	Ammonium persulfate
Asn	Asparagine
A. thaliana	*Arabidopsis thaliana*
GlcDH	Glycolate dehydrogenase
ATP	Adenosine triphosphate
bla	β--lactamase gene for selection in bacteria (ampicillin/carbenicillin resistance).
bps	Base pairs
BSA	Bovine serum albumin
C_2-cycle	Photorespiratory cycle
C_3-cycle	Benson Calvin cycle
CAT	Catalase
Carb	Carbenicillin
cDNA	Complementary DNA
Ci	The internal CO_2 concentration inside plant leaf
CO2	Carbon dioxide
*Cr*GlcDH	*Clamydomonas rheinhardii* glycolate dehydrogenase
CYND	*Pseudomonas stutzeri AK61* cyanindase
DCIP	2,6 dichlorophenolindophenol sodium salt
D-LDH	D(+)-lactate dehydrogenase
DNA	Deoxyribonucleic acid
dNTP	Deoxyribonucleoside triphosphate
DTT	Dithiothreitol
*Dv*DlDH	*Desulfovibrio vulgaris* $_D$lactate dehydrogenase
DW	Dry weight
*Ec*GlcDH	*E. coli* glycolate dehydrogenase
EDTA	Ethylene diamine tetra acetic acid

FW	Fresh weight
G3P	Glyceraldehyde-3-phosphate
GC/MS	Gas Chromatography/Mass Spectrometry
GDC	Glycine decarboxylase
GDC/SHMT	Glycine decarboxylase/serine hydroxymethyl transferase
GST	Glutathione S-transferase fusion protein
GK	Glycerate kinase
*Glc*D	Coding sequence for the D subunit of glycolate dehydrogenase in *E. coli*
*Glc*E	Coding sequence for the E subunit of glycolate dehydrogenase in *E. coli*
*Glc*F	Coding sequence for the F subunit of glycolate dehydrogenase in *E. coli*
GOGAT	Glutamate:glyoxylate aminotransferase
GOX	Glycolate oxidase
GS	Glutamine synthetase
h	Hour
Hepes	N-2-hydroxyethylpiperazine-N´-2-ethanesulfonic acid
His	The coding sequence for His-tag protein
HPR	Hydroxypyruvate reductase
IPTG	Isopropyl-β-D-thiogalactoside
Kan	Kanamycin
kDa	Kilodalton
Km	Michaelis constant
LB medium	Luria Bertani medium
MBP	Maltose binding protein fusion tag
mg	Milligram
min	Minute
mM	Milli mol
ml	Milli liter
mRNA	Messenger RNA
MS medium	Murashige and Skoog Basal medium
mTP	Mitochondrial targeting peptide

µg	Microgram
µl	Micro liter
µM	Micro mol
NAD+/NADH	Nicotinamide adenine dinucleotide (oxidized/reduced form)
NADP+/NADPH	Nicotinamide adenine dinucleotide phosphate (oxidized/reduced form)
OD	Optical density
ON	overnight
p35SS/pA35S	Promotor (duplication) and polyadenylation-/termination sequence from CaMV
PAnos	Polyadenylation promoter of nopaline synthetase gene from *A.tumefaciens*
PCR	Polymerase chain reaction
PCR-cycle	Photosynthetic carbon reduction cycle
PG	Phosphoglycolate
PGA	Phosphoglycerate
PGP	Phosphoglycolate phosphatase
PMS	Phenazine methosulfate
Pnos	Promoter of nopaline synthase gene from *A. tumefaciens*.
PYR	Pyruvate
Rif	Rifampicin
RNA	Ribonucleic acid
rpm	Rotation per minute
RT	Room temperature
RT	Reverse transcriptase
RT-PCR	Reverse transcriptase-polymerase chain reaction
Rubisco	Ribulose 1,5 bisphosphate carboxylase/oxygenase
RuBP	Ribulose 1, 5 bisphosphate
SDS-PAGE	Sodium dodecyl sulphate-polyacrylamide gel electrophoresis
sec	Second
SE	Standard error
SGAT	Serine:glutamate aminotransferase

TAE	Tris-acetate-EDTA-buffer
TEMED	N, N, N´, N´-tetramethyl ethylene diamine
Tris	Tris-acetate-EDTA-buffer
UV	Ultraviolet
x	Times
xg	Apparent gravity
Y(II)	photosynthetic yield
v/v	Volume per volume
w/v	Weight per volume
WT	Wild type

6.3. List of figures

APPENDIX

APPENDIX

6.4. List of tables

6.5. References

Akcil, A. (2003). Destruction of cyanide in gold mill effluents: biological versus chemical treatments. Biotechnol. Adv. **21**: 501–11.

Akcil, A. and Mudder, T. (2003). Microbial destruction of cyanide wastes in gold mining: process review. Biotechnol. Lett. **25**: 445–50.

Altschul, S.F., Madden, T.L., Schäffer, A.A., Zhang, J., Zhang, Z., Miller, W., and Lipman, D.J. (1997). Gapped BLAST and PSI-BLAST: a new generation of protein database search programs. Nucleic Acids Res. **25**: 3389–02.

Andersson, I. (2008). Catalysis and regulation in Rubisco. J. Exp. Bot. **59**: 1555–68.

Ausubel, F.M., Brent, R., Kingston, R.E., Moore, D.D., Seidman, J.G., Smith, J.A., and Struhl, K. eds. (2001). Current protocols in molecular biology. Wiley Interscience, New York.

Bari, R., Kebeish, R., Kalamajka, R., Rademacher, T., and Peterhänsel, C. (2004). A glycolate dehydrogenase in the mitochondria of *Arabidopsis thaliana*. J. Exp. Bot. **55**: 623–30.

Bauwe, H., Hagemann, M., and Fernie, A.R. (2010). Photorespiration: players, partners and origin. Trends Plant Sci. **15**: 330–36.

Bauwe, H. and Kolukisaoglu, U. (2003). Genetic manipulation of glycine decarboxylation. J. Exp. Bot. **54**: 1523–35.

Bertani, G. (2004). Lysogeny at mid-twentieth century: P1, P2, and other experimental systems. J. Bacteriol. **186**: 595–600.

Blankenship, R.E. (2010). Early evolution of photosynthesis. Plant Physiol. **154**: 434–38.

Boldt, R., Edner, C., Kolukisaoglu, U., Hagemann, M., Weckwerth, W., Wienkoop, S., Morgenthal, K., and Bauwe, H. (2005). D-glycerate 3 kinase, the last unknown enzyme in

the photorespiratory cycle in Arabidopsis, belongs to a novel kinase family. Plant Cell **17**: 2413–20.

Bradford, M.M. (1976). A rapid and sensitive method for the quantitation of microgram quantities of protein utilizing the principle of protein-dye binding. Anal. Biochem. **72**: 248–54.

Carvalho, J.D.F.C., Madgwick, P.J., Powers, S.J., Keys, A.J., Lea, P.J., and Parry, M. a J. (2011). An engineered pathway for glyoxylate metabolism in tobacco plants aimed to avoid the release of ammonia in photorespiration. BMC Biotechnol. **11**: 111.

Clough, S.J. and Bent, A.F. (1998). Floral dip: a simplified method for Agrobacterium-mediated transformation of *Arabidopsis thaliana*. Plant J. **16**: 735–43.

Cossins, E.A. and Chen, L. (1997). Folates and one-carbon metabolism in plants and fungi. Phytochemistry **45**: 437–52.

Douce, R., Bourguignon, J., Neuburger, M., and Rébeillé, F. (2001). The glycine decarboxylase system: a fascinating complex. Trends Plant Sci. **6**: 167–76.

Ebbs, S., Bushey, J., Poston, S., Kosma, D., Samiotakis, M., and Dzombak, D. (2003). Transport and metabolism of free cyanide and iron cyanide complexes by willow. Plant, Cell Env. **26**:1467–78.

Edenborn, H.M. and Litchfield, C.D. (1985). Glycolate metabolism by *Pseudomonas sp*., strain S227, isolated from a coastal marine sediment. Mar. Biol. **88**: 199–05.

Eisenhut, M., Ruth, W., Haimovich, M., Bauwe, H., Kaplan, A., and Hagemann, M. (2008). The photorespiratory glycolate metabolism is essential for cyanobacteria and might have been conveyed endosymbiontically to plants. Proc. Natl. Acad. Sci. U. S. A. **105**: 17199–04.

Engel, N., van den Daele, K., Kolukisaoglu, U., Morgenthal, K., Weckwerth, W., Pärnik, T., Keerberg, O., and Bauwe, H. (2007). Deletion of glycine decarboxylase in Arabidopsis is lethal under nonphotorespiratory conditions. Plant Physiol. **144**: 1328–35.

Fahnenstich, H., Scarpeci, T.E., Valle, E.M., Flügge, U.-I., and Maurino, V.G. (2008). Generation of hydrogen peroxide in chloroplasts of Arabidopsis overexpressing glycolate oxidase as an inducible system to study oxidative stress. Plant Physiol. **148**: 719–29.

Foyer, C.H., Bloom, A.J., Queval, G., and Noctor, G. (2009). Photorespiratory metabolism: genes, mutants, energetics, and redox signaling. Annu. Rev. Plant Biol. **60**: 455–84.

Gallagher, L.A. and Manoil, C. (2001). *Pseudomonas aeruginosa PAO1* kills *Caenorhabditis elegans* by cyanide poisoning. J. Bacteriol. **183**: 6207–14.

García, I., Castellano, J.M., Vioque, B., Solano, R., Gotor, C., and Romero, L.C. (2010). Mitochondrial beta-cyanoalanine synthase is essential for root hair formation in *Arabidopsis thaliana*. Plant Cell **22**: 3268–79.

Givan, C. V and Kleczkowski, L.A. (1992). The enzymic reduction of glyoxylate and hydroxypyruvate in leaves of higher plants. Plant Physiol. **100**: 552–6.

Goudey, J.S., Tittle, F.L., and Spencer, M.S. (1989). A role for ethylene in the metabolism of cyanide by higher plants. Plant Physiol. **89**: 1306–10.

Hagemann, M., Fernie, A. R., Espie, G.S., Kern, R., Eisenhut, M., Reumann, S., Bauwe, H., and Weber, A. P.M. (2013). Evolution of the biochemistry of the photorespiratory C_2 cycle. Plant Biol. (Stuttg). **15**: 639–47.

Hansen, R.W. and Hayashi, J.A. (1962). Glycolate metabolism in *Escherichia coli*. J. Bacteriol. **83**: 679–87.

Henny, C.J., Hallock, R.J., and Hill, E.F. (1994). Cyanide and migratory birds at gold mines in Nevada, USA. Ecotoxicology **3**: 45–58.

Herman, P.L., Ramberg, H., Baack, R.D., Markwell, J., and Osterman, J.C. (2002). Formate dehydrogenase in *Arabidopsis thaliana*: overexpression and subcellular localization in leaves. Plant Sci. **163**: 1137–45.

Hew, C.S. and Krotkov, G. (1968). Effect of oxygen on the rates of CO_2 evolution in light and in darkness by photosynthesizing and non-photosynthesizing leaves. Plant Physiol. **43**: 464–66.

Himanen, M., Prochazka, P., Hänninen, K., and Oikari, A. (2012). Phytotoxicity of low-weight carboxylic acids. Chemosphere **88**: 426–31.

Hourton-Cabassa, C., Ambard-Bretteville, F., Moreau, F., Davy de Virville J, Rémy, R., and Francs-Small, C. (1998). Stress induction of mitochondrial formate dehydrogenase in Potato leaves. Plant Physiol. **116**: 627–35.

Husic, H.D. and Tolbert, N.E. (1984). Anion and divalent cation activation of phosphoglycolate phosphatase from leaves. Arch. Biochem. Biophys. **229**: 64–72.

Igarashi, D., Miwa, T., Seki, M., Kobayashi, M., Kato, T., and Tabata, S. (2003). Identification of photorespiratory glutamate☐: glyoxylate aminotransferase (GGAT) gene in Arabidopsis. The plant J. **33**:975-87.

Igarashi, D., Tsuchida, H., Miyao, M., and Ohsumi, C. (2006). Glutamate:glyoxylate aminotransferase modulates amino acid content during photorespiration. Plant Physiol. **142**: 901–10.

Ingvorsen, K., Højer-Pedersen, B., and Godtfredsen, S.E. (1991). Novel cyanide-hydrolyzing enzyme from *Alcaligenes xylosoxidans* subsp. denitrificans. Appl. Environ. Microbiol. **57**: 1783–89.

Jandhyala, D., Berman, M., Meyers, P.R., Sewell, B.T., Willson, R.C., and Benedik, M.J. (2003). CynD, the Cyanide Dihydratase from *Bacillus pumilus*: Gene Cloning and Structural Studies. Appl. Environ. Microbiol. **69**: 4794–05.

Järvi, S., Gollan, P.J., and Aro, E.M. (2013). Understanding the roles of the thylakoid lumen in photosynthesis regulation. Front. Plant Sci. **4**: 434.

Kebeish, R., Niessen, M., Thiruveedhi, K., Bari, R., Hirsch, H.J., Rosenkranz, R., Stäbler, N., Schönfeld, B., Kreuzaler, F., and Peterhänsel, C. (2007). Chloroplastic

photorespiratory bypass increases photosynthesis and biomass production in *Arabidopsis thaliana*. Nat. Biotechnol. **25**: 593–99.

Kornberg, H.L. and Morris, J.G. (1965). The utilization of glycolate by *Micrococcus denitrificans*: the beta-hydroxyaspartate pathway. Biochem. J. **95**: 577–86.

Kornberg, H.L. and Sadler, J.R. (1960). Microbial oxidation of glycolate via a dicarboxylic acid cycle. Nature **185**: 153–55.

Kornberg, H.L. and Sadler, J.R. (1961). The metabolism of C_2-compounds in micro-organisms. VIII. A dicarboxylic acid cycle as a route for the oxidation of glycolate by Escherichia coli. Biochem. J. **81**: 503–13.

Korte, F., Spiteller, M., and Coulston, F. (2000). The cyanide leaching gold recovery process is a nonsustainable technology with unacceptable impacts on ecosystems and humans: the disaster in Romania. Ecotoxicol. Environ. Saf. **46**: 241–45.

Ku, M.S., Agarie, S., Nomura, M., Fukayama, H., Tsuchida, H., Ono, K., Hirose, S., Toki, S., Miyao, M., and Matsuoka, M. (1999). High-level expression of maize phosphoenolpyruvate carboxylase in transgenic rice plants. Nat. Biotechnol. **17**: 76–80.

Laemmli, U.K. (1970). Cleavage of structural proteins during the assembly of the head of bacteriophage T4. Nature **227**: 680–85.

Larsen, M. and Trapp, S. (2006). Uptake of iron cyanide complexes into willow trees. Environ. Sci. Technol. **40**: 1956–61.

Larsen, M., Ucisik, A.S., and Trapp, S. (2005). Uptake, metabolism, accumulation and toxicity of cyanide in Willow trees. Environ. Sci. Technol. **39**: 2135–42.

Lau, W.W.Y., Keil, R.G., and Armbrust, E.V. (2007). Succession and diel transcriptional response of the glycolate-utilizing component of the bacterial community during a spring phytoplankton bloom. Appl. Environ. Microbiol. **73**: 2440–50.

Leegood, R.C., Lea, P.J., Adcock, M.D., and Hausler, R.E. (1995). The regulation and control of photorespiration. J. Exp. Bot. **46**: 1397–14.

Li, R., Moore, M., Bonham-Smith, P.C., and King, J. (2002). Overexpression of formate dehydrogenase in *Arabidopsis thaliana* resulted in plants tolerant to high concentrations of formate. J. Plant Physiol. **159**: 1069–76.

Liang, W.-S. (2003). Drought stress increases both cyanogenesis and β-cyanoalanine synthase activity in tobacco. Plant Sci. **165**: 1109–15.

Liepman, A.H. and Olsen, L.J. (2001). Peroxisomal alanine□: glyoxylate aminotransferase (AGT1) is a photorespiratory enzyme with multiple substrates in *Arabidopsis thaliana*. Plant J. **25**: 487–98.

Lord, J.M. (1972). Glycolate oxidoreductase in *Escherichia coli*. Biochim. Biophys. Acta **267**: 227–37.

Lorenz, T.C. (2012). Polymerase chain reaction: basic protocol plus troubleshooting and optimization strategies. J. Vis. Exp. e3998.

Maier, A., Fahnenstich, H., von Caemmerer, S., Engqvist, M.K.M., Weber, A.P.M., Flügge, U.I., and Maurino, V.G. (2012). Transgenic introduction of a glycolate oxidative cycle into *Arabidopsis thaliana* chloroplasts leads to growth improvement. Front. Plant Sci. **3**: 38.

Manning, K. (1988). Detoxification of cyanide by plants and hormone action. Ciba Found. Symp. **140**: 92–10.

Maurino, V.G. and Peterhansel, C. (2010). Photorespiration: current status and approaches for metabolic engineering. Curr. Opin. Plant Biol. **13**: 249–56.

McMahon Smith, J. and Arteca, R.N. (2000). Molecular control of ethylene production by cyanide in *Arabidopsis thaliana*. Physiol. Plant. **109**: 180–87.

Meyer, T.S. and Lamberts, B.L. (1965). Use of coomassie brilliant blue R250 for the electrophoresis of microgram quantities of parotid saliva proteins on acrylamide-gel strips. Biochim. Biophys. Acta **107**: 144–45.

Miller, G., Suzuki, N., Ciftci-Yilmaz, S., and Mittler, R. (2010a). Reactive oxygen species homeostasis and signalling during drought and salinity stresses. Plant. Cell Environ. **33**: 453–67.

Miller, J.M. and Conn, E.E. (1980). Metabolism of hydrogen cyanide by higher plants. Plant Physiol. **65**: 1199–202.

Miziorko, H.M. and Lorimer, G.H. (1983). Ribulose-1,5-bisphosphate carboxylase-oxygenase. Annu. Rev. Biochem. **52**: 507–35.

Murray, a J., Blackwell, R.D., and Lea, P.J. (1989). Metabolism of hydroxypyruvate in a mutant of Barley lacking NADH-dependent hydroxypyruvate reductase, an important photorespiratory enzyme activity. Plant Physiol. **91**: 395–400.

Murray, A.J., Blackwell, R.D., Joy, K.W., and Lea, P.J. (1987). Photorespiratory N donors, aminotransferase specificity and photosynthesis in a mutant of barley deficient in serine: glyoxylate aminotransferase activity. Planta **172**: 106–13.

Nakamura, Y., Kanakagiri, S., Van, K., He, W., and Spalding, M.H. (2005). Disruption of the glycolate dehydrogenase gene in the high-CO_2-requiring mutant HCR89 of *Chlamydomonas reinhardtii*. Can. J. Bot. **83**: 820–33.

Naveen, D., Majumder, C.B., Mondal, P., and Shubha, D. (2011). Biological treatment of cyanide containing wastewater. Res. J. Chem. Sci **1**: 15–21.

Niessen, M., Krause, K., Horst, I., Staebler, N., Klaus, S., Gaertner, S., Kebeish, R., Araujo, W.L., Fernie, A.R., and Peterhansel, C. (2012). Two alanine aminotranferases link mitochondrial glycolate oxidation to the major photorespiratory pathway in Arabidopsis and rice. J. Exp. Bot. **63**: 2705–16.

Niessen, M., Thiruveedhi, K., Rosenkranz, R., Kebeish, R., Hirsch, H.-J., Kreuzaler, F., and Peterhänsel, C. (2007). Mitochondrial glycolate oxidation contributes to photorespiration in higher plants. J. Exp. Bot. **58**: 2709–15.

Norman, E.G. and Colman, B. (1991). Purification and characterization of phosphoglycolate phosphatase from the cyanobacterium *Coccochloris peniocystis* . Plant Physiol. **95**: 693–698.

O'Leary, B., Preston, G.M., and Sweetlove, L.J. (2014). Increased β-cyanoalanine nitrilase activity improves cyanide tolerance and assimilation in Arabidopsis. Mol. Plant **7**: 231–43.

Ogren, W.L. (1984). Photorespiration: pathways, regulation, and modification. Annu. Rev. Plant Physiol. **35**: 415–42.

Oliver, D.J. (1994). The Glycine decarboxylase complex from plant mitochondria. Annu. Rev. Plant Physiol. Plant Mol. Biol. **45**: 323–37.

Osmond, B., Badger, M., Maxwell, K., Björkman, O., and Leegood, R. (1997). Too many photons: photorespiration, photoinhibition and photooxidation. Trends Plant Sci. **2**: 119–21.

Owen, A. and Zdor, R. (2001). Effect of cyanogenic rhizobacteria on the growth of velvetleaf (*Abutilon theophrasti*) and corn (*Zea mays*) in autoclaved soil and the influence of supplemental glycine. Soil Biol. Biochem. **33**: 801–09.

Parry, M.A.J. (2003). Manipulation of Rubisco: the amount, activity, function and regulation. J. Exp. Bot. **54**: 1321–33.

Patil, Y.B. and Paknikar, K.M. (2000). Biodetoxification of silver-cyanide from electroplating industry wastewater. Lett. Appl. Microbiol. **30**: 33–37.

Peiser, G.D., Wang, T.T., Hoffman, N.E., Yang, S.F., Liu, H.W., and Walsh, C.T. (1984). Formation of cyanide from carbon 1 of 1-aminocyclopropane-1-carboxylic acid during its conversion to ethylene. Proc. Natl. Acad. Sci. U. S. A. **81**: 3059–63.

Pellicer, M.T. (1999). Cross-induction of glc and ace Operons of *Escherichia coli* Attributable to Pathway Intersection. Characterization of the glc promotor. J. Biol. Chem. **274**: 1745–52.

Peterhansel, C., Blume, C., and Offermann, S. (2013). Photorespiratory bypasses: how can they work? J. Exp. Bot. **64**: 709–15.

Peterhansel, C., Horst, I., Niessen, M., Blume, C., Kebeish, R., Kürkcüoglu, S., and Kreuzaler, F. (2010). Photorespiration. Arabidopsis Book **8**: e0130.

Pick, T.R., Bräutigam, A., Schulz, M.A., Obata, T., Fernie, A.R., and Weber, A.P.M. (2013). PLGG1, a plastidic glycolate-glycerate transporter, is required for photorespiration and defines a unique class of metabolite transporters. Proc. Natl. Acad. Sci. U. S. A. **110**: 3185–90.

Poulton, J.E. (1988). Localization and catabolism of cyanogenic glycosides. Ciba Found. Symp. **140**: 67–91.

Queval, G., Issakidis-Bourguet, E., Hoeberichts, F. a, Vandorpe, M., Gakière, B., Vanacker, H., Miginiac-Maslow, M., Van Breusegem, F., and Noctor, G. (2007). Conditional oxidative stress responses in the Arabidopsis photorespiratory mutant cat2 demonstrate that redox state is a key modulator of daylength-dependent gene expression, and define photoperiod as a crucial factor in the regulation of H_2O_2-induced cel. Plant J. **52**: 640–57.

Reumann, S., Ma, C., Lemke, S., and Babujee, L. (2004). AraPerox. A database of putative Arabidopsis proteins from plant peroxisomes. Plant Physiol. **136**: 2587–08.

Reumann, S. and Weber, A.P.M. (2006). Plant peroxisomes respire in the light: some gaps of the photorespiratory C_2 cycle have become filled-others remain. Biochim. Biophys. Acta **1763**: 1496–10.

Sage, R.F. (2004). The evolution of C_4 photosynthesis. New phytologist **161**:341–70.

Saiki, R.K., Gelfand, D.H., Stoffel, S., Scharf, S.J., Higuchi, R., Horn, G.T., Mullis, K.B., and Erlich, H.A. (1988). Primer-directed enzymatic amplification of DNA with a thermostable DNA polymerase. Science **239**: 487–91.

Sallal, A.K. and Nimer, N.A. (1989). The intracellular localization of glycolate oxidoreductase in *Escherichia coli*. FEBS Lett. **258**: 277–80.

Sambrook, J., and Russel, D. W. (2002). Molecular cloning - a Laboratory mannual, Vol 13, 3 edn Cold Spring Habour, New York, Cold Spring Habour Laboratory Press.

Schwarte, S. and Bauwe, H. (2007). Identification of the photorespiratory 2-phosphoglycolate phosphatase, PGLP1, in Arabidopsis. Plant Physiol. **144**:1580-86.

Sharkey, T.D. (1988). Estimating the rate of photorespiration in leaves. Physiol. Plant. **73**: 147–52.

Shiraishi, T., Fukusaki, E., and Kobayashi, A. (2000). Formate dehydrogenase in rice plant: growth stimulation effect of formate in rice plant. J. Biosci. Bioeng. **89**: 241-46.

Siefert, F., Kwiatkowski, J., Sarkar, S., and Grossmann, K. (1995). Changes in endogenous cyanide and 1-aminocyclopropane-1-carboxylic acid levels during the hypersensitive response of tobacco mosaic virus-infected tobacco leaves. Plant Growth Regul. **17**: 109–13.

Siegień, I. and Bogatek, R. (2006). Cyanide action in plants from toxic to regulatory. Acta Physiol. Plant. **28**: 483–97.

Somerville, C. R. and Ogren, W.L. (1982). Genetic modification of photorespiration. Trends Biochem. Sci. **7**: 171–74.

Somerville, C.R. and Ogren, W.L. (1979). A phosphoglycolate phosphatase-deficient mutant of Arabidopsis. Nature **280**: 833–36.

Somerville, C.R. and Ogren, W.L. (1980). Photorespiration mutants of *Arabidopsis thaliana* deficient in serine-glyoxylate aminotransferase activity. Proc. Natl. Acad. Sci. U. S. A. **77**: 2684–87.

Song, T., Toma, C., Nakasone, N., and Iwanaga, M. (2004). Aerolysin is activated by metalloprotease in *Aeromonas veronii*. J. Med. Microbiol. **53**: 477–82.

Spreitzer, R.J. and Salvucci, M.E. (2002). Rubisco: structure, regulatory interactions, and possibilities for a better enzyme. Annu. Rev. Plant Biol. **53**: 449–75.

Sriramachari, S. and Chandra, H. (1997). The lessons of Bhopal [toxic] MIC gas disaster scope for expanding global biomonitoring and environmental specimen banking. Chemosphere **34**: 2237–50.

Stabenau, H., Saftel, W., and Winkler, U. (2003). Microbodies of the alga Chara. Physiol. Plant. **118**: 16–20.

Stabenau, H. and Winkler, U. (2005). Glycolate metabolism in green algae. Physiol. Plant. **123**: 235–45.

Taiz, L. and Zeiger, E. (2010). Plant Physiology, Fifth Edition. Sinauer Associates. Sunderland, MA. (In press).

Taler, D., Galperin, M., Benjamin, I., Cohen, Y., and Kenigsbuch, D. (2004). Plant eR genes that encode photorespiratory enzymes confer resistance against disease. Plant Cell **16**: 172–84.

Tamura, K., Peterson, D., Peterson, N., Stecher, G., Nei, M., and Kumar, S. (2011). MEGA5: molecular evolutionary genetics analysis using maximum likelihood, evolutionary distance, and maximum parsimony methods. Mol. Biol. Evol. **28**: 2731–39.

Tcherkez, G.G.B., Farquhar, G.D., and Andrews, T.J. (2006). Despite slow catalysis and confused substrate specificity, all ribulose bisphosphate carboxylases may be nearly perfectly optimized. Proc. Natl. Acad. Sci. U. S. A. **103**: 7246–51.

Timm, S., Nunes-Nesi, A., Pärnik, T., Morgenthal, K., Wienkoop, S., Keerberg, O., Weckwerth, W., Kleczkowski, L. a, Fernie, A.R., and Bauwe, H. (2008). A cytosolic pathway for the conversion of hydroxypyruvate to glycerate during photorespiration in Arabidopsis. Plant Cell **20**: 2848–59.

Tittle, F.L., Goudey, J.S., and Spencer, M.S. (1990). Effect of 2 , 4-dichlorophenoxyacetic acid on endogenous evolution in seedlings of soybean and barley. Plant Physiol. **94**: 1143–48.

Tolbert, N.E. (1997). The C_2 oxidative photosynthetic carbon cycle. Annu. Rev. Plant Physiol. Plant Mol. Biol. **48**: 1–25.

Trapp, S., Larsen, M., Pirandello, A., and Lyngby, D.-K. (2003). Feasibility of cyanide elimination using plants. **3**: 128–37.

Tural, B. and Moroney, J. V (2005). Regulation of the expression of photorespiratory genes in *Chlamydomonas reinhardtii*. Can. J. Bot. **83**: 810–19.

Voll, L.M., Jamai, A., Renné, P., Voll, H., McClung, C.R., and Weber, A.P.M. (2006). The photorespiratory *Arabidopsis shm1* mutant is deficient in SHM1. Plant Physiol. **140**: 59–66.

Volokita, M., Uniuersity, M.S., Lansing, E., and Foundation, K. (1987). The primary structure of spinach glycolate oxidase deduced from the DNA sequence of a cDNA clone. J Biol Chem. **25**: 15825–28.

Voss, I., Sunil, B., Scheibe, R., and Raghavendra, A.S. (2013). Emerging concept for the role of photorespiration as an important part of abiotic stress response. Plant Biol. (Stuttg). **15**: 713–22.

Watanabe, A., Yano, K., and Ikebukuro, K. (1998). Cloning and expression of a gene encoding cyanidase from *Pseudomonas stutzeri* AK61. Appl. Microbiol. Biotechnol. **3**: 93–97.

Weise, S.E., Schrader, S.M., Kleinbeck, K.R., and Sharkey, T.D. (2006). Carbon balance and circadian regulation of hydrolytic and phosphorolytic breakdown of transitory starch. Plant Physiol. **141**: 879–86.

Whitney, S.M., Houtz, R.L., and Alonso, H. (2011). Advancing our understanding and capacity to engineer nature's CO_2-sequestering enzyme, Rubisco. Plant Physiol. **155**: 27–35.

Wingler, a, Lea, P.J., Quick, W.P., and Leegood, R.C. (2000). Photorespiration: metabolic pathways and their role in stress protection. Philos. Trans. R. Soc. Lond. B. Biol. Sci. **355**: 1517–29.

Xu, H., Zhang, J., Zeng, J., Jiang, L., Liu, E., Peng, C., He, Z., and Peng, X. (2009). Inducible antisense suppression of glycolate oxidase reveals its strong regulation over photosynthesis in rice. J. Exp. Bot. **60**: 1799–09.

Yu, X., Trapp, S., and Zhou, P. (2005). Phytotoxicity of cyanide to weeping willow trees. Environ. Sci. Pollut. Res. Int. **12**: 109–13.

Yu, X., Trapp, S., Zhou, P., Wang, C., and Zhou, X. (2004). Metabolism of cyanide by Chinese vegetation. Chemosphere **56**: 121–26.

Yu, X.-Z., Lu, P.-C., and Yu, Z. (2012). On the role of β-cyanoalanine synthase (CAS) in metabolism of free cyanide and ferri-cyanide by rice seedlings. Ecotoxicology **21**: 548–56.

Zelitch, I., Schultes, N.P., Peterson, R.B., Brown, P., and Brutnell, T.P. (2009). High glycolate oxidase activity is required for survival of maize in normal air. Plant Physiol. **149**: 195–04.

Zhong, H.H., Resnick, A.S., Straume, M., and Robertson McClung, C. (1997). Effects of synergistic signaling by phytochrome A and cryptochrome1 on circadian clock-regulated catalase expression. Plant Cell **9**: 947–55.

6.6. Curriculum vitae

Personal information

Name: Mohamed Hassan Mohamed Ahmed Aboelmy

Date of birth: 13.06.1979

Place of birth: Menia

Nationality: Egyptian

Marital status: Married

Educational data:

1985-1990   Shem primary school (excellent grade) - Menia/Egypt

1990-1993   Shem prep school (excellent grade) - Menia/Egypt

1993-1995   Maghagha secondary school (very good grade) - Menia/Egypt

1996-2000   Bachelor science (Very good grade) - Faculty of science/ Minia University
                   - Menia/Egypt

2003   Diploma in Microbiology (very good grade) – Institute botany South of
                   Valley University, Sohag, Egypt

2009   International Master of Horticulture (plant Biotechnology): Gottfried
                   Wilhelm Leibniz University Hannover, Germany

Since November   PhD student at the Leibniz University Hannover, Institute of Botany,
2009   Christoph Peterhänsel;

                   Research associate at the Leibniz University Hannover, Institute of Botany,
                   Prof. Dr. Christoph Peterhänsel

6.7. Acknowledgements

First and foremost I am grateful to Professor Dr. Christoph Peterhänsel for giving me the chance to work in his laboratory. I am also very thankful for his supervision, his friendship and his hospitality. The critical reading, discussion and correction of this manuscript by him made it possible for me to present this manuscript in its present form.

I would wish to express my special thanks to Prof. Dr. Bernhard Huchzermeyer, Prof. Dr. Jutta Papenbrock and Prof. Dr. Sascha Offermann and other members of Botany Institute for their kindness and cooperation.

I wish to introduce my special thanks to member of AG Peterhänsel for their friendship and their endless help during my work.

I also would like to thank Prof. Dr. Hans Peter Braun for helping with mass spectrometry work.

My special thanks to the Egyptian government for financing my study in Germany from 2007 to 2012. I also thank the Institute for Botany - Hannover University for financing my study from 2012 till the end of this study.

My special thanks to my family and my children Rofida, Rahaf and Retal for their lovely smiles that always refresh my life

6.8. Declaration / Erklärung

Herewith I declare that I have written this PhD thesis myself, using only the referenced literature.

Hiermit versichere ich, dass ich die vorliegende Doktorarbeit selbstständig verfasst und keine anderen als die angebenen Hilfsmittel und Quellen verwendet habe.

Mohamed H Aboelmy

Hannover, 2014